



**1949**

**Intact protein analysis  
using capillary zone electrophoresis-mass spectrometry  
in different capillaries**

Thesis for the Degree of Doctor of Philosophy (PhD)

by **Narmin Hamidli**  
Supervisor: Dr. Attila Gáspár

**UNIVERSITY OF DEBRECEN**  
Doctoral Council of Natural Sciences and Information Technology  
Doctoral School of Chemistry  
Debrecen, 2023

*Hereby I declare that I prepared this thesis within the Doctoral Council of Natural Sciences and Information Technology, Doctoral School of Chemistry, University of Debrecen in order to obtain a PhD Degree in Natural Sciences/Informatics at Debrecen University.*

*The results published in the thesis are not reported in any other PhD theses.*

*Debrecen, 2023*

.....  
*signature of the candidate*

*Hereby I confirm that Narmin Hamidli conducted her studies with my supervision within the K/2 Doctoral Program of the Doctoral School of Chemistry between 2019 and 2023. The independent studies and research work of the candidate significantly contributed to the results published in the thesis.*

*I also declare that the results published in the thesis are not reported in any other theses.*

*I support the acceptance of the thesis.*

*Debrecen, 2023*

.....  
*signature of the supervisor*

# **Intact protein analysis using capillary zone electrophoresis-mass spectrometry in different capillaries**

Dissertation submitted in fulfilment of the requirements  
for the doctoral (PhD) degree in Chemistry

Written by Narmin Hamidli

Prepared in the framework of the Doctoral School of Chemistry of the University of  
Debrecen  
(Coordination and Analytical Chemistry, programme K/2)

Dissertation advisor: Dr. Attila Gáspár

The official opponents of the dissertation:

Dr. ....  
Dr. ....

The evaluation committee:

chairperson: Dr. ....  
members: Dr. ....  
Dr. ....  
Dr. ....  
Dr. ....

The date of the dissertation defense: 2023

## **Acknowledgement**

I would like to express my deepest appreciation to my supervisor *Dr. Attila Gáspár* for his invaluable guidance, patience and understanding.

I also could not have undertaken this journey without *Dr. Melinda András* who supported me personally and professionally in different ways. I deeply appreciate the help and support of *Cynthia Nagy, Ruben Dávid Szabó, Dr. Gyöngyi Gyémánt* and *all other colleagues* who showed me the kindness and friendliness of a Hungarian and made me feel like a part of a family away from home. I am also thankful to *Blerta Pajaziti* for her cooperation in our joint works as well as her friendship.

This endeavor would not have been possible without *Tempus Public Foundation* that honored me with “*Stipendium Hungaricum*” scholarship (#242771) to finance my Ph.D. research between 2019-2023.

I am grateful *to my family* who showed endless support for my studies and life abroad. Despite their initial worries over my civil status at the end of four years abroad, I hope I make them proud now by completing my education as a married woman.

Finally, special thanks to *my husband Maximilian Ullrich*. His belief in me, encouragement and vacation plans has kept my spirit and motivation high during the previous four years.

## TABLE OF CONTENTS

<b>1. PREFACE .....</b>	<b>8</b>
<b>2. LITERATURE REVIEW .....</b>	<b>9</b>
<b>2.1 Top-down proteomic analysis.....</b>	<b>9</b>
<b>2.2 Capillary electrophoresis .....</b>	<b>11</b>
2.2.1 Principle .....	11
2.2.2 Instrumentation .....	13
2.2.3 Capillary zone electrophoresis.....	15
2.2.4 Capillary coatings .....	18
<b>2.3 Mass spectrometry.....</b>	<b>20</b>
<b>2.4 Capillary electrophoresis with mass spectrometric detection</b> <b>.....</b>	<b>24</b>
<b>2.5 Top down CZE-MS analysis of proteins.....</b>	<b>28</b>
2.5.1 General approaches and techniques .....	28
2.5.2 Protein adsorption and its prevention.....	30
2.5.3 CZE-MS determination of intact proteins.....	33
<b>3. EXPERIMENTAL SECTION .....</b>	<b>38</b>
<b>3.1 Chemicals.....</b>	<b>38</b>
<b>3.2 Samples .....</b>	<b>38</b>
<b>3.3 Instrumentation .....</b>	<b>39</b>
3.3.1 CE .....	39
3.3.2 ESI-QTOF-MS.....	40
<b>3.4 Capillary coatings .....</b>	<b>41</b>
3.4.1 Single-layer PB and SMIL-PB coated capillaries.....	41
3.4.2 Preparation of linear polyacrylamide coating .....	42
<b>4. RESULTS AND DISCUSSION.....</b>	<b>43</b>

<b>4.1 Analysis of protein mixtures in different capillaries .....</b>	<b>43</b>
4.1.1 Analysis in BFS capillary .....	43
4.1.2 Analysis in coated capillaries.....	55
4.1.2.1 Analysis in PB-coated capillary .....	55
4.1.2.2 Analysis in LPA-coated capillary.....	61
4.1.3 Comparison of coated and non-coated capillaries for the analysis of venom proteins.....	64
<b>4.2 Analysis of recombinant insulins.....</b>	<b>69</b>
4.2.1 CE-UV analysis of insulins.....	69
4.2.2 Mass spectrometric detection of insulins .....	81
<b>4.3 Applications.....</b>	<b>89</b>
<b>5. SUMMARY .....</b>	<b>97</b>
<b>6. REFERENCES .....</b>	<b>101</b>
<b>7. PUBLICATIONS AND CONFERENCES.....</b>	<b>110</b>

## Abbreviations

<b>BFS</b>	Bare fused silica
<b>BPE</b>	Base peak electropherogram
<b>BUMS</b>	Bottom-up mass spectrometry
<b>CEC</b>	Capillary electrochromatography
<b>CGE</b>	Capillary gel electrophoresis
<b>CID</b>	Collision induced dissociation
<b>CIEF</b>	Capillary isoelectric focusing
<b>CITP</b>	Capillary isotachopheresis
<b>CZE</b>	Capillary zone electrophoresis
<b>EIE</b>	Extracted ion electropherogram
<b>EOF</b>	Electroendosmotic flow
<b>ESI</b>	Electrospray ionization
<b>HILIC</b>	Hydrophilic interaction chromatography
<b>IEX</b>	Ion exclusion chromatography
<b>LPA</b>	Linear polyacrylamide
<b>MALDI</b>	Matrix-assisted laser desorption/ionization
<b>MEKC</b>	Micellar electrokinetic capillary chromatography
<b>MS/MS</b>	Tandem mass spectrometry
<b>NMR</b>	Nuclear magnetic resonance
<b>PB</b>	Polybrene
<b>PEG</b>	Polyethylene glycol
<b>PEI</b>	Polyethyleneimine
<b>pI</b>	Isoelectric point
<b>PTM</b>	Post translational modification
<b>PVA</b>	Poly-vinyl alcohol
<b>Q-TOF</b>	Quadrupole-time of flight
<b>rhGH</b>	Recombinant human growth hormone
<b>RPLC</b>	Reverse-phase liquid chromatography
<b>SDS-PAGE</b>	Sodium dodecyl sulfate–polyacrylamide gel electrophoresis
<b>SL</b>	Sheath liquid
<b>SMIL</b>	Successive multiple ionic-polymer layer
<b>TDMS</b>	Top-down mass spectrometry

## 1. Preface

Proteins possess inherent complexity. This is linked to their high molecular weight, post-translational modifications (PTMs), mutations, isoforms and microheterogeneities. Subtle modifications in the protein structure may induce the formation of functionally varying proteoforms, changing the efficacy and safety of proteins and protein complexes. The latter, in turn, may adversely impact medical and biological activity of molecules. Biopharmaceutical industry has long been willing to address this challenge, which necessitates the effective proteoform identification and characterization, that are usually deduced from the determination of the structure and the precise intact mass of the protein. For decades, mass spectrometry has been primarily responsible for this task.

The complete sequence of intact proteins and protein complexes may be well characterized using intact and native top-down mass spectrometric (TDMS) approaches, accordingly. Upon the intact analysis of therapeutic proteins TDMS often incorporates the chromatographic or electrophoretic separation step prior to MS analysis in order to simplify the distinct proteoform spectra. For the study of intact proteins, capillary electrophoresis has evolved into a mature and appealing technique. Capillary zone electrophoresis (CZE), capillary gel electrophoresis (CGE) and capillary isoelectric focusing (CIEF) have gained prominence in this field, while only CZE enables a straightforward and unchallenging connection with an MS detector for mass determination and protein characterization.

Our group has been involved in intact protein analysis since a few years. Yet during my doctoral studies, we have gained a substantial amount of experience with TDMS on intact as well as native protein analysis with CZE-MS.

## 2. Literature review

### 2.1 Top-down proteomic analysis

Proteomics is an advanced technology for the identification, comprehensive characterization, and quantitation of proteins, proteoforms and proteoform complexes [1]. The term proteome was first stated by Marc Wilkins [2] to signify the “PROTEin complement expressed by a genOME”. While genome is invariable in an organism, the proteome can undergo alterations in response to variety of conditions. Particularly those structural changes, post-translational modifications (PTMs), protein interactions are the subject of interest in proteomics research.

Mass spectrometry (MS) has developed into a potent technique for the study of proteomes over the last 30 years. Top-down (TD) and bottom-up (BU) techniques are two main approaches for MS-based proteomics (Figure 1). TDMS operates at the proteoform level to examine intact or native proteins while maintaining a wide range of molecular complexity. In contrast, BU technique performs at the peptide level, therefore necessitates the digestion of target proteoform prior to analysis [3]. This approach has been widespread for its notably easier execution, simple application to complex proteoforms, high-throughput performance, remarkable sensitivity and for the availability of advanced data screening tools and data bases. Even with all the benefits listed above, the BU approach has not become a routine proteomics technique yet. The reason of this is that the detected peptides do not accurately reflect the whole sequence of an intact protein or the entire collection of PTMs, just as puzzle pieces do not depict the entire image [4]. To fully characterize proteoforms and comprehend PTMs, genetic variants, and alternative splicing isoforms, TDMS-based proteomics is a valuable tool. It is necessary for deciphering fundamental biological functions, discovering disease pathways, and uncovering novel biomarkers [5].

Since it was initially explored in 1997 [6], several advancements in sample front-end fractionation strategies, MS equipment and whole protein ion dissociation techniques have aided TD proteomics become an appealing technology with growing significance. However, TDMS-based proteomics still faces a number of difficulties. Those are particularly with regard to proteome complexity, solubility, data processing and analytical output for targeted therapy. Further advancements in MS-competent efficient separation techniques, protein extracting and solubilizing surfactants, front-end protein enrichment strategies, user-friendly data deconvolution sets, and technological advancements for characterization of large proteins (>50 kDa) or nanoproteomics are all required to address these challenges [5].

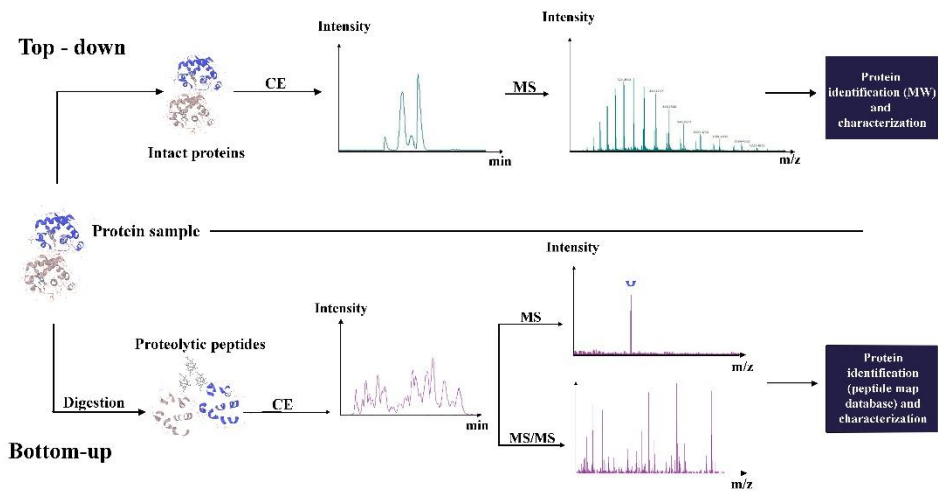


Figure 1. Basic approaches for MS-based proteomics analysis [7].

Components of complex proteome samples must be separated before being introduced into MS. When coupled to MS, the commonly utilized chromatographic or electrophoretic separation methods boost efficiency and minimize sample handlings. The most frequent separation procedure for assessing intact proteoforms is liquid chromatography (LC), which includes reversed-

phase liquid chromatography (RPLC), hydrophilic interaction liquid chromatography (HILIC), and ion exchange (IEX) chromatography. In these chromatographic techniques analytes are selectively partitioned between a liquid mobile phase and a stationary phase. Electrophoretic techniques, on the other hand, separate charged analytes based on differential migration velocities in an applied electric field. Given that conventional SDS-PAGE and alternative capillary electrophoresis (CE) modes such as capillary isoelectric focusing (CIEF) and capillary gel electrophoresis (CGE) are not fully adequate to TDMS, capillary zone electrophoresis (CZE) has grown in favor among electrophoretic methods.

Following the separation, proteoforms need to be transferred into the gas phase and ionize prior to detection. Ionization methods that are regularly performed for proteins comprise matrix-assisted laser desorption ionization (MALDI) and electrospray ionization (ESI). While utilizing MALDI often produces singly or doubly protonated ions, ESI yields multiple charged ions. Since ESI-MS and flow systems may be readily connected online, ESI is a favored ion source for intact protein analysis [8].

## **2.2 Capillary electrophoresis**

### **2.2.1 Principle**

Hjerten's study [9], which first demonstrated the feasibility of separating numerous analytes by electrophoresis in free solutions in 1967, serves as the basis for current CE. It was occasionally called tube electrophoresis, since the apparatus at the time comprised of 3 mm inner diameter (ID) quartz capillary tube besides a high voltage power source and a detector. Later, further enhancements to the instrumentation - even narrower glass and Teflon capillary applications with ID of 200  $\mu\text{m}$  followed by Virtanen and Mikkers [10],

respectively. In 1981 Jorgenson [11] proposed using 75  $\mu\text{m}$  ID glass capillaries as well as outlined the theory and the correlations between operating parameters and separation performance. Herewith CE has grown into a mature and adaptable separation technology since the commercialization of instrument in 1988 [12].

A modern CE is a technique that employs an applied electric field to separate components based on their charge, size and shape. That is, the separation occurs through differential electrophoretic mobilities of components, which increase with smaller size and higher charge of the spherical components [13] (Equation 1).

$$\mu_e = \frac{q}{6\pi\eta r} \quad (1)$$

where  $\mu_e$ : electrophoretic mobility,  $q$ : ion charge,  $\eta$ : solution viscosity,  $r$ : ion radius.

Introduction of narrower capillaries (25-75  $\mu\text{m}$  ID) offered various benefits as well as challenges. The greater surface area to volume ratio allowed Joule heating to be distributed evenly throughout the capillary. This not only reduced the thermal diffusion effect but also inhibited significant current generation even at high voltages up to 30 kV [14]. On the other hand, it supported the formation of a unique plug flow known as electroendosmotic flow (EOF). This phenomenon arises when a liquid (electrolyte) near a charged surface is subjected to an electrical field, driving the liquid at that surface to move in bulk [15]. EOF is often directed towards the cathode (negatively charged electrode) where detection takes place. As a result of this driving force, for the first time, both charged and uncharged components could be analyzed in a single run. As a pH dependent component, EOF becomes significant at high pH values. When the magnitude of the EOF surpasses the mobilities of the analytes, they will be

flushed fast toward the detection end of the capillary, resulting in short, inefficient separation and resolution [16].

Several electrophoretic separation modes, including CIEF, CGE and isotachopheresis (ITP) frequently need EOF suppression, while CZE, micellar electrokinetic chromatography (MEKC) and capillary electrochromatography (CEC) usually take advantage of it. The concepts and applications of these distinct CE operating modes differ considerably. For instance, CZE as the straightforward approach employs background electrolytes (BGE) in the electrode reservoirs and capillary. When an electric field is applied, the BGE and sample begin to be drawn by the proper electrode, yielding in the separation and detection of each component [17]. Separation in MEKC, in contrast, is accomplished by analyte interaction with micelles. In CIEF, ampholytes serve to create a pH gradient in the capillary, and separation takes place when the components attain a net charge of zero ( $pI=pH$ ). One of the oldest methods, CITP, employs two distinct buffer systems between which analytes are separated based on their effective mobilities. CEC resembles HPLC in that it uses an electrolyte (mobile phase) within a packed capillary-like column and it applies a combination of chromatographic and electrophoretic interactions [14].

### **2.2.2 Instrumentation**

Despite the fact that there are variety of CE modes of operation, they can all be performed using the same instrument. A conventional CE is basically made up of a high voltage power supply, two electrodes, an injection system and a detector. In brief, following the sample loading at the inlet end of the capillary, a high voltage application takes place between the ends of the electrodes immersed in BGE. Hereby, the applied voltage assists the electrolyte solution in transferring the sample to the detector. An on-capillary detector

positioned at the opposite end of the capillary detects the separated analyte zones and transmits the raw data to a computer in the form of electropherograms as an illustration of peaks indicating analytes as a function of migration time [17].

The CE makes use of a dual polarity power source designed to supply up to  $\pm 30$  kV while limiting current levels to 200-300  $\mu\text{A}$ .

Sample introduction into the capillary is usually performed via hydrodynamic or electrokinetic methods. Hydrodynamic injection, which incorporates loading by pressure, gravity flow or vacuum suction, is favorable for low viscosity samples. Electrokinetic injection, on the contrary, is accomplished by applying voltage to the sample reservoir. Since the loaded quantity of individual analytes is dependent on their own mobility, in this technique, often the injection of unequal amounts of species may take place [14]. In either scenario, the length of the injected plug should not exceed 1-2% of the entire length of the capillary. Otherwise, it might result in broad peak widths or peak distortions (tailing or leading), both compromising the good resolution. The quantity of loaded solutes can be calculated in both hydrodynamic (Equation 2) or electrokinetic (Equation 3) injection methods [13].

$$V = \frac{\Delta P d^4 \pi t}{128 \eta L} \quad (2)$$

$$Q = \frac{(\mu_e + \mu_{EOF}) V \pi r^2 C t}{L} \quad (3)$$

where V: injected volume,  $\Delta P$ : pressure difference across the capillary, d: inner diameter of the capillary, t: injection time,  $\eta$ : buffer viscosity, L: total length of capillary, Q: injected quantity in mol,  $\mu_e$ : analyte mobility,  $\mu_{EOF}$ : EOF mobility, V: voltage, r: capillary radius, C: analyte concentration.

Nowadays, besides the conventional instruments, numerous microfabricated [18] as well as portable [19] CE counterparts serve as popular fields of research due to their enhanced performance and speed. Unlike CE, in miniaturized devices fluid is transferred, mixed, separated via microchannels etched onto glass or polymer microfabricated chip substrates [20]. The flow is regulated either by devices integrated on the microchip or externally by pressure controllers. In the following chapters, however, only conventional CE applications will be exclusively reviewed.

CE instruments are equipped with on-capillary detection, which is typically UV-Visible absorption spectrometry using the wavelength range from 190 nm to 600 nm. However, a broader array of alternative optical, electrochemical, off-capillary mass spectrometry, NMR detectors have been also extensively investigated [21]. High sensitivity, broad dynamic range, rapid response time, low volume detection cells, selective and unselective detection are the key considerations for proper choice of detectors. Yet, since it is difficult to meet all of these requirements on a single detector, each of them has particular applications [17].

### **2.2.3 Capillary zone electrophoresis**

As previously stated, CZE separates analytes based on their electrophoretic mobilities. Yet, achieving a selective separation is not always straightforward and the control over the interactions between the capillary wall, BGE and analytes is necessary. CZE analysis is commonly conducted in bare fused silica (BFS) capillaries possessing free silanol groups on the inner surface. They deprotonate at pH values higher than 4, become protonated at low pH. Very low pH values ( $\text{pH} < 2$ ) do not exhibit EOF due to complete neutralization of the wall. However, in the pH range of 3 to 9, alterations in EOF magnitude

with minor variations in capillary surface charge are more likely, producing irreproducible migration time and area values. Therefore, the most significant demand for the BGE is its high buffering capacity. Besides, effective buffer systems also exhibit low absorbance at the detection wavelength and possess low conductivity [22]. Often additives - surfactants, chiral selectors, organic modifiers - are added to BGE solution to regulate EOF and Coulomb interactions between the solute and the wall [23]. Furthermore, the change in ionic strength of the buffer systems is also capable of modifying EOF. Increasing ionic strength of the BGE entails larger charge density on the double-layer of the wall that is inversely proportional to zeta potential and slows EOF mobility [24] (Equation 4).

$$\mu_{EOF} = \frac{\varepsilon\zeta}{\eta} \quad (4)$$

where  $\mu_{EOF}$ : EOF mobility,  $\varepsilon$ : dielectric constant,  $\zeta$ : zeta potential,  $\eta$ : solution viscosity.

Increasing ionic strength or applying extreme pH to achieve high resolution may not always be beneficial to the target analyte due to denaturation, precipitation, or adsorption of solutes.

CZE is capable of analyzing a variety of solutes: small drugs, amino acids, peptides, proteins and monoclonal antibodies (mAbs) are some of them. A variety of routine analyses have been implemented in industrial, pharmaceutical, forensics and biological labs. CZE can determine inorganic ions, organic acids, and carbohydrates present in food, plants and biological materials. The majority of them barely exhibit UV absorbance, making UV photometry impractical. Thus, the indirect CZE-UV approach incorporating carrier electrolytes and UV-absorbing probes has gained acceptance in the industry [25].

CZE is an essential orthogonal approach in the process of quality control for monitoring the active pharmaceutical components, their excipients and impurities of small drugs. The majority of drugs include one or more ionizable groups, making them favorable for CZE separation. Reminek et al. [26] have recently summarized the standard CZE procedures for over 68 minor pharmaceuticals, their degradation products and contaminants. CZE-UV and CZE-MS are often used for glycosylation profiling and charge variant analysis of mAb-based biopharmaceuticals. One of the routine CZE-UV techniques for charge heterogeneity profiling utilizes 300-600 mM  $\epsilon$ -aminocaproic acid (EACA) as BGE with addition of hydroxypropyl methylcellulose (HPMC) at pH values between 4.5 and 6.0 [27]. Using CZE-MS, mAbs may be assessed in their intact, reduced, incomplete and completely digested states [28].

Proteomics is one of the many applications of CZE. It is highly suitable for the determination of proteins and their characterization thanks to its low solute and reagent consumption as well as its rapid and efficient separation capacity. CZE has long been a preferred procedure for profiling the serum proteins [29, 30]. The analysis featuring the separation of albumin,  $\alpha$ ,  $\beta$ , and  $\gamma$ -globulins was conducted utilizing barbital-based buffer systems in alkaline pH values via online UV detection at 200/214 nm. CZE has also been effective throughout the quality control processes in order to guarantee the safety, integrity, and purity of therapeutic recombinant and food proteins [31, 32]. Besides top-down proteomics applications, peptide mapping (bottom-up proteomics) serves as one of the most effective uses of CZE. It involves the analysis of enzymatically digested proteins to identify the subtle changes in their molecule. UV and MS detection are used extensively in research for this objective [23, 33].

### 2.2.4 Capillary coatings

The analysis in BFS capillaries might be obstructed by a number of constraints. The electrostatic and hydrophilic interactions (Mathe et al. [34] and Kubiak-Ossowska et al. [35] assume the presence of hydrophobic interactions as well) between the capillary wall and solute referred to as adsorption is capable of causing EOF instabilities compromising proper separation efficiency, resolution, and precision. As previously noted, techniques using extreme pH settings or ionic strength alterations may not totally alleviate the adsorption problem, but they may result in irreversible structural changes in the molecule [36]. Coating the capillary surface becomes an alternative when the aforementioned solutions conflict with the application. In general, an ideal coating is expected to meet the following requirements: (i) the coating layer must be homogenous and exhibit full coverage over the silanol groups as a shield; (ii) it has to prove its high stability at the target pH range and rather against organic solvents; (iii) it should exhibit hydrophilicity thus induce no interactions with the analyte of interest and BGE components; and (iv) it has to deliver good separation performance and repeatability [23, 37]. Typically, they are categorized as dynamic and static coatings. Dynamic coatings (or additives) are commonly integrated into the separation medium and serve as a coating by reversibly adsorbing onto the surface [38]. In contrast, static coatings may covalently adhere or strongly attach to the silanol groups. The latter is occasionally referred to as semi-static coating too. The coatings are also classified based on their charge (neutral or charged coatings) as well as hydrophobicity (hydrophilic or hydrophobic coatings).

Neutral coverage on the BFS surface is preferable for effectively inhibiting EOF and any potential electrostatic interactions with charged components. In contrast, positive coatings may modify the EOF direction, while negatively charged coatings intensify it.

Each kind of coating has benefits and drawbacks. Dynamic coatings are user-friendly and may be optimized for various applications. Since the modifier contained in the BGE constantly recovers the coating material, concern about instability is resolved. Amines have been reported often in the scientific literature as possible dynamic modifiers in acidic or neutral condition when these amines are protonated (cationic) [36]. Furthermore, dynamic additives are often not suitable for sensitive post-column analyses involving mass spectrometry. Cationic polyamines and polysaccharides are often exploited to be dynamically adsorbed onto the counter-charged silanol groups. Chitosan, cetyltrimethylammonium bromide and polyethyleneimine (PEI) are a few examples. As neutral dynamic coatings, dextran, hydroxypropylmethylcellulose (HPMC), poly (vinyl alcohol) (PVA) and polyethylene oxide have been extensively employed [37].

Another coating strategy is covalently adhering the coating agent (predominantly polymers) to the silanol groups. Although the preparation phase is arduous and time-consuming, they often do not require regeneration and are hence very stable. Si-O-Si-R or Si-R bonds may be used to achieve covalent attachment. The coupling via the silylation step is susceptible to hydrolysis at even mildly alkaline pH ranges, whilst direct coupling is more stable (pH 2–10) [37]. In CZE applications, linear polyacrylamide (LPA), PVA, and polysaccharide coatings are broadly used [12]. Coatings like PVA and HPMC can be used as dynamic coatings in BGE or as static coatings when a chemical reaction is accomplished with thermal capillary treatment (140 °C) [36, 39].

Semi-static coatings, including cationic polybrene (PB), poly(diallyldimethylammonium chloride), anionic poly(vinyl sulfonate), and dextran sulphate (DS) are typically generated by a simple rinsing step (in a similar way

to dynamic layer preparation), but can be detached and regenerated easily. After a series of runs, “bleeding” of the coating from the surface may be encountered due to the inferior durability of the coatings. Therefore, these coatings are often applied in several layers for greater stability and thicker coverage of silanol groups. In this manner, so-called successive multi-ionic layer (SMIL) coatings [40] are formed which include the sequential application of 3 to 5 layers of cationic and anionic coatings.

Finding a universal coating that meets all demands appears to be challenging. However, highly stable coatings are often favored for the study of biomolecules using CZE-MS.

### **2.3 Mass spectrometry**

Mass spectrometry is a powerful technique for assessing the mass-to-charge ratio ( $m/z$ ) of analytes. It yields a mass spectrum, which represents a plot of ion abundance versus  $m/z$  and delivers insights on the molecular mass, characteristics, and structure of the components. For decades after its emergence, MS has been confined mostly to the study of small organic molecules. Prior to the genomics revolution in the 1970s, biomolecules used to be detected through UV absorbance or fluorescence spectroscopy [41]. The most compelling demand for MS in the instrumental development was a methodology for ionizing and transferring complex molecules into the gas phase. This was not attainable until the late 1980s, when ESI and MALDI ionization strategies were introduced [42]. This innovation made MS a thriving technology. Nowadays, diverse range of specialized MS instruments are routinely performed and extensively employed for the identification as well as quantification of complex biological probes. Modern MS instruments are equipped with three principal domains: ionizer, mass analyzer and detector.

Numerous ionization sources, including gas phase, spray, and desorption approaches, have been implemented to MS. The choice of ion source in MS is a key step and is dependent on the analyte of interest and the intended purpose. Two of the soft ionization methods, ESI and MALDI, which enable ionization with minor or no fragmentation of analytes, have emerged as the most prominent ionization techniques.

ESI serves to desolvate and ionize liquid-phase analytes into the gas phase. The initial formation of charged analyte droplets is facilitated by a static electric field-induced spray. The solute travels through a capillary exposed to high voltages (2–5 kV) in a near-atmospheric-pressure-heated chamber. In the positive ion mode, a generic electrochemical oxidation process takes place at the positive electrode - at the liquid/metal interface of the spray capillary. Sample is expelled constantly from the capillary end which leads to the formation of the Taylor cone, a distorted capillary outflow where a fine mist of charged components is emitted by the aid of nebulizing gas (N<sub>2</sub>). The resultant droplets undergo desolvation and Coulomb fission until the droplets acquire the extra charge and transform into gas phase ions [12, 43, 44]. Ions freed from the solvent travel to the mass analyzer.

Further advancements in ESI involve miniaturization in the dimensions substantially in terms of capillary inner diameter and solvent flow rates. Alongside conventional ESI with capillary ID > 100 μm and flow rate > 500 nL/min, microESI (10 μm < ID < 100 μm, 100 nL/min < flow rate < 500 nL/min) and nanoESI (10 μm ID and 100 nL/min) setups are also accessible for intensified desolvation process [43, 45]. Regardless of their size, ESI simplifies the analysis of polar, charged components of varying molecular weights, including big macromolecules. For the latter, ESI generates ions with multiple charges, thereby allowing analyzers with a low mass limit to analyze large molecules.

The sensitivity is even further enhanced when ESI combines MS with one of the separation techniques. Yet, ion suppression is a persistent problem in ESI. It is caused by the presence of nonvolatile salts, drugs, metabolites or ion-pairing agents in the solution. These components hinder adequate desolvation and ionization, hence reduce sensitivity [45, 46].

In MALDI, laser irradiation is used for ionization process. Typically, the analyte of interest is blended with a crystalline matrix that is able to absorb the laser light. Following that, the mixture is deposited on a MALDI plate and dried. Pulsed laser irradiation on the dried droplets facilitates matrix desorption and ionization, which is then followed by secondary ionization of the sample molecules. For high throughput MALDI analysis, the selection of matrix, laser settings, and sample drying are critical stages [43]. MALDI is competent in the analysis of thermally unstable and non-volatile materials. Major application areas involve complex organic components and proteomics, the latter of which is largely based on peptide mass fingerprinting [47]. Unlike ESI, MALDI yields singly or at most doubly charged ions, making the analysis of intact components challenging. However, MALDI may be advantageous over ESI due to its high tolerance for salts and buffers [45].

The ionic species generated by ion source are subsequently transferred to the mass analyzer. Simply, this is the section where ions are separated based on their  $m/z$  ratio. Key criteria for mass analyzers encompass high resolving power, sensitivity, mass accuracy and the capacity to generate information-dense mass spectrum [48]. The four distinct mass analyzers are quadrupole (Q), ion trap (IT), time of flight (TOF), and Fourier-transform ion cyclotron resonance (FT-ICR). Hybrid approaches, such as Q-TOF, Q-q-Q, TOF-TOF, and Q-LIT (quadrupole-linear ion trap), are also accessible by merging the competences of several analyzers (Table 1.) [49].

The quadrupole mass analyzers feature four parallel electrically connected cylindrical rods. Between the pair of countercharged rods direct current (DC) and radio frequency (RF) voltages are applied, the ratio of which enables the estimation of  $m/z$  in mass analysis. Thus, the ions having stable paths in the dynamic electric field corresponding to a certain  $m/z$  are filtered out among others. Due to their low cost, quadrupole mass filters have been actively exploited during the last decades. However, its mass resolution, accuracy (often hundreds of ppm), and upper  $m/z$  limit (4000) are sometimes unsatisfactory while it is often utilized with some chromatographic methods (e.g., gas chromatography) [45]. IT analyzers exhibit comparable performance characteristics. In IT analyzers, ions are captured for a period of time and exposed to mass analysis. They are recognized by their sensitivity and speed upon MS/MS analysis [41].

*Table 1. Performance comparison of common mass analyzers [41, 49, 50].*

MS	Resolving power	Accuracy (ppm)	Sensitivity (LOD)	Ion source	MS <sup>n</sup>	Proteomics capacity
IT	4000	<1000	medium	ESI	MS <sup>n</sup>	BU-MS
TOF	20000	<20	high	MALDI	MS <sup>2</sup>	BU/TD-MS
Q-q-Q	1000	<1000	high	ESI	MS <sup>2</sup>	BU-MS
TOF-TOF	20000	<20	high	MALDI	MS <sup>2</sup>	BU/TD-MS
Q-q-TOF	20000	<20	high	ESI and MALDI	MS <sup>2</sup>	BU/TD-MS
FTICR	750000	<2	high	ESI and MALDI	MS <sup>n</sup>	BU/TD-MS
Orbitrap	100000	<5	high	ESI and MALDI	MS <sup>n</sup>	BU/TD-MS

TOF, FT-ICR, and Orbitrap are the preferred analyzers for applications seeking outstanding resolving power and accuracy. In linear TOF spectrometers, ions are driven through a long tube (0.5 to 2 meters) after being accelerated by an electric field of a known strength (1–20 kV). Ions are separated following their decreasing velocities, with increasing  $m/z$ . Even higher resolution is offered by reflectron TOF analyzers. They feature a reflectron with the

ability to distinguish identical  $m/z$  ions with slight velocity differences [45]. TOF analyzers provide a limitless mass range, resolution in the tens of thousands and mass accuracy in less than 10 ppm. Typically, they are hybrids with quadrupole analyzers (Q-q-TOF), ensuring excellent resolution and mass accuracy. In this scenario, quadrupole directs the ions to be separated by TOF analyzers in MS, whilst in MS/MS analysis it accomplishes the fragmentation of the selected ions as well. In FT-ICR, ions are separated solely by their cyclotron frequencies in the presence of a combined high magnetic field and a slight electrical field [51, 52]. The frequencies may be evaluated with great precision, which implies high resolution and mass accuracy at the ppm and sub-ppm levels.

The ions finally reach the detector, where MS signals are generated (with the exception of the FT-ICR, which functions as both a detector and an analyzer). Major detector attributes may include strong amplification, high detection efficiency, low noise, quick response, a broad dynamic range, and a low cost. Electron multipliers (EM), photomultiplier conversion dynodes, Faraday cups (FC), and array detectors are the most prominent kinds of detectors in MS [53].

#### **2.4 Capillary electrophoresis with mass spectrometric detection**

The introduction of advanced and modified ion sources has encouraged the hyphenation of CE with MS (Fig. 2). Mainly, online coupling of CE to MS has been conducted using ESI in order to determine organic ionic compounds. Other ionization techniques, like MALDI [54] and inductively coupled plasma (ICP) [55], have not delivered an automated and straightforward solutions, offering far less application possibilities than ESI [50]. The transfer of analyte flow from CE to MS via ESI was, however, demanding in the following ways:

(1) the electrical currents from CE do not correlate with ESI currents, exhibiting always an order of magnitude greater current values; (2) the flow rate of CE (0-100 nL/min) is not as high as in ESI (1-10  $\mu$ L/min); and (3) the acceptable BGE solutions for ESI-MS are very limited, restricting the inclusion of non-volatile elements (for instance, surfactants, gel-like matrix) that may cause analyte signal suppression as well as ion source contamination. This makes CZE the most popular CE mechanism interfaced with MS [12, 56, 57].

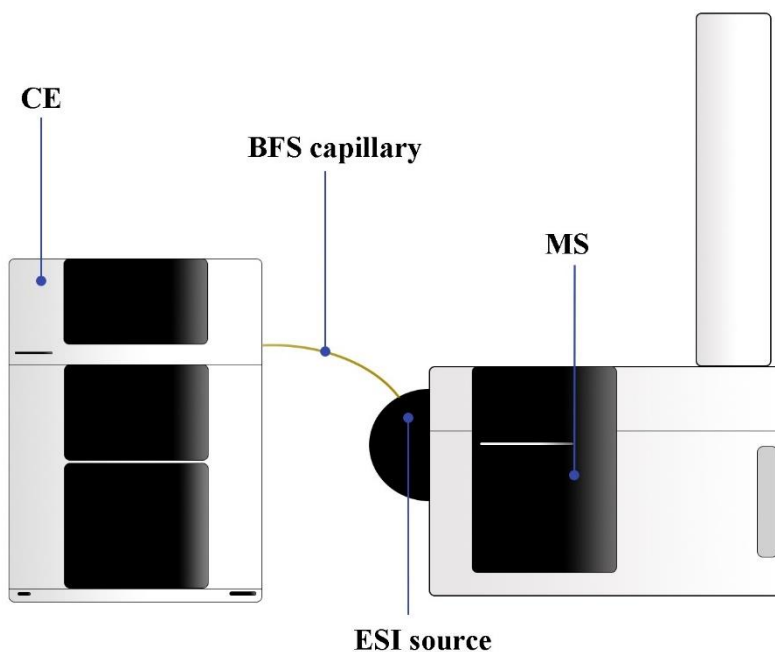


Figure 2. Visualization of CE-MS coupling.

Numerous interface strategies have been proposed in response to the aforementioned difficulties in order to provide a homogeneous electrical field, steady electrospray, and high MS detection sensitivity. These methods are referred to as sheath liquid (SL) and sheathless interfaces.

The coaxial (triple-tube setup) SL interface is a regular sheath flow approach. In this configuration, SL flow is delivered via a wider tube neighboring

the CE capillary, which acts as a makeup flow to close the CE electrical circuit, guarantees spray stability and ionization efficiency. SL consists mainly of 50–80% organic solvents (usually methanol or isopropanol) for spray stability and a small quantity of ionic species (formic/acetic acid or ammonium salt) to enable enhanced spray formation. Frequently, nebulizing gas flow is also supplied via the outermost (third) tube to enhance spray generation. Besides its electrospray-friendly nature, the SL interface also allows flexibility in the choice of BGE, which is favored for CE separation. However, the SL significantly dilutes the CE effluent traveling at lower flow rates, compromising the signal sensitivity [58]. This challenge was intended to be resolved via liquid-junction techniques by inserting the CE capillary end into the ESI emitter. Using an extra SL tee junction, the effluent was mixed with conductive flow in minute quantities. Yet, this interface struggled to achieve a uniform electric field and a high resolution [56, 57].

Avoiding the use of SL, which refers to sheathless interfaces, is yet another approach for mitigating the dilution effect. Typically, electrical contact is achieved by coating the outer wall of the capillary sprayer tip with conductive metals or by installing the wire electrode directly into the CE capillary. This interface attains the nanoliter per minute flow rates necessary for electrospray by achieving excellent sensitivity. Due to the electrochemical processes, reliable spray formation was still an unmet objective for this system besides its limited durability and low reproducibility [57, 59]. Thus, a nanoflow interface with a porous tip was suggested. This unique interface incorporates etching the CE capillary end and introducing conductive liquid into the pores to establish electrical contact [60].

Independent of the connection interface, CE BGE plays a key role in the ionization process. BGEs are required to assist ion formation and exhibit

high volatility as well as low ionic strength. Therefore, the most prevalent BGEs for CE-MS online applications are restricted to formic acid, acetic acid for acidic, and their ammonium salts or buffers for neutral and alkaline pH [61]. Furthermore, the electrolyte should be compliant with the SL. This implies that the electrophoretic mobilities or conductivities of counterions in both solutions should be similar, which is particularly beneficial under conditions with low or no EOF to prevent back flow. This issue is addressed, however, by selecting the same counterions for both SL and BGE [12].

The hyphenation with MS allows CE to achieve more than a mere separation. Given the application areas, two significant aspects of CE may be outlined: (1) CE-MS has made feasible to identify the composition of biological materials that are available only in low volumes. This CE-MS feature has boosted biomarker identification from body fluids and metabolomic studies which was followed by the progress in sample preparation and enrichment strategies [62]. As a matter of fact, Nevedomskaya et al. [63] have demonstrated the possibility of mouse urine metabolomic profiling using CE-MS with in-capillary sample preconcentration. (2) CE-MS also exhibits the capability to provide information on sample specific properties such as complex dissociation/association or protein conformational structure. This feature has been implemented in pharmaceutical, biotechnological fields for characterization, structural sequencing of proteoforms, their complexes and aggregates [64]. A reliable approach for accomplishing this is native CE-MS, which was used by Belov et al. [65] to separate the monomer of enolase from its homodimer and isozyme in their active state. Separation of monomer and homodimer was adequate enough for quantitation and deconvolution of species. In one of the recent reviews, Stolz et al. [50] provided an overview of CE-MS applications. Proteomics comprised 22% among all CE-MS applications based on a survey of over 140 studies. Besides, 18% of them featured in biomarker discovery,

15% in food and environmental studies, 14% in metabolomics, 13% in the pharmaceutical industry and 9% in glycopeptide analysis.

## **2.5 Top down CZE-MS analysis of proteins**

### **2.5.1 General approaches and techniques**

Chains of amino acid residues make up the massive biomolecules known as proteins. They have important roles in the cells, including regulating gene expression, transporting metabolites, aiding metabolic reactions, and guaranteeing structural stability. Proteins feature a heterogeneous structure comprising various proteoforms and PTMs. These alterations may sometimes be linked with medical conditions. For instance, abnormalities in phosphorylation are connected with neurological disorders and type II diabetes, yet glycosylation is often associated with cancer and inflammation [66]. Thus, the determination of subtle structural modifications is of key importance. For decades, protein identification and characterization have centered around their analyses following proteolytic digestion [67]. However, when the whole polypeptide chains are examined using TDMS, more informational layers may be retrieved.

TDMS can conduct intact as well as native protein analyses. In the light of recent biotechnological breakthroughs, CZE-MS has evolved into a potent tool for achieving this objective. Analysis of intact proteins incorporates the study of denatured or unfolded protein structures. The process of denaturation disorganizes protein structure, disrupts its rigidity, leaving behind a flexible open chain. Numerous physical and chemical stimuli, including temperature, pressure, acidic or alkaline conditions, organic solvents, UV radiation, and even shaking may induce the unfolding of protein. Upon exposure to one of

the conditions, they lose their quaternary, tertiary, and in most cases also secondary structural linkages, producing an intact chain of amino acids [68]. Analyzing intact proteins may be effective for acquiring qualitative information about their naturally occurring isoforms, impurity content, and stability (degradation products). Many affinity and bioactivity assays also require the analysis of proteins in their intact forms. Moreover, information on conformational changes and folding mechanisms can be retrieved by intact analysis [12, 69].

While intact protein MS focuses on individual protein analysis, native MS (nMS) investigates protein complexes [70]. By maintaining physiological conditions, nMS aims to preserve the non-covalent interactions between proteins, subunits, and other assemblies. Under these settings, proteins maintain quaternary structures and remain functionally active, understanding of which is essential for the development of drug design and disease monitoring [71].

There are some differences in the sample preparation, the choice of BGE, SL and accordingly in the mass spectra depending on the target study. During intact analysis, sample matrices and BGE may contain modest quantities of acids or organic solvents to facilitate protein denaturation. The same holds true for sheath liquids as well. In contrast, native analysis is confined to using only aqueous formate, bicarbonate, or acetate salts/buffers at neutral pH values (pH 6.5-7) [66, 72]. In native analysis, a small quantity of MeOH, acids present in the SL, BGE, or sample buffer that is usual for intact analysis may give rise to inadvertent disruption of non-covalent interactions [73].

The denaturation expands the protein's contact surface, leading to many protonation sites and therefore, multiple charge states in the MS spectrum. In contrast to their denatured counterparts, folded proteins have less protonation, leading to fewer charge states and hence higher  $m/z$  values [65]. The latter demands powerful equipment and carefully adjusted MS parameters.

Consequently, high resolution mass analyzers (FTICR, Orbitrap) are frequently used in native analysis [71, 73]. On the other hand, utilizing nanoflow or ultra-low flow ESI as well as sheathless porous tip interfaces promotes the more effective ionization of native components, leading to high sensitivity [65].

### **2.5.2 Protein adsorption and its prevention**

Compared to compact, rigid and smaller components, proteins may exhibit a variety of different characteristics based on their amino acid composition, net charge, structural stability, and intramolecular interactions. In turn, they are susceptible to changes during separation when exposed to pH, ionic strength, temperature, and capillary surface derivatization strategies. Regarding their "unique molecular personality", their adsorption characteristics are hard to comprehend [74].

Adsorption of proteins on the capillary wall has unfavorable effect on the separation performance. It may cause permanent conformational changes to protein structure, rendering them functionally inactive. On the other hand, prolonged contact with the wall might alter the capillary surface, resulting in fluctuations in the EOF that degrades migration time and area values. As a result of this behavior the overall separation efficiency and resolution becomes deteriorated [12].

Protein adsorption can be initiated by external effects, the attributes of proteins, and the surface. External factors encompass pH, ionic strength, temperature, and the composition of the BGE. At pH levels greater than the isoelectric point of a protein, the net charge becomes negative and conversely, protein holds the net positive charge at pH values considerably below its isoelectric point. When pH approaches the proteins' pI value, it is rather vulnerable

to adsorption due to the presence of both positively and negatively charged amino acids in the chain. Elevating temperature stimulates the diffusivity of proteins to the surface, whereas low ionic strength fosters electrostatic interactions [74].

The adsorption mechanism is governed mainly by electrostatic and hydrophilic interactions. Briefly, after the proteins are introduced into the capillary, the oppositely charged groups of the proteins are attracted electrostatically to the (typically negatively charged) capillary wall. This initial attachment of proteins to the surface is often reversible. If the protein is incapable of reversing the interactions, they remain on the surface and become susceptible to conformational changes. There are a few works where hydrophobic interactions between the siloxane (Si-O-Si) bridges and hydrophobic moieties of protein are assumed to occur as a result of the unfolding event, which initiate the protein's permanent attachment to silanol groups [34, 35, 75]. The occurrence of the last step relies greatly on the physicochemical features of the proteins.

The initial interactions are ruled by the quantity of charged species on a polypeptide chain. The abundance of charged amino acids, namely arginine and lysine, raises the likelihood of interactions. One of the most important characteristics of proteins is their flexibility or rigidity, which is defined by the number of aromatic clusters as well as  $\pi$ - $\pi$  interactions [34]. A greater number of aromatic species (tyrosine, phenylalanine, tryptophan, and histidine) in the chain aid in maintaining their folded configuration and inhibiting irreversible adsorption. These are frequently referred to as "hard" proteins. In contrast, "soft" proteins lack substantial internal cohesion and adsorb irreversibly under circumstances favorable to adsorption (Fig. 3). Furthermore, the hydrophobic/hydrophilic moieties of proteins dictate the reversibility of adsorption. Large proteins containing lipid groups, for instance, may adsorb rapidly owing

to their high affinity, while hydrophilic glycan groups are inert to interactions [74].

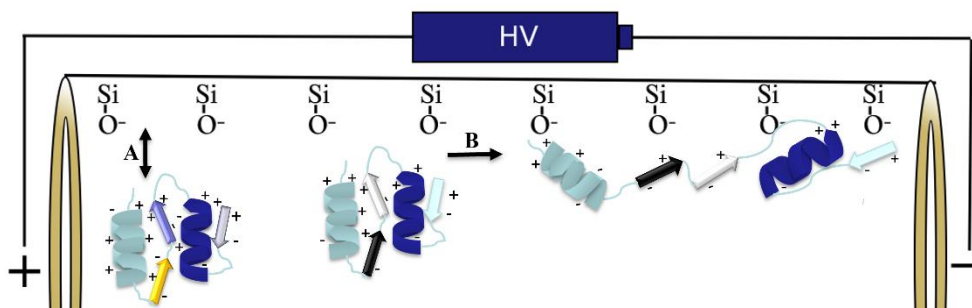


Figure 3. Interaction of hard (A) and soft (B) proteins with the BFS capillary wall.

If protein is one mediator of protein-wall interactions, the surface is yet another. To comprehend the adsorption mechanism, surface morphology, charge, polarity, and energy need to be examined [74]. Frequently, capillary wall coatings are applied to inhibit such interactions. It is still an effective approach for modifying the aforementioned surface properties. The chapter 2.2.4 comprehends the commonly used coatings and their competencies. Additionally, a number of reviews [23, 69, 72] highlighted the most adequate capillary coatings for protein analysis by CZE-MS. Due to their compatibility with MS, covalent and physically adsorbed coatings are the most prevalent types of coatings. To effectively eliminate electrostatic and hydrophilic interactions, silanol groups are often covered by neutral polymers such as LPA and PVA. Polymer binds to the intermediate layer generated by silanization over the surface hydroxyl groups. In an ideal scenario, these settings restrict EOF, and proteins meet the detector without encountering adsorption or structural modifications. In terms of charged coatings, one or more polyelectrolytic layers of PB or PEI are regarded as the most effective. They offer a positively charged surface and change the EOF direction. These coatings are operable in settings of reversed

polarity and acidic pH. As a result of the reversed EOF and protein electrophoretic mobilities, these coatings enable a separation with a high degree of resolution [39].

### **2.5.3 CZE-MS determination of intact proteins**

Principally, intact protein analysis with CZE-MS is conducted for separating and determining different proteins in a sample but also for profiling and identification of isoforms in order to gain expertise on protein degradation, glycosylation heterogeneities, charge or size variances, and other modifications [76]. Since unnoticed isoforms or variations might have adverse effects on consumers' health, the biopharmaceutical field puts emphasis primarily on developing reliable screening methods to discover these modifications. Smith et al. [77] undertook the first on-line CZE-MS analysis of intact proteins by separating bovine insulin, whale, and horse myoglobins. The separation was carried out in a BFS capillary at basic pH values (pH 11 and 8.4) using MS-incompetent buffers such as Tris/HCl and sodium phosphate. Nevertheless, these findings still sparked a huge interest and research on intact protein analysis by CZE-MS.

Analysis of intact proteins has been restricted by major constraints, one of which being adsorption of proteins on the BFS capillary wall. To eliminate adsorption, one approach was to employ BGE solutions with very low or high pH values and therefore neutralize or deprotonate the silanol groups accordingly. Shen and coworkers [78] sought to characterize a PEG sample containing myoglobin by CZE-ESI-MS. By using 0.5% formic acid as BGE and 1M urea in the sample, they succeeded in the separation of myoglobin and PEG. The presence of urea in the sample hindered the formation of protein-PEG complexes and appeared to increase run-to run reproducibility. Later, adopting

the same principle, Stutz et al. [79] examined the separation performance of volatile and non-volatile BGEs at very acidic pH levels for metal-binding proteins. By comparing formic acid, acetic acid, propionic and ortho-phosphoric acids in the pH range of 1.62 to 2.37, they revealed that 1M formic acid was more competent to efficiently and repeatably resolve 6 proteins including 2 globin chains of hemoglobin.

The incorporation of organic solvents into the BGE was yet another alternative to inhibit adsorption. Following the findings by Deterding et al. [80], apolipoproteins A-I and A-II could only be characterized when 10–20% ACN was introduced into 50 mM ammonium bicarbonate buffer (pH 9.0). The addition of an organic solvent to the buffer further resolved the oxidized species of proteins. Similarly, four proteins of *S. platensis* microalgae were identified using 40 mM ammonium hydrogen bicarbonate with 50% acetonitrile and 5% isopropyl alcohol by Simo and his group [81]. In the studies by Staub et al. [75, 82], the application of a similar approach to three model proteins with variable rigidity can also be encountered in the scientific literature. The impact of ACN on protein adsorption in basic and acidic BGEs has been explored. The findings suggested that 10–20% ACN in BGE enhances the sensitivity and efficiency at basic pH for insulin, at acidic pH for growth hormone (rhGH), however, stimulates the adsorption of hemoglobin under similar settings. This indicates ACN may assist in the reversible adsorption of rigid proteins like insulin and growth hormone, while it fails to reverse the adsorption of flexible hemoglobin. Thus, authors recommended considering the use of organic solvents on a case-by-case basis.

When examining numerous review articles [69, 72, 83, 84], it is noticeable that over the years the scientific community's interest in the study of intact proteins has shifted from BFS to coated capillaries. As discussed before, CE-

MS coupling necessitates a stable coating film on the CE capillary wall in order to eliminate signal suppression by dynamic reagents. Thus, the application of physically adsorbing and covalent coatings has expanded in this field. Polybrene has been actively exploited from basic protein separations to isoform characterization, mAb analysis to glycoform profiling. For instance, single PB-layer coated capillary has been successfully utilized by Neuss et al. [85] for glycoform characterization of intact human erythropoietin by CE-ESI-TOF-MS. As a consequence, 44 glycoforms were successfully separated based on their size and the number of sialic acid groups. The approach was able to characterize 135 isoforms in total, including acetylated and oxidized forms. Attempts have been made to enhance the effectiveness of PB coating by depositing one or more polyelectrolyte layers in an effort to thicken the layer and impede adsorption more efficiently. Catai and colleagues [86] were capable of separating long time stored rhGH from its desamido form by coating the PB layer with additional polyanion poly(vinyl sulfonic acid) (pH 8.5). Using the same technique, a few years later Haselberg et al. [87] identified additional degradation products for heat-exposed rhGH. In addition, they assessed the usefulness of CZE-MS for examining the glycan profile of biopharmaceutical products using recombinant interferon-1 $\alpha$  as a reference. In three-layered PB-DS-PB-coated capillaries, ten glycoforms with variable numbers of sialic acid groups were characterized, demonstrating the effectiveness of CE-MS for the detection of protein modifications with charge variations. CE-MS analysis of human body fluids also appeared to be promising for clinical diagnosis [88, 89]. For instance, Ullsten et al. [89] examined the proteins from human plasma and cerebrospinal fluid using 15 mM ammonium formate BGE (pH 2.2). The separation was conducted using an uncommon PolyE-323 coated capillary which authors reported to demonstrate a high tolerance for complex sample matrices over the broad pH range (pH 2-10).

In the last decade, the rising number of biopharmaceuticals and biosimilars has contributed to the expansion of the intact protein analysis research. The demand to identify complex macromolecules, such as mAbs and their isoforms, required the development of reliable CE-MS settings. 2D CZE-MS of trastuzumab has been conducted by Jooss et al. [90], who identified two acidic charge variants attributed to deamidation. The first dimension was used to separate charge variants by the conventional EACA-based BGE (pH 5.7) system in uncoated capillaries, while the second dimension was employed to separate MS interfering species from the component of interest in a PVA-coated capillary. In the study of intact biopharmaceuticals, LPA-coated fused silica capillaries also have gained prominence. Han et al. [91], for example, could prove this way the feasibility of CZE-MS not only for the analysis of basic standard protein mixtures but also for the characterization of deglycosylated IgG1 and free chains of mAbs.

Although the coated capillaries have gained popularity in the last few decades for use in protein analysis, numerous established methods continue to rely on BFS capillaries. According to the summary of Haselberg et al. [83], a significant proportion (45%) of the studies (out of 94 publications) documented the use of BFS capillaries in CE-MS applications, whereas the most frequently applied coatings, PB and LPA, accounted for only 14% and 9% of the applications, respectively. A number of studies in the scientific literature compare the performance of BFS capillaries to that of their coated counterparts. However, these comparisons are often presented in an unfair manner [92-94]. The overlooked fact in these research is that the methods designed for protein analysis in coated capillaries may not necessarily be applicable to BFS capillaries, which need further adjustment of conditions (particularly pH) for optimum performance and a fair comparison.

Furthermore, since the analysis of insulin analogues is included in our studies, it is noteworthy that numerous studies with CE [95-98] and HPLC [99-102] have reported the analysis of insulin mixtures to demonstrate the applicability of a given method. While a large number of CZE applications involve BGE solutions with basic pH values (pH 6.5–9.2) to reduce protein adsorption, the use of acidic pH BGEs or capillary coatings is often disregarded.

Based on the survey of the literature about intact protein analysis using CZE-MS the goals of my PhD research are:

- study of the separation parameters for BFS, PB and LPA coated capillaries, enabling proper MS coupling;
- the comparison of the analytical performance obtained with different capillaries;
- investigation of CE-UV and CE-MS sensitivities attainable for simple and complex protein mixtures;
- application of the proposed CZE-MS methods for pharmaceutical and biological samples.

### 3. Experimental Section

#### 3.1 Chemicals

All chemicals were of analytical grade. The following chemicals were purchased from Sigma Aldrich (St. Louis, MO, USA): formic acid (FA), acetic acid, ammonia, ammonium acetate (NH<sub>4</sub>Ac), acetonitrile, 2-propanol (IPA), 3-(trimethoxysilyl)propyl methacrylate, sodium hydroxide, hydrochloric acid and methanol. The compounds used throughout the PB and SMIL coating production hexadimethrine bromide (polybrene, PB) and dextran sulfate (DS) were acquired from Sigma Aldrich and Merck Millipore (Darmstadt, Germany), respectively. Tris-HCl, N,N,N',N'-tetramethyl ethylenediamine (TEMED), ammonium persulfate, and acrylamide were obtained from Sigma Aldrich to be utilized in the LPA coating generation. For the latter coating procedure, a polymerization solution containing 1 mL of degassed, 4% m/m acrylamide dissolved in Tris-HCl (pH = 7.0), 1  $\mu$ L of TEMED, and 10  $\mu$ L of 10% m/v ammonium persulfate solution (aqueous) was employed. For the preparation of aqueous solutions, deionized water (Millipore Synergy UV) was used. Prior to use, BGEs were degassed in an ultrasonic bath for five minutes and filtered via membrane filters with pore sizes of 0.45  $\mu$ m. The stock solutions were kept at +4 °C. Unless otherwise stated, before its initial usage, the BFS capillary was rinsed using 1 M NaOH for 18 min, acetone for 6 min and BGE solution for 20 min.

#### 3.2 Samples

Human serum albumin (HSA), human hemoglobin, lysozyme from chicken egg white, myoglobin from horse muscle tissue, thyroglobulin from bovine thyroid were purchased from Sigma Aldrich in lyophilized powder form (St. Louis, MO, USA). Insulin solutions of 100 units/mL (3.47 mg/mL)

concentration comprised human insulin (Humulin R) and lispro (Humalog) obtained from Lilly (France), glargine (Lantus) and glulisine (Apidra) by Sanofi (France), aspart (Novorapid), degludec (Tresiba), and detemir (Levemir) by Novo Nordisk (Denmark). Snake venom sample (*Naja melanoleuca*, #304) used in the comparative study has been provided by Dr. Vladimir Petrilla from the Department of Biology and Physiology, University of Veterinary Medicine and Pharmacy, Kosice, Slovakia.

### **3.3 Instrumentation**

#### **3.3.1 CE**

The CE 7100 System (Agilent, Waldbronn, Germany) was used to perform CE separations. Unless otherwise specified, fused silica capillaries (50  $\mu\text{m}$  I.D. and 370  $\mu\text{m}$  O.D., Polymicro, Phoenix, AZ, USA) with the length of 65 cm (effective length ( $L_{\text{eff}}$ ): 57 cm for UV) were chosen for the analyses with UV as well as MS detection. A 200 nm detection wavelength was selected for UV on-capillary detection. A sample introduction has been always performed hydrodynamically (50 mbar, 2 s) at the cathodic end of the PB, SMIL coated capillaries and at the anodic end of the BFS and LPA coated capillaries. The separation voltage was found to be optimal as +20 kV for BFS, +30 kV for LPA and -30 kV for PB and SMIL capillaries. The current values in uncoated and coated capillaries did not appear to exceed 30  $\mu\text{A}$  during CE-MS analyses. A nitrogen cylinder was utilized for the high pressure (max. 8 bar) rinsing. The operation of the CE instrument and the interpretation of the collected data have been accomplished by OpenLAB CDS Chemstation software (version B.04.02, Agilent).

### 3.3.2 ESI-QTOF-MS

The MS analysis was carried out via the MaXis II Ultra High-Resolution ESI-QTOF MS (Bruker, Karlsruhe, Germany) instrument. By the use of the co-axial ESI sprayer interface (G1607B, Agilent), CE and MS coupling has been made possible. The sheath liquid, which contained isopropyl alcohol and water (1:1) with 0.1% v/v FA (at 0.7  $\mu$ L/min flow rate), was delivered using a 1260 Infinity II isocratic pump (Agilent). External mass calibration was conducted on MS analyses using ESI-MS Tuning mix (part number: G2431A, Agilent) and on MS/MS analyses using Na-formate calibrant solutions. Background correction has been applied to electropherograms. The MS electrospray ion source settings for the five protein mixture analyses were as follows: capillary voltage: 4.5 kV; end plate offset: 500 V; nebulization pressure: 0.5 bar; dry gas temperature: 220 °C; dry gas flow rate: 8.0 L/min; MS scan range: 500-2400 m/z; spectra rate: 1.5 Hz. The following parameters have been applied throughout the analysis of human insulin and its analogues: capillary voltage: 4.5 kV; end plate offset: 500 V; nebulization pressure: 0.3 bar (following 500 s no pressure application after sample introduction); dry gas temperature: 200 °C; dry gas flow rate: 4.0 L/min; MS scan range: 600-2500 m/z; spectra rate: 3 Hz. The mass resolution for the insulin formulations were in the range of 65000-94000. MS/MS settings were tuned in a following way: mass scan range: 20-1800 m/z; spectra rate: 1 Hz; collision energy (CID): 45 eV. As a precursor ion, the most abundant charge state (5+) was selected. The measurements were monitored through otofControl software version 4.1 (build: 3.5, Bruker) and evaluated using Compass DataAnalysis software version 4.4 (build: 200.55.2969).

### 3.4 Capillary coatings

#### 3.4.1 Single-layer PB and SMIL-PB coated capillaries

Prior to the preparation of the PB coating layer, silanol groups were deprotonated by 1 M NaOH solution rinsing for 20 min. Following the water wash for the next 20 min, the capillary was further flushed with 10% w/v PB solution and BGE for 30 and 40 min, respectively [103]. Washing of the capillary has been achieved at 1 bar of pressure. Single-layer PB coated capillaries demonstrated considerable bleeding, necessitating the coating regeneration. The latter has been achieved by 5 min rinsing of the capillary with PB and BGE solutions following each run. During the coating regeneration, the CE capillary was detached from the ESI chamber. Despite the PB bleeding, there was no discernible ionization suppression or increased background signal [104].

The process reported by Haselberg et al. [105] was implemented to generate SMIL coating. 10% (m/v) PB and 3% (m/v) DS were employed as coating solutions after being filtered. Following the capillary rinsing with 1 M NaOH for 30 minutes and water for 15 minutes, the three ionic layers of the coating are produced by the following sequential capillary flushing at 1 bar: 20 min PB, 10 min water, 20 min DS, 10 min water, 20 min PB and 10 min water. The capillary did not involve an incubation period and could be utilized in a CZE analysis immediately afterwards. A 3-minute BGE preconditioning was conducted between runs. After being inactive overnight, the coating was activated with a 5-minute water and 5-minute BGE rinse, followed by a 10-minute application of +10 kV to the inlet electrode. Capillary then was rinsed with water for 10 min and stored with both ends submerged in water.

### 3.4.2 Preparation of linear polyacrylamide coating

The LPA coating was generated relying on the suggested technique by Hjerten [93]. Freshly cut capillaries were successively flushed at 60°C as follows: acetone (1 min, 6 bar), 1 M NaOH (5 min, 6 bar), deionized water (1 min, 6 bar), 1 M HCl (5 min, 6 bar), deionized water (1 min, 6 bar) and acetone (3 min, 6 bar). By applying nitrogen flow, the capillaries were dried (30 min, 6 bar). Later, the silane mixture, containing 3-(trimethoxysilyl)propyl methacrylate and acetonitrile in a 1:1 ratio, was injected (5 min, 3 bar) into the capillary. The capillary was then left at 60 °C immersed in the reagent for an hour. Later, the capillary was flushed with acetone (2 min, 2 bar, 25 °C) in order to remove the unbound silane and dried by nitrogen flow (30 min, 6 bar). Subsequently, LPA polymerization solution was introduced in the capillary (5 min, 6 bars) and it was stored at 50 °C overnight. Capillaries could be used after manually removing excess polymer solution with water the next day. For storage, LPA capillaries were washed with water (10 min, 1 bar) and kept submerged in water vials. Each run's preconditioning included a 5-minute flushing phase with a running buffer (1 bar). No usage of organic solvents or aqueous solutions with pH values between 2 and 8 were permitted.

## **4. Results and discussion**

### **4.1 Analysis of protein mixtures in different capillaries**

#### **4.1.1 Analysis in BFS capillary**

In the scientific literature BFS capillaries have been widely reported for analyses of proteins, while they are often reported to cause protein adsorption and irreproducible outcomes. Thereby, we closely studied the impact of various parameters on the analytical performance of BFS capillaries. With the aim of investigating whether intact proteins could be separated in BFS capillaries, BGEs of "extreme" pH values (pH = 1.8 and 10.8) and frequently preferred moderate pH values (pH = 6.8 and 9.6) have been examined. At very low pH values, as a result of utterly protonated silanol groups, a neutral silica surface is produced. Proteins, meanwhile, gain a significant net positive charge due to possessing pI values far above the empirical pH. In contrast, BGE with a rather high pH value, initiates the entire deprotonation of the silanol groups, leaving the capillary wall with negative charges. In this settings, proteins possess large negative charges as well. In either scenario, given the presence of repulsive forces between the proteins and the capillary surface, narrower protein peaks were predicted to be obtained due to the restricted adsorption. As a matter of fact, the acquisition of the narrowest insulin and HSA peaks at pH = 1.8 and in contrast, less intense, tailed peaks with a larger width at moderate pH values due to the possible electrostatic and hydrophilic interactions, justified the expectations (Fig.4).

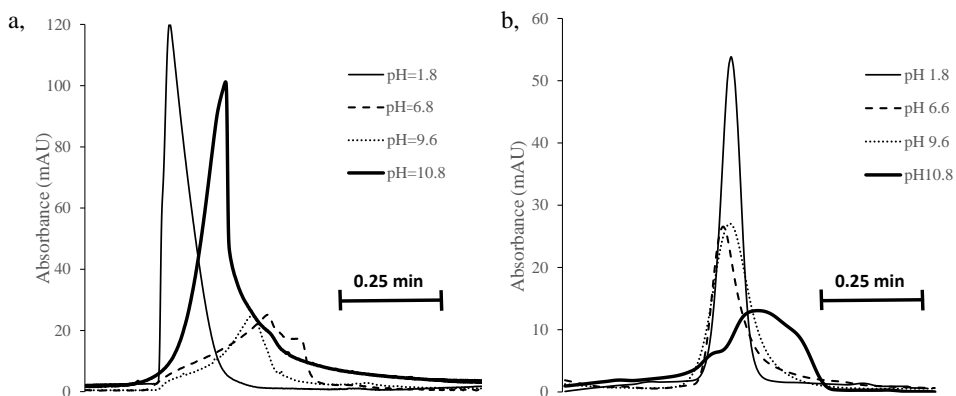


Figure 4. (a) human insulin and (b) human serum albumin (0.5 mg/mL concentration each) peaks recorded by CE-UV at various pH values (only the segments of the electropherograms are shown). Capillary  $L_{eff}$ : 23 cm; separation voltage: +20 kV; BGE: 1 M FA (pH 1.8), 50 mM  $NH_4Ac$  (pH 6.8 and 9.6), 100 mM  $NH_4OH$  (pH 10.8); conditioning: rinsing with 1 M NaOH (5 min), water (2 min) and BGE (5 min).

Yet, rather extreme pH may induce protein denaturation or/and precipitation. In the latter scenario, species produce markedly distorted peak patterns as a consequence of asymmetric sample zone migration. Similarly, small and irregular peak morphologies acquired at pH 10.8 could be attributed to protein coagulation. It becomes clear from Fig. 4 that only in the case of a low pH milieu an adequate number of theoretical plates could be reached in both small (insulin, pI: 5.35; Mr: 5.8 kDa) and large protein (HSA, pI: 4.7; Mr: 66 kDa) examples. In the case of insulin, the plate numbers were at least a magnitude higher at lower pH values than the plate numbers obtained at pH values over 3. These findings are consistent with the previous studies discussed in the academic literature [79]. As previously outlined in chapter 2.5.3, BFS capillary protein separation at various BGE solutions (ortho-phosphate, acetic, propionic and formic acid) has been accomplished by Stutz et al. [79], where they

also deduced that 1M FA exhibited the highest relevance for optimal peak efficiency and resolution.

A right-angled peak distortion can also be observed for human insulin even at  $\text{pH} = 1.8$ , whereas the HSA peak appears as a narrow symmetrical peak. The right-angled peak morphology of insulin may be due to a mismatch in the electrophoretic mobilities of the solute and the electrolyte ion, which is usually referred to as electrodispersion. The similar fronting peak shape of insulin was also recorded by others [106]. For small components, this phenomenon is commonly investigated; however, it has not been addressed for proteins. Yet, reducing the analyte concentration can effectively minimize the effects of both electrodispersion as well as overloading. Indeed, the peak distortion of insulin was suppressed following 125-fold dilution, increasing the number of theoretical plates from 27000/m to 243000/m (Fig. 5).

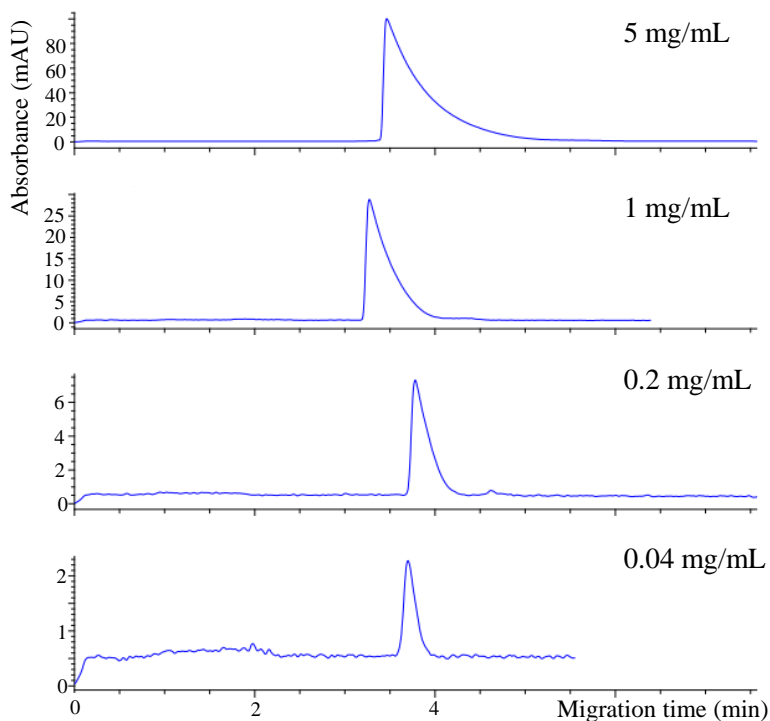


Figure 5. Insulin analyses at varying concentrations. Capillary  $L_{\text{eff}}$ : 23 cm; separation voltage: +20 kV; BGE: 1 M FA ( $\text{pH} 1.8$ ); conditioning: rinsing with 1 M NaOH (5 min), water (2 min) and BGE (5 min).

When the pH value approaches the isoelectric point of the protein (particularly, for insulin at pH 6.8), analyte adsorption and hence capillary surface alterations become inevitable. As a result, EOF mobility changes and further adsorption of components from subsequent samples proceeds, resulting in distorted peak morphologies (Fig. 4).

In our investigation, the examined standard mixture included proteins ranging in size, with insulin being the smallest and albumin being the largest. The adsorption behavior of these two proteins of varying sizes has been compared with that of a small component (imidazole) in Figure 6.

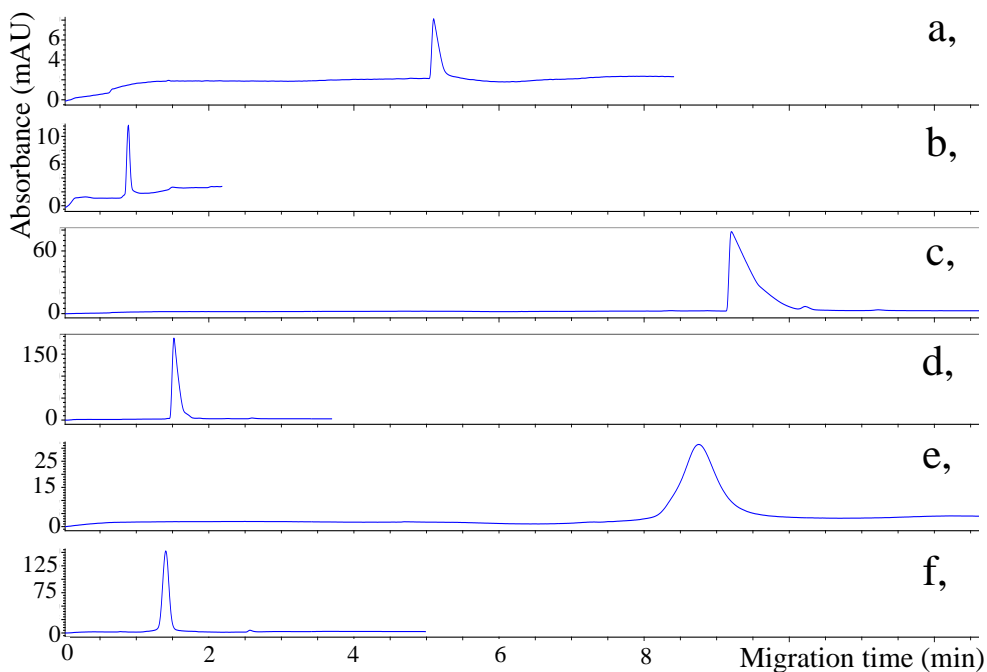
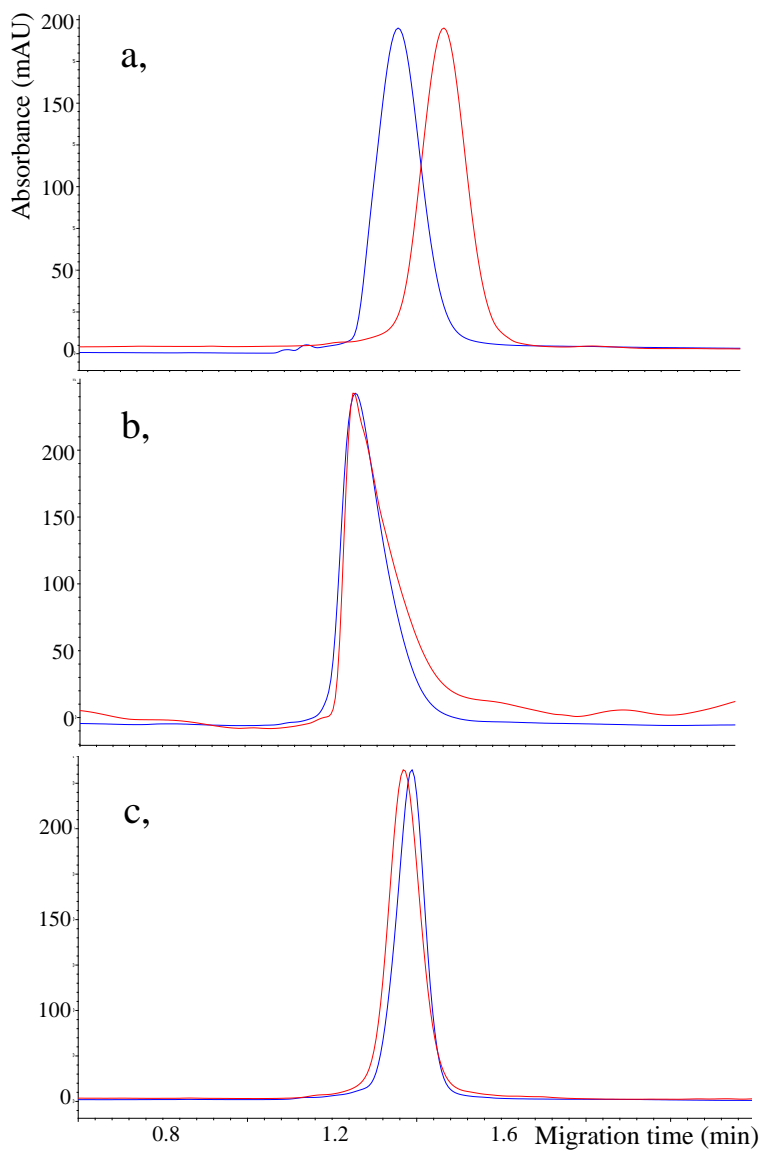


Figure 6. CE-UV measurements of (a, b) imidazole, (c, d) human insulin, and (e, f) thyroglobulin in (a, c, e) a long –  $L_{eff}$ : 57 cm - and (b, d, f) a short -  $L_{eff}$ : 8 cm – capillary. Separation voltage: +25 kV; BGE: 1 M acetic acid (pH 2,5); conditioning: MeOH (5 min), 1 M NaOH (5 min), water (2.5 min), 1 M HCl (5 min), BGE (15 min).

Generally, the bulkier proteins are thought to have a greater propensity for adsorption since they feature more amino acid groups that may readily interact with charged surfaces [107]. However, it is shown in Fig. 6 (e, f) that even large proteins, such as thyroglobulin (Mr: 660-690 kDa, pI = 4.5), can produce rather narrow peak shapes. They are reminiscent of the insulin peaks (Fig 6. c, d) in both capillaries, with short and long effective lengths. The extension of the separation length contributed to the peak broadening of small and large proteins at a similar extent. Although imidazole peak also demonstrates a slight broadening in the longer capillary, it is not to the comparable extent as proteins.

Yet, besides a right pH, another major element to mitigate adsorption was a thorough washing of the capillary inner wall following each separation. Even when very low pH BGE is applied, vigorous capillary prerinsing with a strong base (usually 1 M NaOH was used), and/or a strong acid (e.g., 1 M HCl or FA), appeared to improve precision values. The impact of capillary conditioning was investigated by analyzing thyroglobulin in non-conditioned, 2-step (with 1M HCl and BGE) conditioned, and 5-step (with MeOH, 1M NaOH, water, 1M HCl, and BGE) conditioned capillaries (n = 20). Compared to non-conditioned capillary separation, proper conditioning (5-step conditioning) reduced the RSD% for the migration time of thyroglobulin from 5.3% to 0.8% and for peak areas from 6.3% to 2.7% (Fig. 7).



*Figure 7. The comparison of different conditioning procedures for thyroglobulin analysis in BFS capillary: blue line depicts the 1st and red line depicts the 20th measurements. Capillary  $L_{\text{eff}}$ : 8 cm; separation voltage: +20 kV; BGE: 1 M formic acid (pH 1.8); (a) no conditioning; (b) 2-step conditioning: 1M HCl (8 min), BGE (2 min); (c) 5-step conditioning: MeOH (5 min), 1 M NaOH (5 min), water (2.5 min), 1 M HCl (5 min), BGE (15 min).*

Our regular capillary treatment to separate simple protein mixtures (Table 2) with CE-UV also involved a long rinsing procedure with 18 min of 1M NaOH, 6 min of acetone and 20 min of BGE sequential washing (3-step conditioning) at 1 bar pressure. Nevertheless, during the protein separation at moderate pH values, the suggested long conditioning procedure was unable to reduce the arising migration time shifts and wide peak areas. Given that the adsorption behavior of analytes varies in line with their pI and the pH of the separation buffer, at neutral pH, some proteins readily adsorb (Fig. 8), making it harder to receive a symmetric analyte signal (if any) [37, 72].

*Table 2. The theoretical molecular masses and the isoelectric points (pI) of the studied protein standards(based on Sigma Aldrich information sheets).*

<b>Sample proteins</b>	<b>Mass (Da)</b>	<b>pI</b>
lysozym	14307	11.35
human serum albumin	66437-66600	4.7
myoglobin	16951.49	7.3
hemoglobin ( $\alpha$ )	15126.4	6.9
insulin	5867.2	5.35
thyroglobulin	660000-690000	4.5

The proteins in the 5 protein mixture are well-known, commonly and often used proteins, those were also easily available in our lab. We selected these proteins for our studies since these proteins exhibit different mass, pI values (Table 2), dynamic structures and MS responses. As the proteins with comparable properties (similar pI or molecular mass) may not always be present in the actual biological or pharmaceutical samples, the developed CE-MS method for selected proteins exhibit a wide application range.

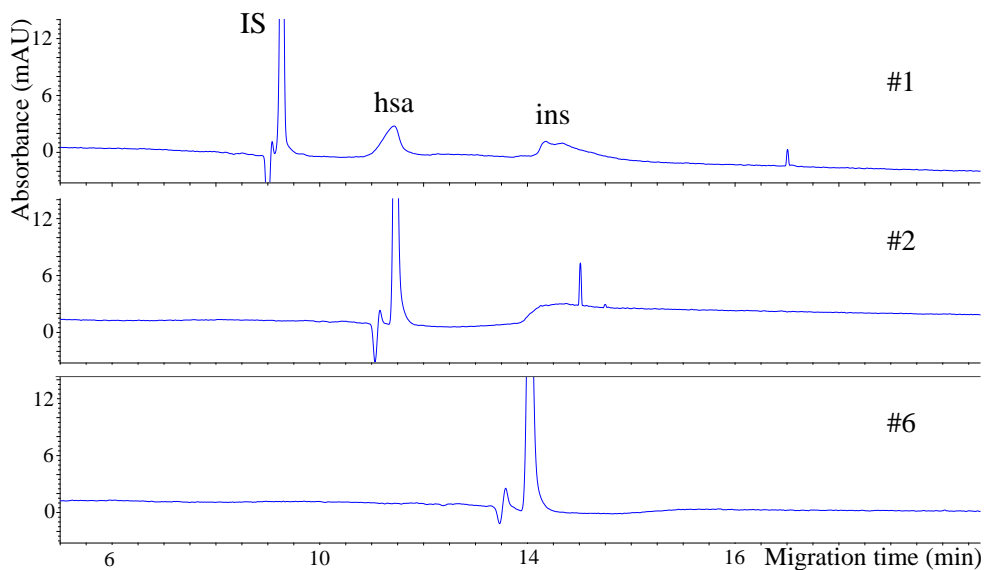


Figure 8. The separation of 5 protein mixture in neutral conditions ( $pH=6.8$ ) using BFS capillary. Capillary  $L_{eff}$ : 57 cm; separation voltage: +20 kV; BGE: 50 mM  $NH_4Ac$  ( $pH 6.8$ ); 3-step conditioning: 1 M NaOH (18 min), acetone (6 min), BGE (20 min); IS: *m-cresol*.

While performing at  $pH 9.6$ , lysozyme as an alkali protein ( $pI = 11.35$ ) with a positive net charge (similar to  $pH 6.8$ ) (Fig. 9), is strongly driven to the oppositely charged capillary surface electrostatically and adsorbed. As a result, the lysozyme peak was not observed in the electropherogram. In the meantime, the remaining proteins demonstrate an adsorption propensity through the repetition, lowering the separation efficiency and precision results.

The proteins in the 5 protein mixture are well-known, commonly and often used proteins, those were also easily available in our lab. We selected these proteins for our studies since these proteins exhibit different mass,  $pI$  values (Table 1), dynamic structures and MS responses. As the proteins with

comparable properties (similar pI or molecular mass) may not always be present in the actual biological or pharmaceutical samples, the developed CE-MS

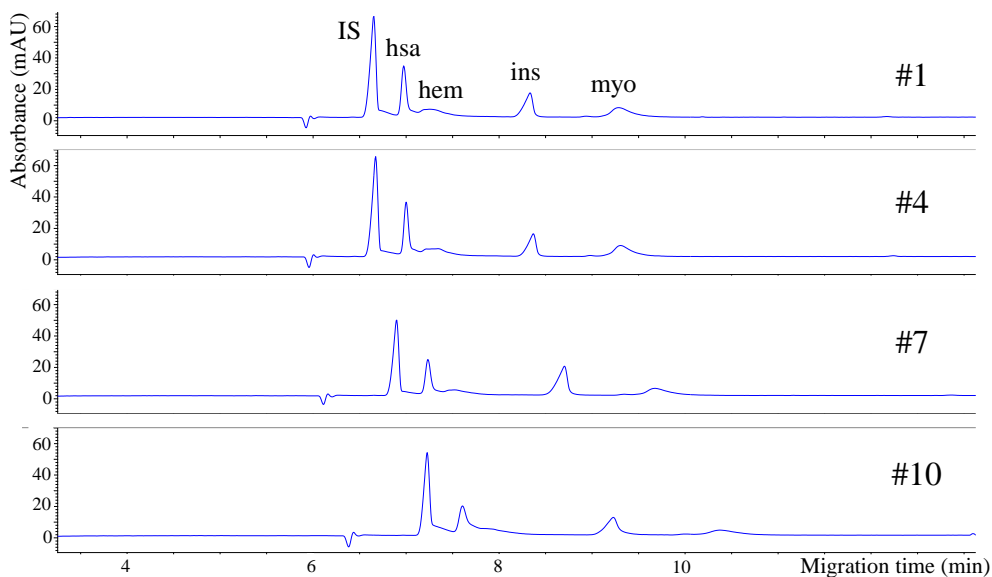


Figure 9. The separation of protein mixture at basic conditions ( $pH=9.6$ ) using BFS capillary. Capillary Leff: 57 cm; separation voltage: +20 kV; BGE: 50 mM  $NH_4Ac$  ( $pH$  9.6); 3-step conditioning: 1 M NaOH (18 min), acetone (6 min), BGE (20 min); IS: *m*-cresol.

Combining the aforementioned capillary conditioning procedure with 1 M FA separation buffer at  $pH$  1.8 for protein analysis produced efficient and highly reproducible separation even in uncoated capillaries (Fig. 10). The analysis revealed that the precision data for migration time was lower than 1 RSD%, while for peak areas, better than 4 RSD% (excluding hemoglobin) was obtained.

The first electropherogram of repetition typically appeared to exhibit smaller migration time shifts, because of which the first analysis is proposed to be treated as a preconditioning run. Therefore, the first run was not ad-

dressed in the precision calculations. Through the repetitions, hemoglobin exhibits a notable peak area decline that is assumed to be attributed to the subtle changes in protein rather than adsorption. Insulin peak exhibits a wide peak area, which has been shown to be vastly reduced by further dilution. Electropherograms are often normalized in order to acquire high-quality precision data. Since BFS capillary analyses at low pH already resulted in acceptable RSD% values, there was no need for normalization. At neutral and basic pH, however, two time reference points for migration time normalization were necessary. Yet, the normalization did not improve the peak area precision below 6% RSD% (Fig. 9).

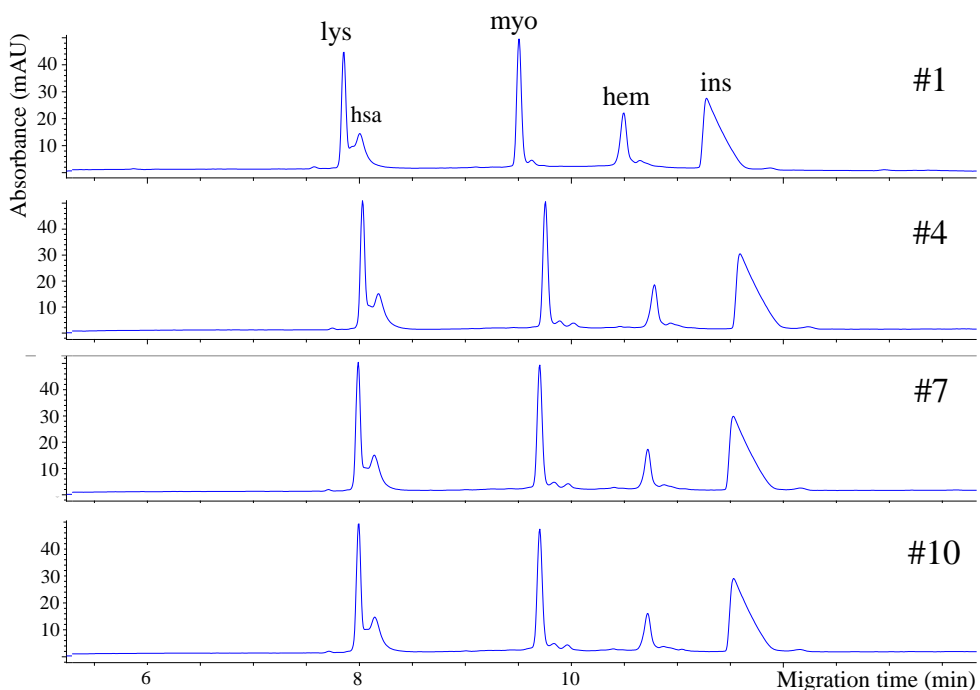


Figure 10. BFS capillary separation of 5 protein mixture. The repetitions are reflected by the 1st, 4th, 7th and 10th electropherograms. Capillary  $L_{\text{eff}}$ : 57 cm; separation voltage: +20 kV; BGE: 1 M FA (pH 1.8); 3-step conditioning: 1 M NaOH (18 min), acetone (6 min), BGE (20 min); sample: 0.5 mg/mL lysozyme (lys), human serum albumin (hsa), insulin (ins), 1 mg/mL hemoglobin (hem) and myoglobin (myo).

As the detection technique changes from UV to MS, the following system parameters become affected: (1) detection sensitivity degrades and (2) off-capillary MS detection reduces the separation efficiency. On the other hand, in ESI, the proteins generate mass spectra with different numbers of charge states and adducts, resulting in distinct detection responses (Fig. 11), whereas UV detection is restricted to revealing the similar spectra for all proteins. HSA, for example, produced more than 40 charge states (they were too ambiguous to identify), while insulin was present only in 3 charged forms. As proteins form a higher number of charge states, the signal intensity for a given analyte peak reduces. Following a proper deconvolution, based on the charge numbers and  $m/z$  values given by the software, the accurate mass of the analytes could be obtained (Table 3).

A minor (~1-5%) loss in separation efficiency during MS detection is commonly encountered as a result of laminar flow induced by a slight vacuum at the CE capillary outlet end in the ESI interface. This phenomenon is referred to as the "siphon effect", which affects all components (proteins) independent of the capillaries (coated or uncoated) utilized. It could, however, be diminished by turning the nebulization pressure in the ESI interface off during sample introduction and the first several minutes of the electrophoretic run (20–30 s prior to the detection of the first analyte) [108].

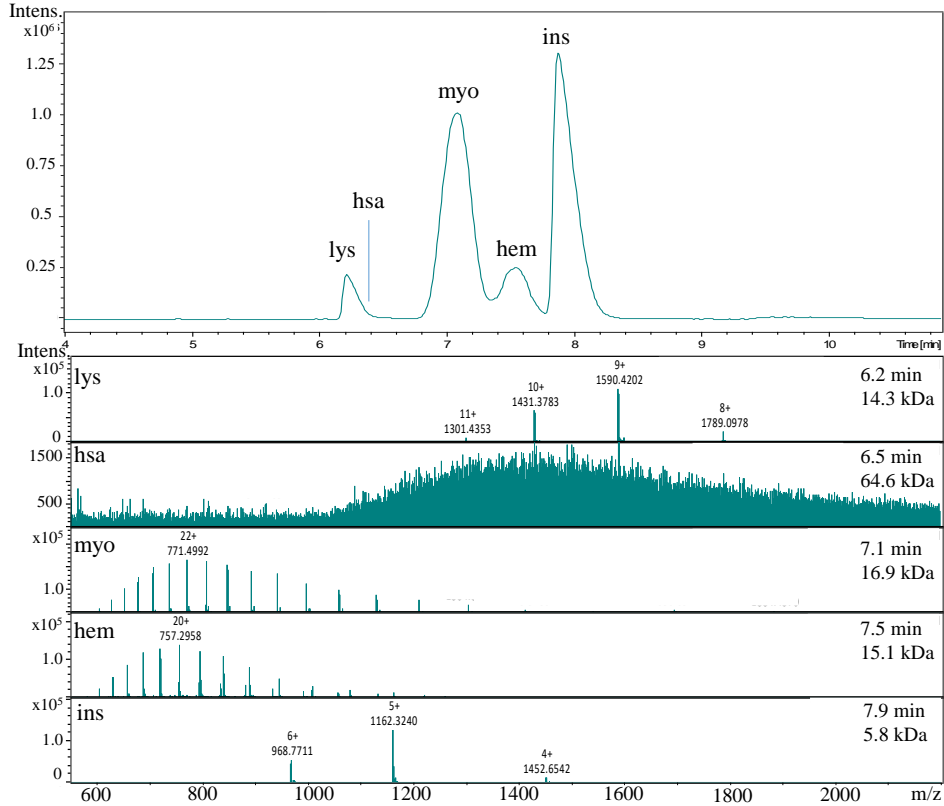


Figure 11. CZE-MS analysis of a protein mixture. (a) A base peak electropherogram and (b) mass spectra of separated proteins. Capillary: 90 cm; separation voltage: +20 kV; BGE: 1 M FA (pH 1.8); 3-step conditioning: 1 M NaOH (18 min), acetone (6 min), BGE (20 min); capillary voltage: 4.5 kV; end plate offset: 500 V; nebulization pressure: 0.5 bar; dry gas temperature: 220 °C; dry gas flow rate: 8.0 L/min; MS scan range: 500-2400 m/z; spectra rate: 1.5 Hz.

Table 3. The theoretical and experimentally obtained molecular masses ( $M$ ) of the studied protein standards. The theoretical values were obtained from Sigma Aldrich.

peak #	t (min)	m/z [M+H] <sup>+</sup>	M (theor.), Da	M (exp.), Da	protein
1	6.21	1590.309	14307	14304.78	lysozyme
2	6.49	1396.8023	66437-66600	64614.63	HSA
3	7.09	771.4992	16951.49	16950.98	myoglobin
4	7.55	757.2957	15126.4	15125.91	hemoglobin $\alpha$
		794.3643	15867.2	15867.28	hemoglobin $\beta$
5	7.87	1162.3241	5807.72	5806.62	insulin

#### 4.1.2 Analysis in coated capillaries

##### 4.1.2.1 Analysis in PB-coated capillary

The performance of semi-static PB, SMIL and static LPA-coated capillaries for the protein separation has been examined. Each CZE separation parameter has been optimized for intact protein analysis by considering the use of MS-compatible electrolytes and washing solutions. In the case of PB-coated capillary, PB agent generates a positively charged layer on the silica surface that is independent of the pH, induces the anode-directed EOF. In these settings, acidic pH electrolytes appear to be the proper choice in order to separate the components bearing a net positive charge. In line with previous studies, 1 M AA (pH = 2.5) proved to be adequate for PB-coated capillary separations [92, 103]. The separation performance of PB-coated capillary has been depicted in Figure 12.b. The electropherogram exhibits the presence of an EOF marker prior to protein peaks, where the proteins appear in the exact reverse order of that in the BFS capillary. The migration direction also appears to be against the EOF, leading to longer analysis time. The latter, in its turn, produced broadened peak areas and therefore equivalent or inferior results com-

pared to BFS performance (Fig. 12.a). For instance, while the resolution between hemoglobin and myoglobin peaks in BFS capillary reached 4.12, in PB-coated capillary it was 3.21.

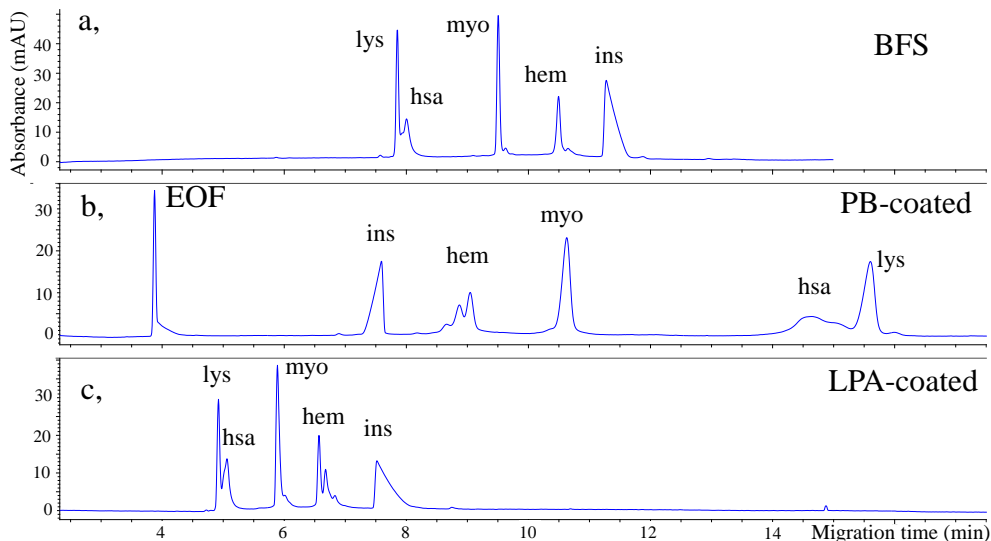


Figure 12. (a) BFS, (b) PB-coated and (c) LPA-coated capillary separation of a protein mixture. Capillary Length: 57 cm; (a) separation voltage: +20 kV; BGE: 1 M FA (pH 1.8); 3-step conditioning: 1 M NaOH (18 min), acetone (6 min), BGE (20 min); (b) separation voltage: -30 kV; BGE: 1 M acetic acid (pH = 2.5); preconditioning: polybrene (5 min) and BGE (5 min); postconditioning: BGE (5 min). (c) separation voltage: +30 kV; BGE: 50 mM FA (pH 2.6); conditioning: BGE (5 min).

However, PB-coated capillary was more effective at resolving several components, namely, the various proteoforms of hemoglobin. In particular, the separation of hemoglobin globin chains ( $\alpha_a$  and  $\beta_a$  with M of 15125 Da and 15867 Da, accordingly) as well as a few unrecognized proteoforms have been achieved in this capillary (Fig. 13). Globin chains separation of hemoglobin in PB-coated capillary has also been disclosed elsewhere [92]. The same number of hemoglobin proteoforms could be separated using both UV and MS detection techniques, despite the number of theoretical plates with on-line UV detection being relatively higher ( $N = 36\,000/m$ ) than with MS ( $N = 30\,000/m$ ).

However, MS detection was the one that could identify the various forms (Fig.14).

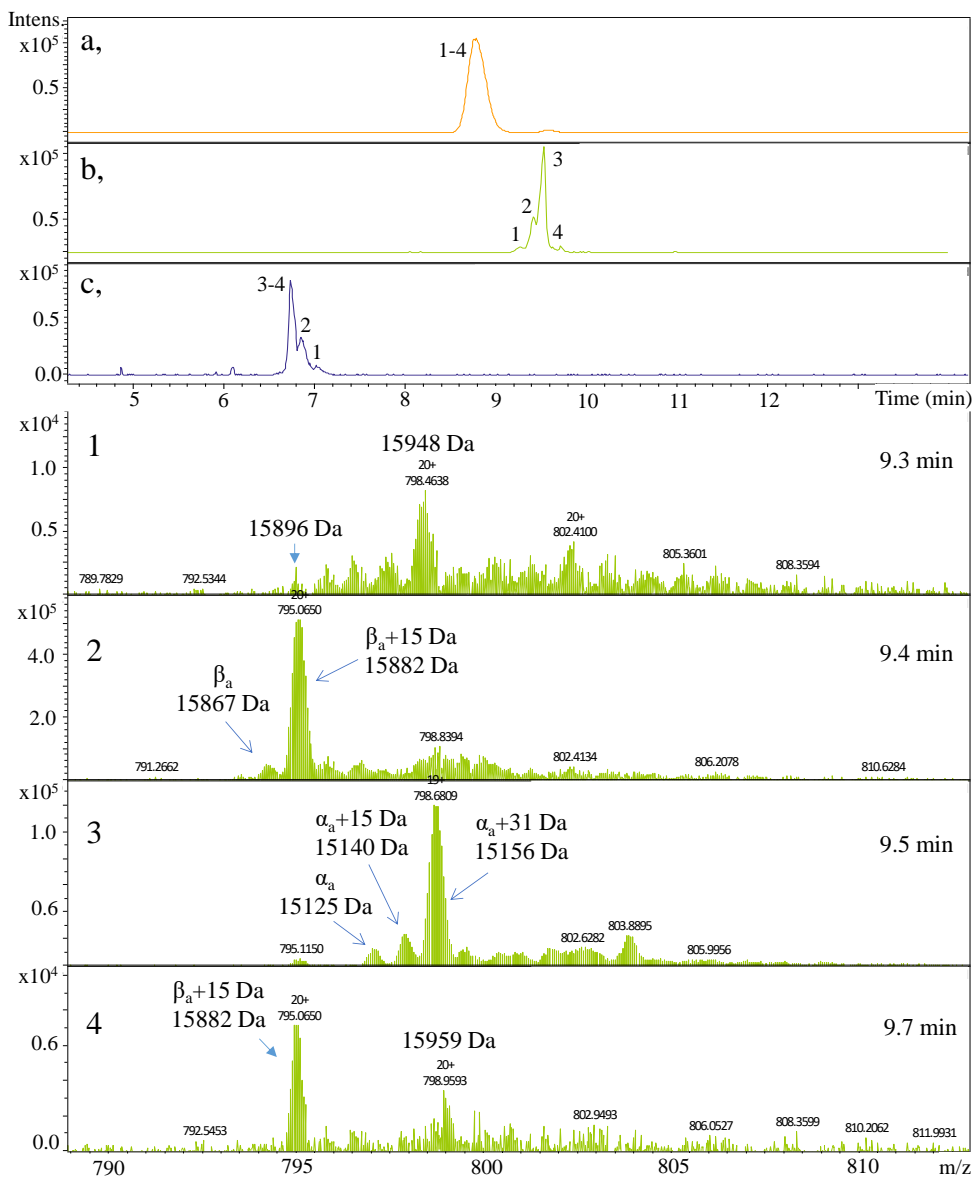


Figure 13. Hemoglobin analysis in (a) BFS, (b) PB-coated and (c) LPA-coated capillaries using CZE-MS. 1-4 indicate the spectra from (b). Sample: 5 mg/mL hemoglobin; capillary voltage: 4.5 kV; end plate offset: 500 V; nebulization pressure: 0.5 bar; dry gas temperature: 220 °C; dry gas flow rate: 8.0 L/min; MS scan range: 500-2400 m/z; spectra rate: 1.5 Hz; the identical CZE conditions as in Fig. 12 were applied.

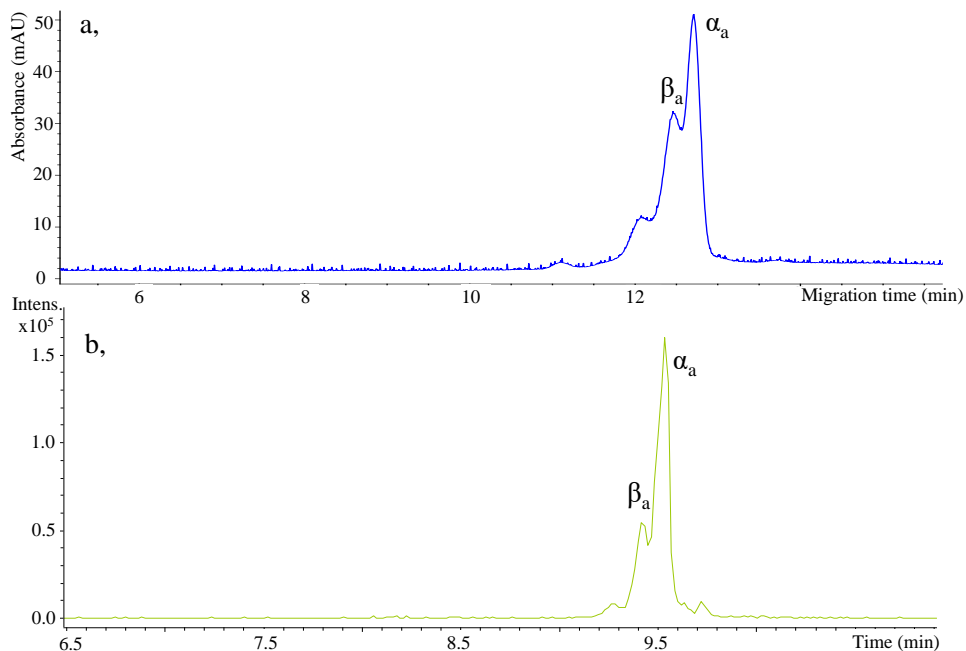


Figure 14. The separation of hemoglobin subunits in PB-coated capillary using (a) UV and (b) MS detection. (a) Capillary  $L_{\text{eff}}$ : 57 cm; separation voltage: -30 kV; BGE: 1 M acetic acid (pH = 2.5); preconditioning: polybrene (5 min) and BGE (5 min); postconditioning: BGE (5 min); (b) capillary: 65 cm; the rest of the CZE parameters are same as in (a); capillary voltage: 4.5 kV; end plate offset: 500 V; nebulization pressure: 0.5 bar; dry gas temperature: 220 °C; dry gas flow rate: 8.0 L/min; MS scan range: 500-2400 m/z; spectra rate: 1.5 Hz.

A healthy adult human hemoglobin (HbA) is a tetramer protein composed of non-covalently bound two  $\alpha$  and two  $\beta$  chains. Each subunit (globin chain) contains a heme prosthetic group ( $\text{Fe}^{2+}$  protoporphyrin IX) that can be liberated during the autoxidation of Hb to produce methemoglobin ( $\text{Fe}^{3+}$  protoporphyrin IX ligated to  $\text{OH}^-$ ) [109]. Acquired masses in the MS spectra (Figure 13.2,3) for the  $\alpha$  and  $\beta$  subunits correspond to heme-free masses known as apo-subunits ( $\alpha_a$  and  $\beta_a$ ). Throughout a human's life (as an embryo, fetus or adult), distinct globin chains with slightly variable amino acid compositions

dominate. For instance, embryonic hemoglobin (Hb Gower 1, Gower 2) contains  $\zeta$  or  $\epsilon$  subunits, fetal hemoglobin (HbF) contains  $\gamma$ , and a small amount of hemoglobin (HbA<sub>2</sub>) contains  $\delta$  subunits in late adulthood. The further substitution of amino acids in a globin chain (most commonly in the  $\beta$  chain) may lead to the formation of mutant Hbs or hemoglobinopathies [110], which may be indicative of an underlying illness. The most prevalent of these abnormalities are HbS, HbE, and HbH, which correlate to sickle cell disease, hemolytic anemia, and thalassemia, respectively. The masses determined by Hb analysis in PB-coated capillaries do not correspond to the masses of these variations. The rarer Hb mutations are recorded in the online database (<https://globin.bx.psu.edu/hbvar/>), where over 1800 Hb variants have been reported. The same database also features instructions to locate the potential point mutations correlating to mass differences, from which the experimental subunit masses may be inferred. Using these instructions, the intensive +15 Da mass difference in the  $\alpha$  (15140 Da) and  $\beta$  (15882 Da) chains might be explained by leucine  $\rightarrow$  glutamine or isoleucine  $\rightarrow$  lysine substitution, while +31 Da mass difference (15156 Da) in the  $\alpha$  chain could be attributed to proline  $\rightarrow$  glutamine replacement. The mass differences of +29 Da (15896 Da), +52 Da (15948 Da) (Fig. 13.1), and +92 Da (15959 Da) (Fig. 13.4) do not correlate to any point mutations that instructions suggest when they are considered as a variation in the  $\beta$  chain as well.

The need for further progress in separation efficiency and stability of PB coating resulted in the emergence of the SMIL technique, where three, five or more layers of polyelectrolytes are successively coated. For protein samples, SMIL-coating proved to exhibit an outstanding separation performance [40, 111]. Our research also covered the application of a three-layer PB coating

besides one-layer PB. The trilayer coating helped enhance the precision results, in particular for migration times (Fig. 15, Table 4).

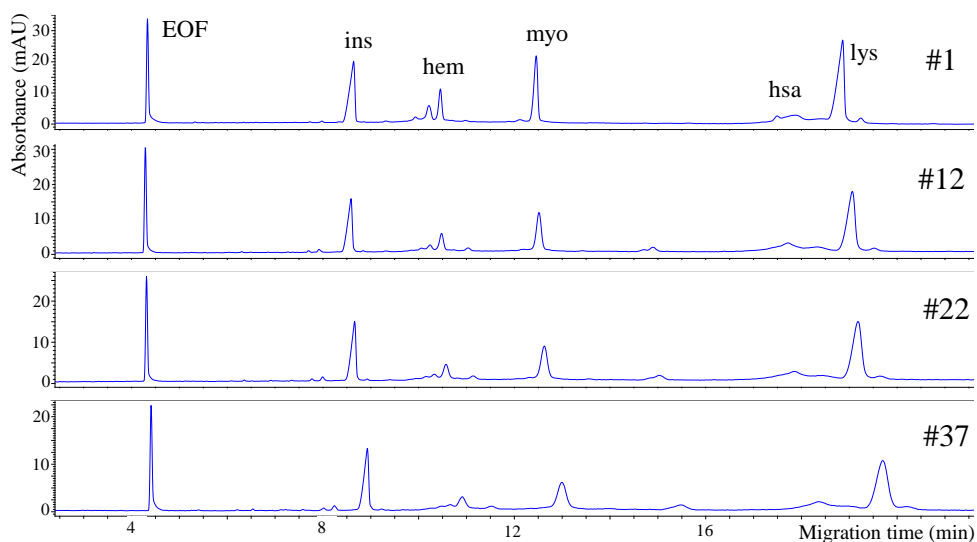


Figure 15. Separation of protein mixture in a multilayer PB-DS-PB (SMIL) coated capillary. Capillary  $L_{eff}$ : 57 cm; separation voltage: -30 kV; BGE: 1 M acetic acid (pH = 2.5); conditioning: BGE (3 min).

Table 4. Precision data obtained for proteins using single-layer and three-layer (SMIL) PB-coated capillary.

	PB-coated capillaries			
	Single-layer		Three-layer (SMIL)	
protein	RSD% (t)	RSD%(area)	RSD% (t)	RSD%(area)
lysozym	0.59	4.52	0.19	3.77
HSA	0.69	3.45	0.17	3.17
myoglobin	0.62	2.36	0.34	2.72
hemoglobin	0.75	12.7	0.39	7.87
insulin	0.69	5.54	0.38	3.49

#### 4.1.2.2 Analysis in LPA-coated capillary

As a neutral covalent coating, LPA has been verified to be effective for protein separation [23, 93, 94, 111, 112, 113, 114]. The benefits of LPA include the elimination of the need for coating renewal, the minimal interactions between the coating and the proteins, and the coating's flexibility to be manufactured in laboratories with standard facilities. However, LPA's incompatibility with BGE solutions with  $\text{pH} < 2$  and  $\text{pH} > 8$ , as well as solutions containing organic solvents, is a significant disadvantage.

The stability and capillary-to-capillary repeatability of LPA-coated capillaries have been investigated by many research groups. Bodnar et al. [94], for instance, have undertaken the protein analysis at  $\text{pH} 6.0$  in LPA-coated capillaries and compared their performance to that of BFS ( $n = 100$  in both cases) in the same analytical settings. These conditions have favored the LPA-coated capillary performance by producing good precision data (0.14-0.55 RSD% for migration times), while BFS failed to achieve adequate separation performance (8.51-14.43 RSD% for migration times). However, it should be emphasized that the comparison is not fair at the specified  $\text{pH}$ . Due to the substantial protein adsorption in BFS capillary in these conditions, sufficient separation performance cannot be anticipated.

Similar comparison in the performance of two capillaries at  $\text{pH} 2.5$  have been shown at Figure 16. Since there is no EOF in the neutral LPA-coated capillary at  $\text{pH} = 2.5$ , migration times comparable to those observed with BFS capillary are expected with LPA (Fig. 16.a, c). In the case of BFS capillary, when the similar parameters are employed (particularly capillary conditioning), due to the continuous adsorption of positively charged proteins onto the silica surface, the steady development of a counter directed EOF still could not be eliminated (Fig 16.a-g).

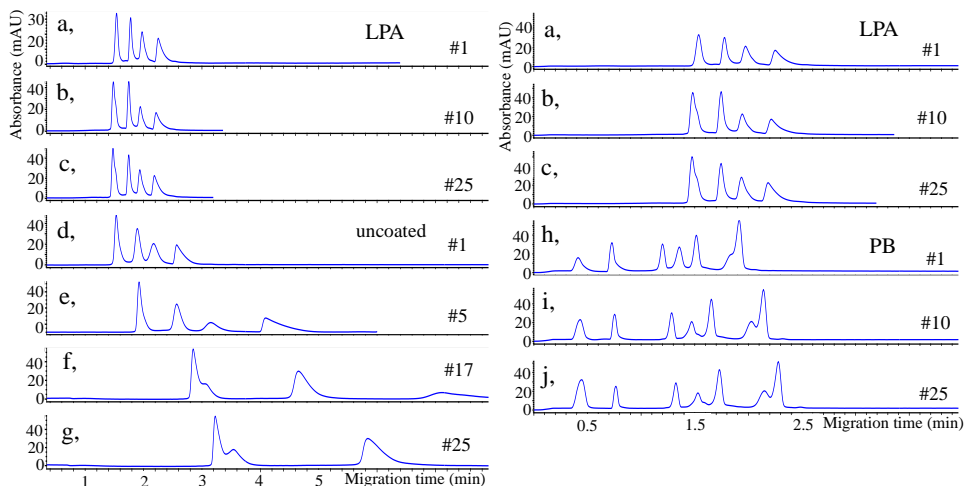


Figure 16. The comparison of repeated separations of proteins in different capillaries. Capillary  $L_{\text{eff}}$ : 25 cm; (a-c): LPA-coated capillary; separation voltage: 25 kV; BGE: 50 mM FA (pH 2.6); conditioning: BGE (5 min); (d-g): BFS capillary; separation voltage: 25 kV; BGE: 1 M FA (pH 1.8); conditioning: BGE (5 min); (h-j): PB-coated capillary; separation voltage: -30 kV; BGE: 1 M acetic acid (pH = 2.5); preconditioning: polybrene (5 min) and BGE (5 min); postconditioning: BGE (5 min).

As seen in the Figure 16.h-j, PB-coated capillaries had somewhat inferior reproducibility (for migration times it was 0.59–0.75 RSD%, while for peak areas it showed 2.4–13 RSD%), and yet no significant protein adsorption or peak widening was encountered. The noticeable migration time changes could be adequately improved if internal time reference points or triple layer (PB-DS-PB) coating (SMIL) was applied [115].

In order to achieve maximum separation, it is necessary to determine the optimal length of the capillary (65–100 cm) that guarantees adequate plate numbers as well as a coupling of CE to MS. During CE-UV analysis, a capillary must be at least 30 cm long, albeit using short-end injection, this may be reduced to 8 cm. Resolution usually improves by increasing the capillary length, but this in turn extends the analysis duration. In fact, in LPA-coated

capillary, with a length of 85 cm, the peaks of Hb subunits and also possibly myoglobin, and HSA minor components were the most clearly resolved, accompanied by a severe peak broadening (Fig. 17). Therefore, 65 cm capillary was selected as an ideal length.

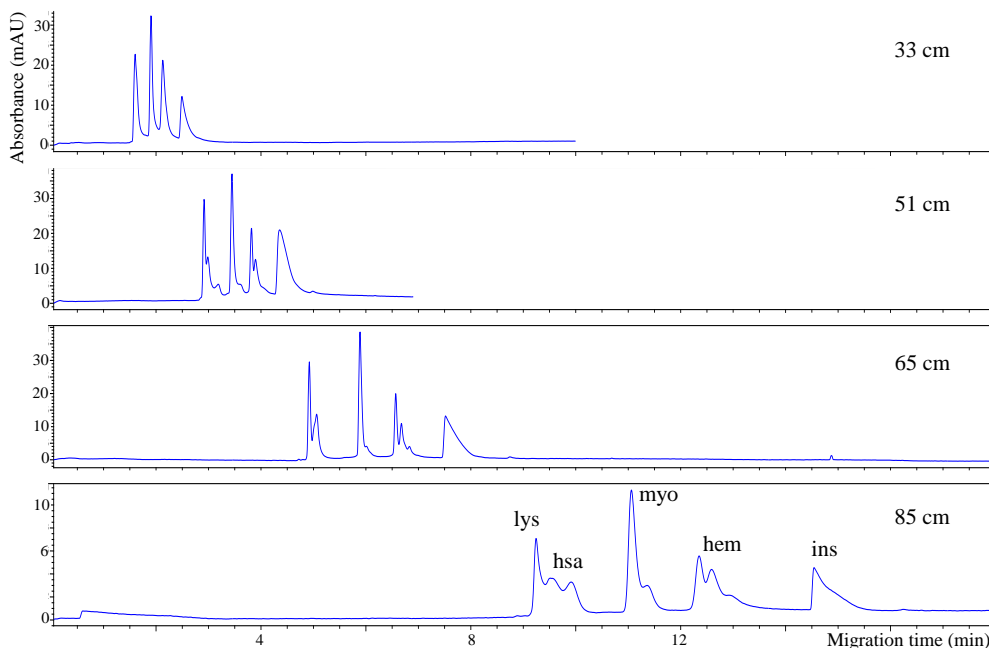


Figure 17. The comparison of protein separation in different lengths of LPA-coated capillaries. Capillary  $L_{eff}$ : 57 cm; separation voltage: +30 kV; BGE: 50 mM FA (pH 2.6); conditioning: BGE (5 min).

The resolution of the various hemoglobin proteoforms in LPA-coated capillary might be indicative of a higher separation efficiency in comparison to that achieved in BFS capillary (Fig. 12.a). Separation of the Hb proteoforms was enhanced by the use of PB-coated capillary rather than LPA-coated. As seen from Table 5, the separation efficiency data in coated and uncoated capillaries may be in a comparable range (for example, 7 000/m to 27 000/m for insulin in LPA and BFS capillaries, respectively), but can also be quite distinct (for example, 39 000/m to 322 000/m for myoglobin in PB and BFS capillaries,

respectively). Uncoated capillaries yielded the greatest number of theoretical plates. It is noteworthy that during the proteins' separation in a BFS capillary achieved by Stutz et al. [79] using 1M FA as a BGE, the highest plate number obtained was 165 000/m. LPA-coated capillaries offered excellent precision values (0.18–0.49 RSD% for migration times and 3.2–4.9 RSD% for peak areas) in 25 repetitions, even when the conditioning included only a 5-minute BGE wash. The stability analyses of this coating has been performed in LPA-coated capillary that had previously been used for over a hundred protein separations. In regard to resolution, PB or LPA-coated capillaries revealed the highest capacity, specifically for the separation of proteoforms of hemoglobin.

*Table 5. The precision and separation efficiency data for 5 protein analysis obtained in different capillaries. The separation parameters are given in Fig. 12.*

protein	BFS			Semi-static coating (PB)			Static coating (LPA)		
	RSD% (t)	RSD%(area)	N (/m)	RSD% (t)	RSD%(area)	N (/m)	RSD% (t)	RSD%(area)	N (/m)
lysozym	0.56	2.76	177090	0.59	4.52	44205	0.18	3.16	84062
HSA	0.54	3.44	47706	0.69	3.45	5381	0.20	3.38	17047
myoglobin	0.64	1.66	321771	0.62	2.36	39006	0.31	3.96	75232
hemoglobin	0.70	6.54	193451	0.75	12.7	36387	0.43	4.33	117988
insulin	0.78	2.91	26676	0.69	5.54	18971	0.49	4.86	7127

### 4.1.3 Comparison of coated and non-coated capillaries for the analysis of venom proteins

Cobra venom is a naturally occurring substance with a very rich and diverse protein composition [116]. Using all three previously examined capillaries as well as separation conditions, the analytical performance of CZE-MS methods for the analysis of complex venom proteins has been evaluated and demonstrated in Fig. 18. Each capillary applied in proper separation conditions proved to be relevant for the analysis of the protein-rich sample. As a result, BFS and LPA-coated capillaries allowed for the identification of 32 components (including proteins and peptides) of venom (29 proteins by uncoated and

31 by LPA-coated capillaries). PB-coated capillary, however, could achieve to separate 52 components, 38 of them being proteins. Table 6 depicts the comprehensive list of identified proteins and smaller components with CE-MS. In PB-coated capillary the increased throughput may be attributed to an extended analysis time and/or its superior resolving ability for smaller species, which have only smaller charge.

ESI-MS possesses a fairly good detection sensitivity for components with molecular masses lower than 25 kDa, while it may be less sensitive for bigger proteins with a broad distribution of charged forms (and with various adducts). As a result, MS is unable to confirm the presence of the numerous large proteins present in venom (for instance, snake venom metalloproteinases with masses varying between 30 and 100 kDa). Even though those proteins can be determined by UV detection, the identification is not yet achievable. Eventually, UV spectrometry yielded a comparable number of separated components as MS did (Fig. 19). It was because MS detection was not sensitive for the detection of the larger species and UV detection was unable to determine smaller components of venom without a chromophore group, but larger components were well detectable.

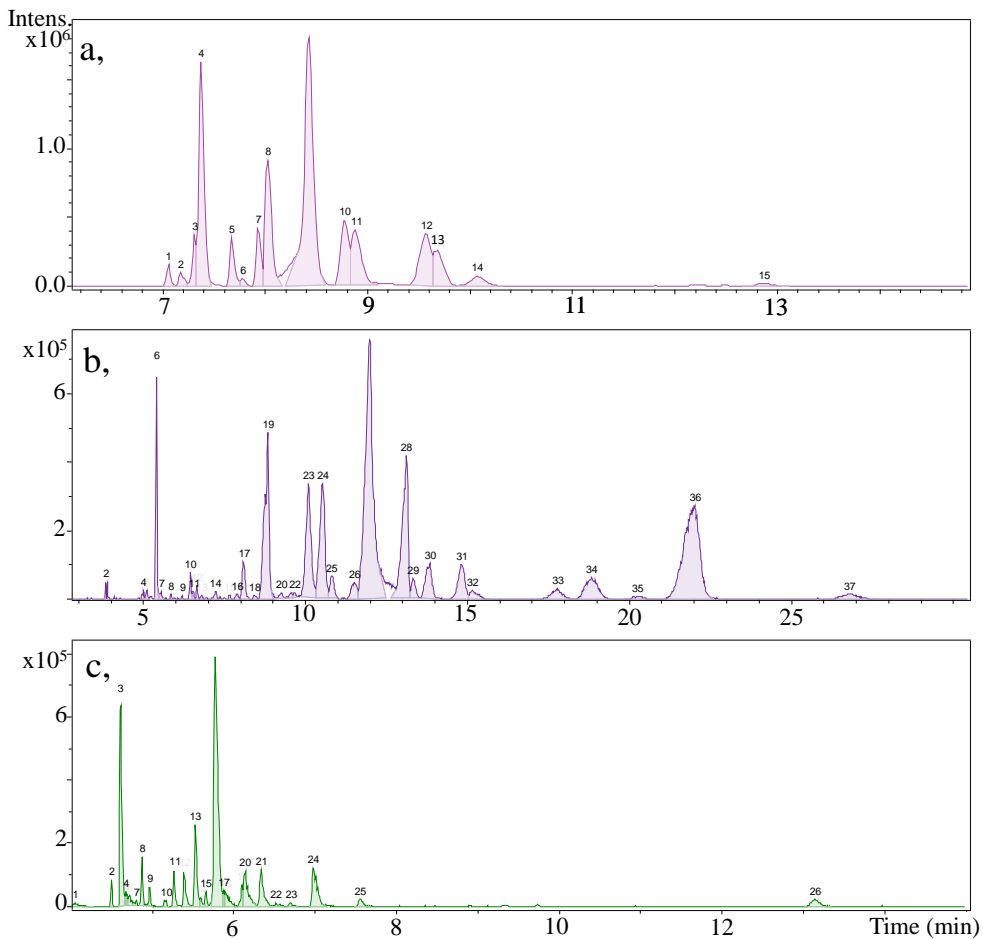


Figure 18. CE-MS analysis of cobra venom in uncoated and coated capillaries. (a) BFS capillary, (b) PB-coated capillary, (c) LPA-coated capillary. Capillary Leff: 57 cm; (a) separation voltage: +20 kV; BGE: 1 M FA (pH 1.8); 3-step conditioning: 1 M NaOH (18 min), acetone (6 min), BGE (20 min); (b) separation voltage: -30 kV; BGE: 1 M acetic acid (pH = 2.5); preconditioning: polybrene (5 min) and BGE (5 min); postconditioning: BGE (5 min); (c) separation voltage: +30 kV; BGE: 50 mM FA (pH 2.6); conditioning: BGE (5 min); capillary voltage: 4.5 kV; end plate offset: 500 V; nebulization pressure: 0.5 bar; dry gas temperature: 220 °C; dry gas flow rate: 8.0 L/min; MS scan range: 500-2400 m/z; spectra rate: 1.5 Hz.

Table 6. The mass list of cobra venom components.

Mass list (Da)			
BFS capillary	PB-coated capillary		LPA-coated capillary
6757.37	657.15	1181.52	6744.26
7559.29	615.02	7457.005	6851.28
7304.14	525.03	13344.57	7559.35
6851.36	457.1	6311.63	7532.33
7066.99	572.21	13353.53	7414.25
7532.42	406.12	13401.57	7050.97
13420.73	1073.36	25002.28	7066.91
6790.97	719.74	7389.2	13422.61
6669.2	944.36	7304.22	7391.25
6292.86	971.84	7787.4	6687.12
7756.48	2231.76	7756.4	8502.73
7442.38	2718.0819	6292.79	6790.87
13398.57	1162.62	6669.13	6669.12
13353.6	3379.3	6790.89	8014.48
13401.58	1405.56	7391.26	6292.78
13344.6	1084.45	13421.67	7789.34
4970.128	780.33	7066.92	7757.38
4616.96	942.38	7050.99	13308.54
4214.82	562.26	7533.33	7792.35
823.25	653.27	7561.37	7442.28
4374.84	1371.53	6851.3	7307.14
5213.11	1413.55	6744.28	7773.33
		38 peptides/proteins, 15 other components	
4638.03	1397.56		7389.16
5842.87	1251.5		7504.21
4780.1	5199.15		25000.17
936.36	822.27		7421.19
5195.09	4782.16		13354.48
5082.03	4640.08		13402.49
5841.85	724.31		13340.44
653.26	1669.61		13384.43
2224.02	4217.85		1114.02
29 peptides/proteins, 3 other components			31 peptides/proteins 1 other component

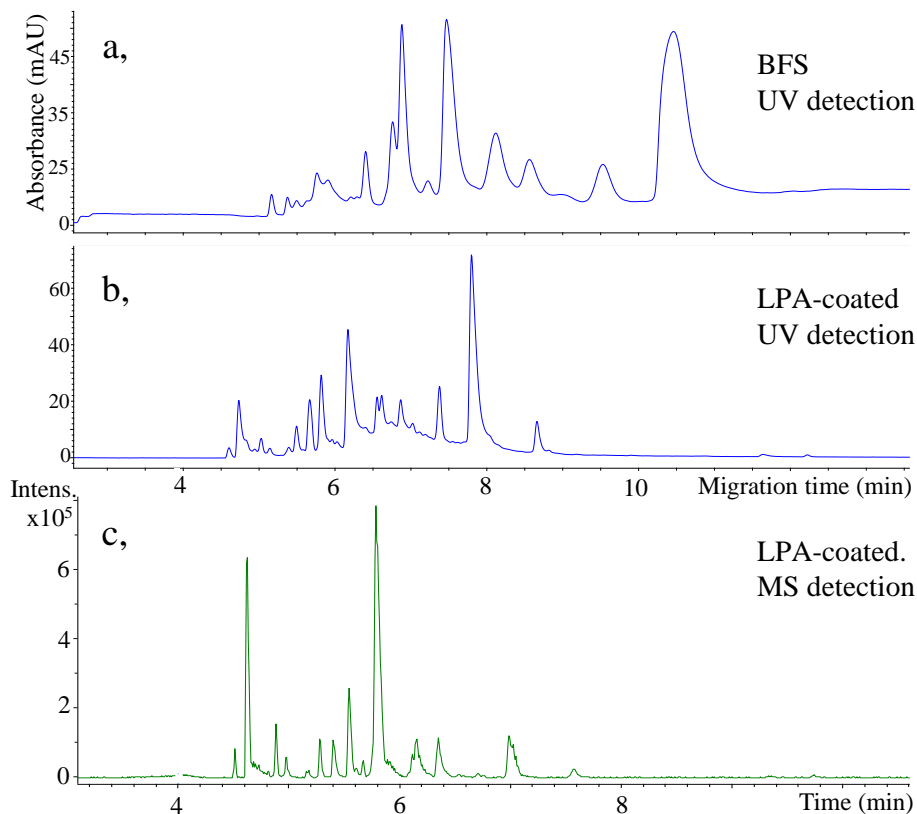


Figure 19. Cobra venom analysis in (a) BFS capillary and in (b and c) LPA coated capillaries. Capillary  $L_{\text{eff}}$ : 57 cm; (a) separation voltage: +20 kV; BGE: 1 M FA (pH 1.8); 3-step conditioning: 1 M NaOH (18 min), acetone (6 min), BGE (20 min); (b and c) LPA coated capillaries: separation voltage: +30 kV; BGE: 50 mM FA (pH 2.6); conditioning: BGE (5 min); (c) capillary voltage: 4.5 kV; end plate offset: 500 V; nebulization pressure: 0.6 bar (the first 240 sec was turned off); dry gas temperature: 220 °C; dry gas flow rate: 8.0 L/min; sheath liquid flow rate: 0.6  $\mu\text{L}/\text{min}$ ; MS scan range: 500-2400 m/z; spectra rate: 2 Hz.

## 4.2 Analysis of recombinant insulins

### 4.2.1 CE-UV analysis of insulins

Insulin has a crucial function in the regulation of blood glucose levels [95]. A malfunction in the body's response to insulin, which may be due to a shortage of insulin, an autoimmune reaction, or insulin resistance, may result in type 2 diabetes [99]. Recombinant DNA technology facilitates the manufacture of human insulin and numerous analogues with varying effects, all of which are currently used in the treatment of insulin-dependent diabetes mellitus. Each insulin possesses a unique pharmacokinetic and pharmacodynamic profile due to structural modifications and formulation preparation (Fig. 20). However, they are also a common target for fraudulent activities [96, 117], which makes reliable and uncomplicated quality control methods necessary.

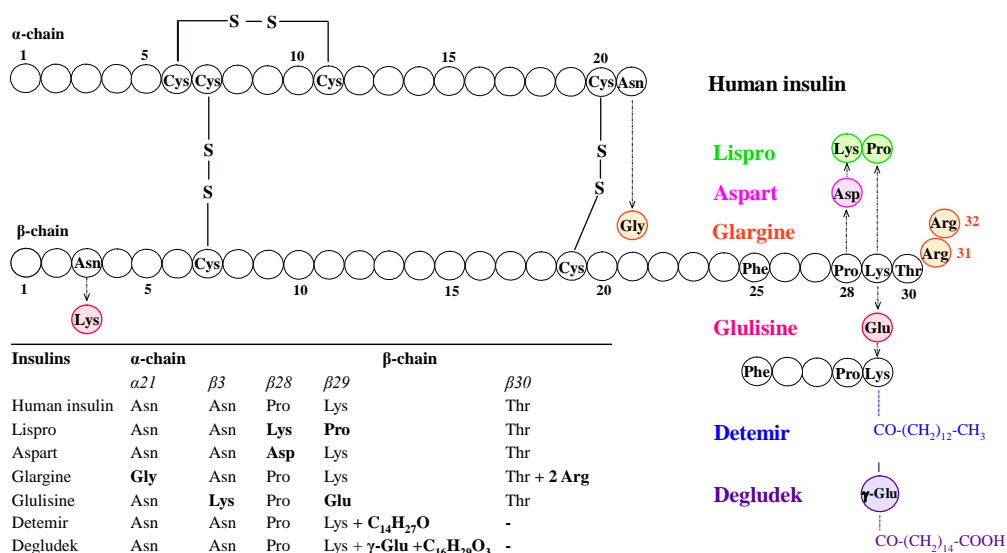


Figure 20. The structure of human insulin and its six analogues

Similarly, to our prior investigations on protein mixtures, the separation of human insulin and other six analogues (with the final concentration of 0.76 mg/mL) has been examined in very acidic (pH = 1.8), neutral and basic

pH (pH = 10) BGE milieus. Although the human insulin's pH-dependent behavior has been previously addressed (Fig. 4), the development of a similar tendency in analogue insulins remained doubtful.

At high pH values, the CE-UV analysis of seven insulins exhibited an insufficient separation pattern (Fig. 21.c), with few insulins displaying narrow and acceptable peak geometries (glargine, aspart and degludec), while some of them (lispro and human insulin, detemir and glulisine) overlapped. A large peak appearing first in the electropherogram is m-cresol (a typical preservative used in insulin infusions), which holds negative charges at basic pH and hence migrates adjacent to insulin peaks. In these settings, one may assume that extending the capillary length would assist in resolving the overlapped insulin peaks. This strategy may often result in a higher separation efficiency for small analytes. However, this is generally not the case for proteins. In longer capillaries, protein adsorption and peak broadening are more pronounced, which often compromises the resolution as well as separation efficiency. Moreover, as previously shown (Fig. 9), basic pH may not be the optimal detection condition for alkali proteins, enabling only acidic proteins to be detected in mixtures.

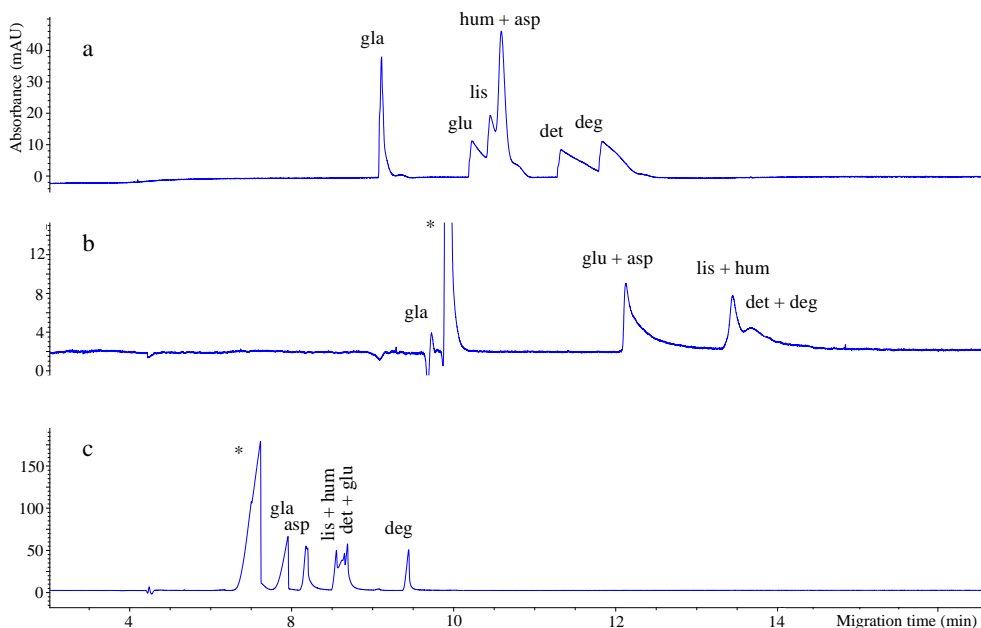


Figure 21. The CE-UV analysis of the human insulin and its six analogues in (a) acidic, (b) neutral and (c) basic BGE in an uncoated capillary. Capillary  $L_{\text{eff}}$ : 57 cm; separation voltage: +25 kV; 3-step conditioning: 1 M NaOH (18 min), acetone (6 min), BGE (20 min); BGE: (a) 1 M FA (pH=1.8); (b) 50 mM  $\text{NH}_4\text{HAc}$  (pH=7.0); (c) 50 mM  $\text{NH}_4\text{HAc}$  (pH=10.0); sample: hum-human insulin; lis-lispro; gla-glarginine; glu-glulisine; asp-aspart; deg-degludec; det-detemir, \* m-cresol.

Yet, as expected, in an uncoated capillary very acidic BGE could achieve a higher selectivity for the separation of more insulin analogues. (Fig. 21. a). In contrast, when the BGE solutions with neutral pH were used, the separation was progressively less selective. In these settings, insulins exhibit fairly comparable charge/size ratios as well as significant adsorption on the BFS wall, which yields the co-migrating and overlapping peaks (Fig. 21. b). Adsorptive interactions amongst insulins and capillary surface at neutral pH (pH = 7.0) could be attributed to positively charged regions of the protein (even though insulins possess a slight net negative charge) and the negative charges of the BFS surface.

In terms of resolution, very low pH remained the most promising; however, when it comes to efficiency, the acidic pH was not sufficient. As illustrated in Fig. 21.a, insulin analogues (particularly degludec and detemir) produced broad peak area with fronting which resembles electrodispersion. This peak broadening may be the result of a hydrophobic interaction with the capillary surface due to the presence of fatty acids in the peptide chain.

The separation performance of BFS capillaries was also compared to that of static LPA-coated and semi-static SMIL-coated capillaries. LPA-coated capillary use is often articulated to be adequate for the research of large proteomes, while several studies reporting its potency for the analysis of proteolytic peptides can also be encountered in the literature [118, 119]. Its suitability for smaller components allowed us to analyze the insulin mixture as well. At neutral pH, where the insulins contain nearly the same number of positive and negative charges (particularly glargine,  $pI = 6.7$ ), therefore they migrate fairly slow in the absence of EOF in LPA-coated capillary, the detection of the components would fail. Given the limited operational pH range of LPA-coating (pH 2–8), it was possible to separate the seven elements of the mixture at pH 2.6 using 50 mM formic acid. However, identical to the outcomes in BFS capillary, the LPA-coated capillary also displayed broad and fronting peaks. The triangle shape of the peaks was attempted to be reduced by dilution of the sample mixture, as previously done (Fig. 5). Nevertheless, the triangle morphology of the peaks (specially degludec and detemir, with very low plate numbers 935 and 3635, respectively) persisted until the peaks shrank and became undetectable (Fig. 22. b, c). As seen, broad peaks did not only contribute to peak overlaps, but they also deteriorated the sensitivity of the detection.

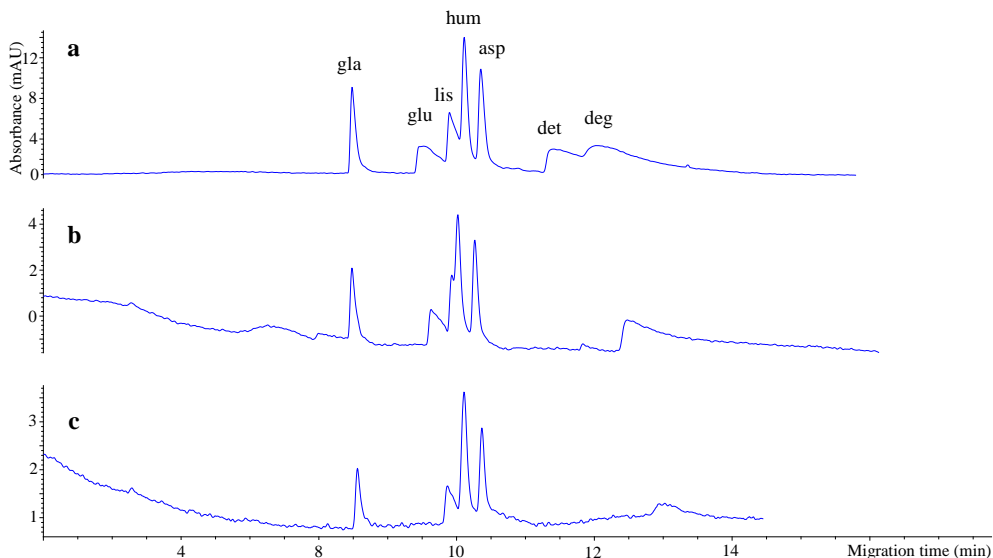


Figure 22. The effect of sample dilution on separation with LPA capillary. Capillary  $L_{eff}$ : 57 cm; separation voltage: +30 kV; BGE: 50 mM FA (pH 2.6); conditioning: BGE (5 min); concentration of insulin mixtures: (a) 1.2 mg/mL; (b) 0.6 mg/mL; (c) 0.35 mg/mL.

This finding once again contradicts the common assumption that larger proteins exhibit a higher tendency to adsorb onto the silica surface. Even as a large protein, HSA (at least 10 times larger than insulin) was found to exhibit significantly narrower peak morphology than insulin peaks in LPA-coated capillary (Fig. 23). This demonstrates that the size of the analytes has no bearing on adsorption. Instead, the role of the isoelectric point and capillary inner surface charge is more significant. Seemingly, a wide sample zone is partly triggered by the slower migration of insulins (due to the low charge/size ratio), although it may also be affected by the interactions as well as pH differences across insulin and the BGE solutions [120].

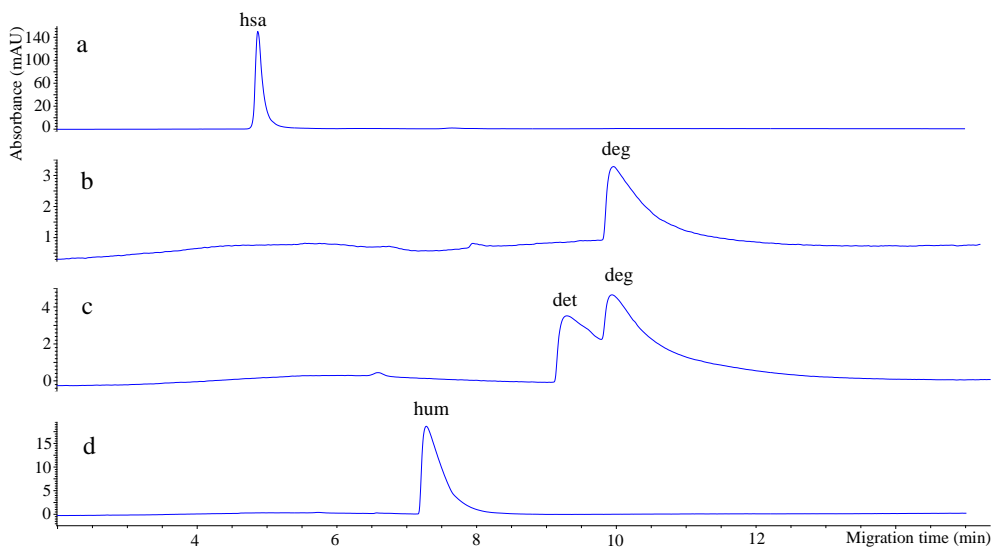


Figure 23. The comparison of (a) HSA, (b) degludec, (c) detemir and degludec mixture and (d) human insulin obtained in LPA capillary. Capillary  $L_{eff}$ : 57 cm; separation voltage: +30 kV; BGE: 50 mM FA (pH 2.6); conditioning: BGE (5 min).

For varying lengths of LPA-coated capillaries, the previous findings regarding the wide insulin peaks (Fig. 22 and Fig. 23) remained consistent (Fig. 24). A higher resolution between insulin analogues was anticipated with the longer (100 cm) LPA-coated capillary, however, this was not the case despite the extended analysis time and still occurring adsorption interactions. In light of this, 65 cm of capillary (the shortest length feasible for CE-MS coupling) was chosen for the subsequent measurements.

Switching to SMIL-coated capillaries made the capillary fabrication and conditioning processes substantially easier than those of LPA-coated capillaries. This semi-static, positively charged coating was formed by the three-step consecutive coating with polyelectrolyte layers of PB, DS (negatively charged) and once more PB. Operational pH for the SMIL coating is mainly an acidic pH, where anode directed EOF migrates in the opposite direction of insulins' effective electrophoretic mobilities.

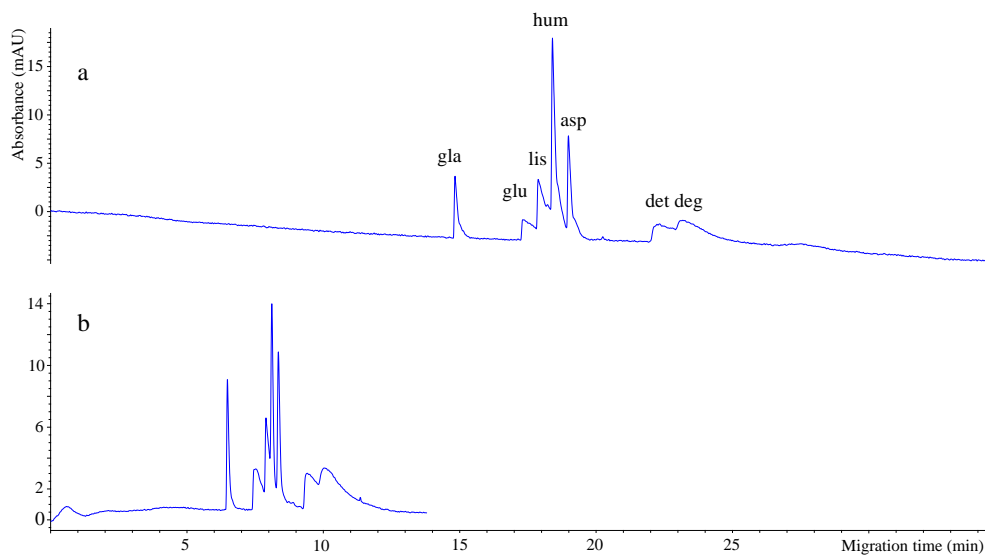


Figure 24. The comparison of electropherograms of 7 insulins obtained in (a) 100 cm and (b) 65 cm LPA capillary. Separation voltage: +30 kV; BGE: 50 mM FA (pH 2.6); conditioning: BGE (5 min).

For seven insulin analyses the BGE and pH were further adjusted for SMIL-coated capillary. It became clear that even small differences in pH had a significant impact on the way the SMIL-coated capillary separated all seven insulins. For instance, while 0.3 M formic acid (pH 2.3) offered the highest resolution for human insulin and aspart, they were not resolved when 0.75 M formic acid (pH 2.1) was employed (Fig. 25).

Comparable separation of human insulin and its analogues has also been performed in a single-layer PB, which is favorable in regard to shorter fabrication time (about 40 min less than SMIL-coated capillaries). Yet, in a single-layer PB capillary unsatisfactory reproducibility values of migration time and peak areas have been encountered. Additionally, it required adequate conditioning of the capillary (with PB and BGE to renew the coating) in each run, which extended the entire analysis duration. During CE-MS analysis, the requirement of preconditioning posed a challenge since the disconnection of

the capillary from the MS was necessary prior to each run to avoid contamination of the ESI chamber with a high concentration of PB.

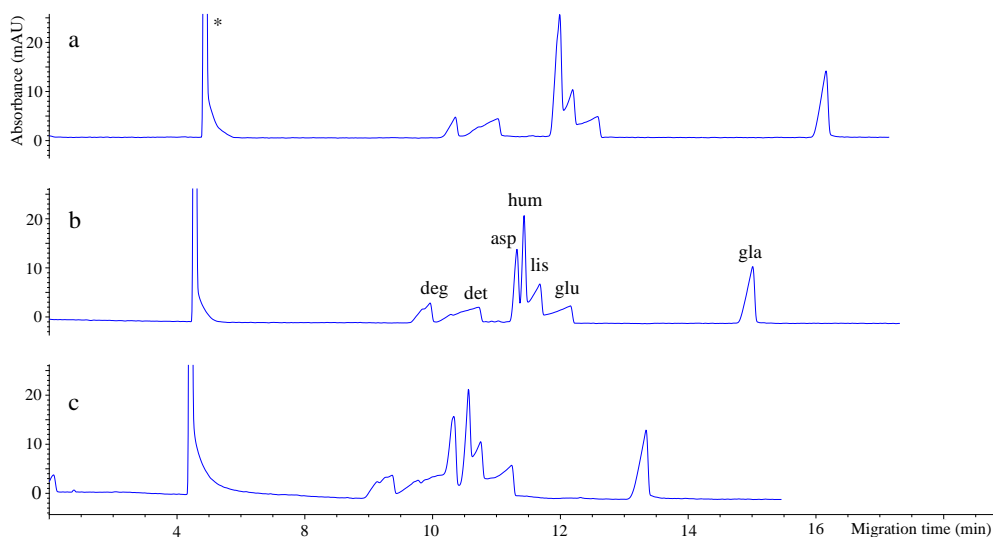
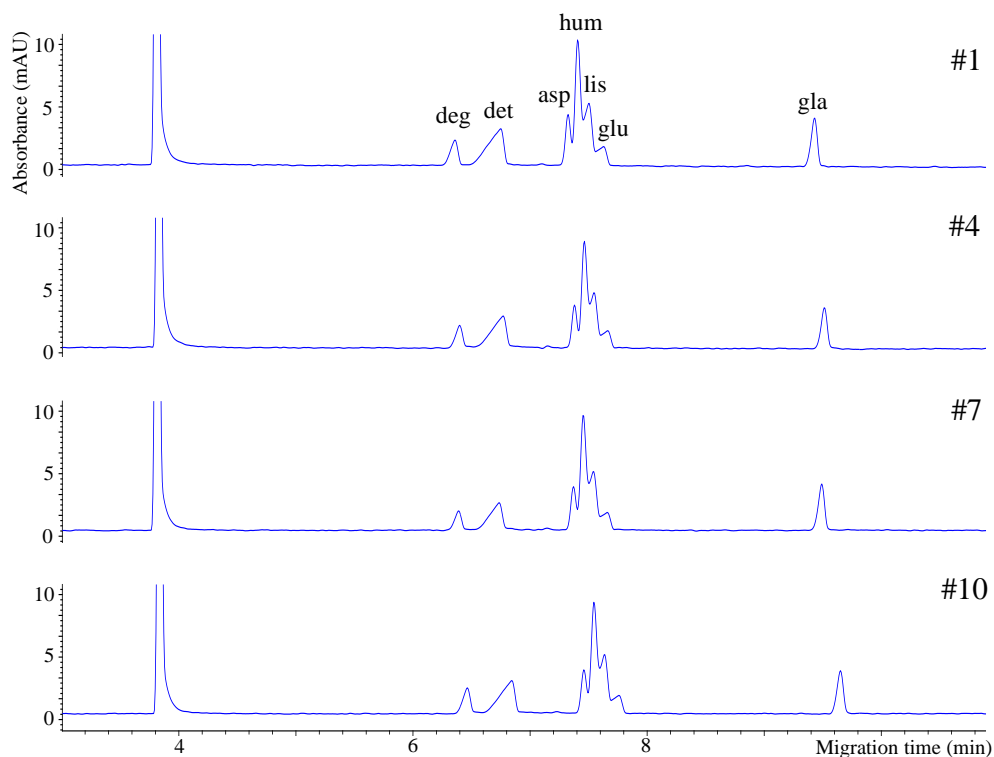


Figure 25. The optimization of BGE and pH for the separation of 7 insulins performed in the SMIL-coated capillary. Capillary  $L_{eff}$ : 57 cm; separation voltage: -30 kV; BGE: (a) 0.75 M FA (pH 2.1); (b) 0.3 M FA (pH 2.3); (c) 0.5 M AA (pH 2.6); conditioning: BGE (3 min); \**m*-cresol.

SMIL coating alleviated the latter concerns. The results obtained based on SMIL-coated capillary repetitions (Figure 26,  $n = 10$ ) are illustrated in Table 7. Moreover, as the SMIL coating did not require a regular coating regeneration but only a 3-min BGE rinse prior to the injection, it could also be readily employed with MS. The efficacy of a three-layer PB coating over a single-layer PB has been investigated by Haselberg et al. [121]. Using atomic force microscopy, the group have measured the thickness of the coated layers. Coating layer thicknesses of around 1 nm for single-layer PB and 5 nm for PB-DS-PB three-layer coating indicated that the polymer layers laid flat on the BFS surface due to intramolecular electrostatic interactions. Atomic force microscopy examinations of the coated capillary walls revealed that the three-layer

SMIL coating ensures entire surface coverage, while the single-layer PB coating fails to do so. The stability of the SMIL coating has also been found [115] to endure for more than 100 runs, whereas after 200 separations at pH 2.8, only 60% of the EOF was reported to be generated. The coating was found to be resistant to organic and alkaline solvents but detachable with a 0.1 M HCl solution. Concerning the capillary-to-capillary reproducibility, the performance of SMIL on five different capillaries was tested, and the RSD% of the EOF and the analytes was found to be less than 1%, demonstrating outstanding repeatability.



*Figure 26. The consecutive analysis of the insulin mixture performed in SMIL capillary ( $n=10$ ). The repeated separations were represented by the 1st, 4th, 7th and 10th runs. Capillary  $L_{\text{eff}}$ : 57 cm; separation voltage: -30 kV; BGE: 0.3 M FA (pH 2.3); conditioning: BGE (3 min).*

Based on our personal expertise, the SMIL coating exhibited a satisfactory level of stability throughout the consecutive forty runs before its regeneration. With the correct capillary storage (described in 3.4.1 chapter), it could even be exploited for up to four weeks. The capillary-to-capillary repeatability in an acidic medium was outstanding, with an RSD% of 0.63%. The comparison of electropherograms achieved in uncoated and coated capillaries under ideal conditions for each capillary is shown in Fig. 27. The greatest resolution of seven insulins was attained in capillaries coated with SMIL.

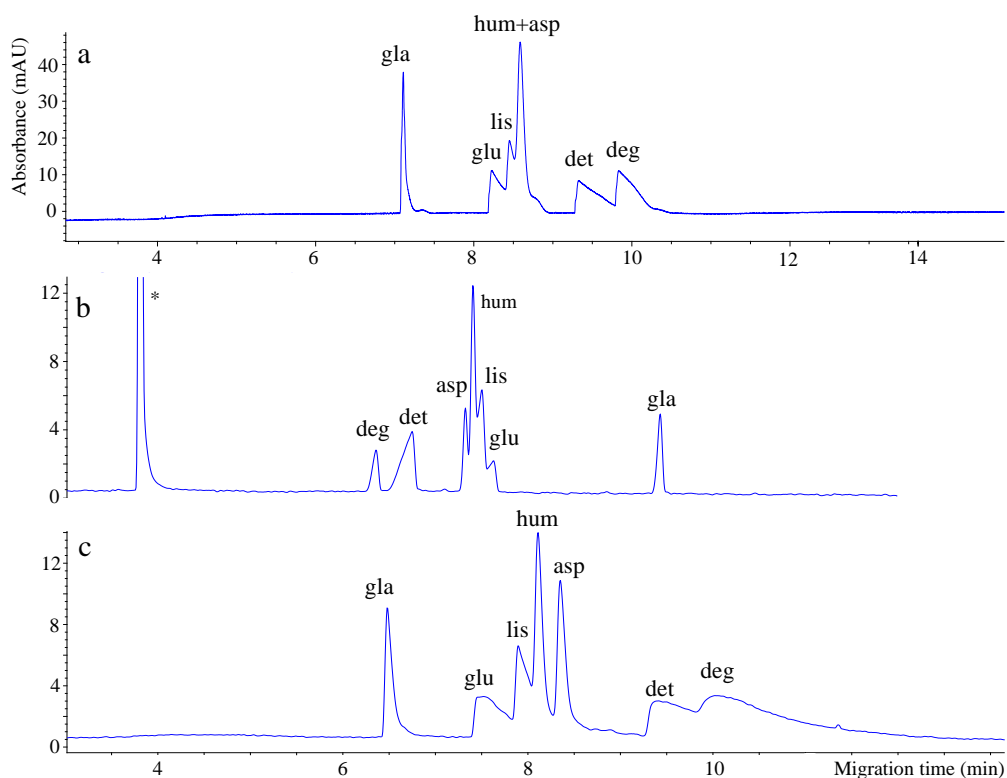


Figure 27. The comparison of CZE-UV separations obtained in optimized conditions of three different capillaries. Capillary  $L_{eff}$ : 57 cm; (a) BFS capillary: separation voltage: +25 kV; BGE: 1M FA (pH 1.8); 3-step conditioning: 1 M NaOH (18 min), acetone (6 min), BGE (20 min); (b) SMIL-PB coated capillary, separation voltage: -30 kV; BGE: 0.3 M FA (pH 2.3); conditioning: BGE (3 min); (c) LPA-coated capillary, separation voltage: +30 kV; BGE: 50 mM FA (pH 2.6); conditioning: BGE (5 min) \**m*-cresol.

The precision data was calculated considering 10 consecutive repetitions of seven insulin analyses in the SMIL-coated capillary. The migration time reproducibility was high, particularly for detemir (0.5 RSD%). As a time reference point, m-cresol peak was chosen, as it was present in majority of insulin formulations. However, this time reference correction did not produce better peak area RSD% data (instead, the corrected values were in the range of 5.8–8.8 RSD%). The elevated RSD% data were primarily attributable to the subtle modifications in adsorbed proteins each run, which led to the higher integration errors induced by the peak distortions and/or overlappings.

Baseline separation of all insulin peaks was not achievable due to the relatively comparable charge/size ratios as well as the widened peak areas. This reveals the great disparity between the results on theoretical plate numbers and resolution (Table 7). The SMIL-coated capillaries enabled the greatest plate numbers to be achieved. Although the separation efficiency of many analogues was poor, for the baseline-separated glargine peak, the plate numbers were the greatest with 192 000/m.

In terms of LPA-coated capillary, the coating was robust for up to hundred separations, under ideal settings. For human insulin, capillary demonstrated remarkable precision results ( $n = 25$ ), comprising 0.5 RSD% for migration time and 4.9 RSD% for peak area.

	Degludec	Detemir	Aspart	Humulin	Lispro	Glulisin	Glargine
pH of formulation <sup>a</sup>	7.6	7.4	7.2-7.6	7.0-7.8	7.0-7.8	7.3	4
pI <sup>a</sup>	5.5	5.5	5.1	5.4	5.6	5.5	6.7
Average mass value (Da)	6102.3	5916.7	5825.6	5807.6	5807.6	5821.2	6063.8
Monoisotopic mass value (Da)	6099.8	5912.7	5821.6	5803.6	5803.6	5818.6	6058.8
Equation for calibration graphs <sup>b</sup>	y=19.766x - 0.0859						
x-intercept <sup>b</sup>	-0.00435	-0.00274	-0.00035	-0.00016	-0.13454	0.01866	-0.00264
R <sup>2</sup>	0.9988	0.9901	0.9984	0.9998	0.9908	0.9917	0.9997
Linear range (mg/L) <sup>b</sup>	4-500	1-300	2-500	2-500	3-500	3-500	2-500
LOD (mg/L) <sup>b</sup>	1.2	0.3	0.6	0.5	0.9	1.1	0.5
LOD (MS) (mg/L)	3.4	1.4	1.1	1.1	1.9	2.9	1.0
RSD% (min)	0.21	0.5	0.08	0.1	0.2	0.33	0.37
RSD% (area) <sup>d</sup>	7.5	7.3	8.5	5.8	7.7	8.8	7.9
Resolution	26.1 <sup>e</sup>	2.07	2.32	0.51	0.43	0.48	15.3
Number of theoretical plates/m (SMIL)	62115	17218	161018	139076	89815	62783	192216
Number of theoretical plates/m (BFS)	11158	8051	54464	56464	76162	23237	142912
Number of theoretical plates/m (LPA)	938	3635	40598	50762	23814	4465	42600

*Table 7. The main characteristics and the validation results based on the separation of human insulin and its analogues in SML-coated capillary; a-those were provided by the producer; b-obtained with UV detection; c-calculated between m-cresol and degludec peaks; d-m-cresol is used as internal standard.*

#### 4.2.2 Mass spectrometric detection of insulins

For human insulin and its analogues, besides comprehensive qualitative data, MS detection also delivered a comparable sensitivity to that of UV detection. Due to their smaller size, insulins generate easily manageable mass spectra with few number of charge states. Smaller insulins, for instance, exhibited  $[M+6H]^{6+}$  as the highest charge state at low pH (pH = 2.1). Glargine, in contrast, produced more charge forms,  $[M+8H]^{8+}$  being the highest. The basic media (pH = 9.0) reduced the number of charge forms for all insulins to  $[M+5H]^{5+}$ . The results from CE-MS analysis of seven insulin analogues are illustrated in Figure 28. The empirical molecular mass of insulins were consistent with the theoretical mass values within a 1 ppm range (Fig. 29). To eliminate the syphon effect and attain a high resolution of analytes, the ESI nebulization pressure was switched off for 8.4 min following sample introduction. However, a laminar flow due to the syphoning action still must have been present during the remaining period of the separation. Specifically, when compared to UV detection, the glargine peak appears as an asymmetric peak in CZE-MS electropherogram, which may have been caused by this action.

While examining insulin analogues, structural data may be required in addition to the separation that could be obtained through the fragmentation of the molecular ions. There are a number of fragmentation methods, the most notable of which are collision-induced dissociation (CID), electron capture dissociation (ECD), electron transfer dissociation (ETD) and ultraviolet photodissociation (UVPD)—all of which generate a detailed molecular "fingerprints". Conformational data may be better represented when multiple techniques are coupled, since together they may generate more complete sets of data.

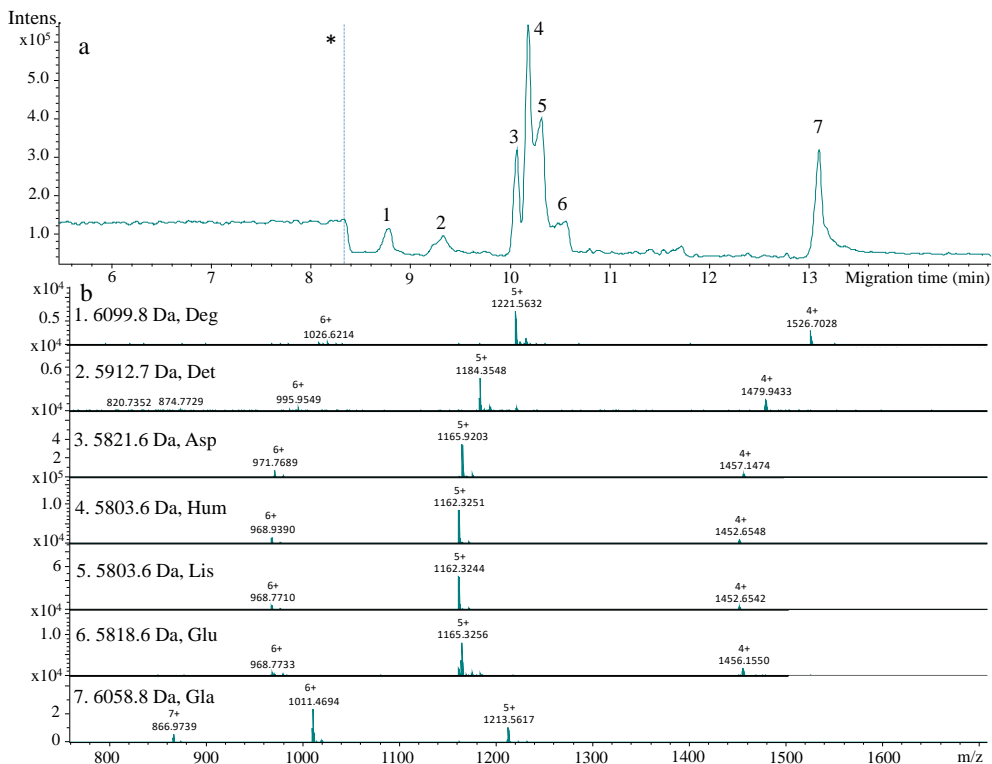


Figure 28. The CZE–MS separation of human insulin and its 6 analogues in SMIL-coated capillary. (a) base peak electropherogram; (b) mass spectra of separated insulins. Capillary: 65 cm; separation voltage: -30 kV; BGE: 0.3 M FA (pH 2.3); conditioning: BGE (3 min); capillary voltage: 4.5 kV; end plate offset: 500 V; nebulization pressure: 0.3 bar (following 500 s no pressure application after sample introduction); dry gas temperature: 200 °C; dry gas flow rate: 4.0 L/min; MS scan range: 600–2500 m/z; spectra rate: 3 Hz. \* the point that ESI nebulization pressure was turned on.

In practice, TD research on proteins with intact structures may be complex, particularly when the proteins feature a few disulfide bonds between cysteine residues. Although the disulfide bridges could be efficiently disrupted using some fragmentation strategies (such as ECD, which is usually supplied in FTICR-MS instruments) [122], they commonly appear to be resistant to the CID technique. When S-S bonds containing proteins are fragmented using the CID technique, the preferred cleavage sites are located on the peptide chain

beyond the disulfide linkage, producing large uncleaved parts of the chain. Yet, several studies [123, 124] have revealed the possibility of disrupting the disulfide linkages under positive CID parameters. In these trials, protein reduction (using tris(2-carboxyethyl)phosphine-HCl) prior to analysis was reported to be beneficial for enhanced fragmentation at the cost of extended analysis duration.

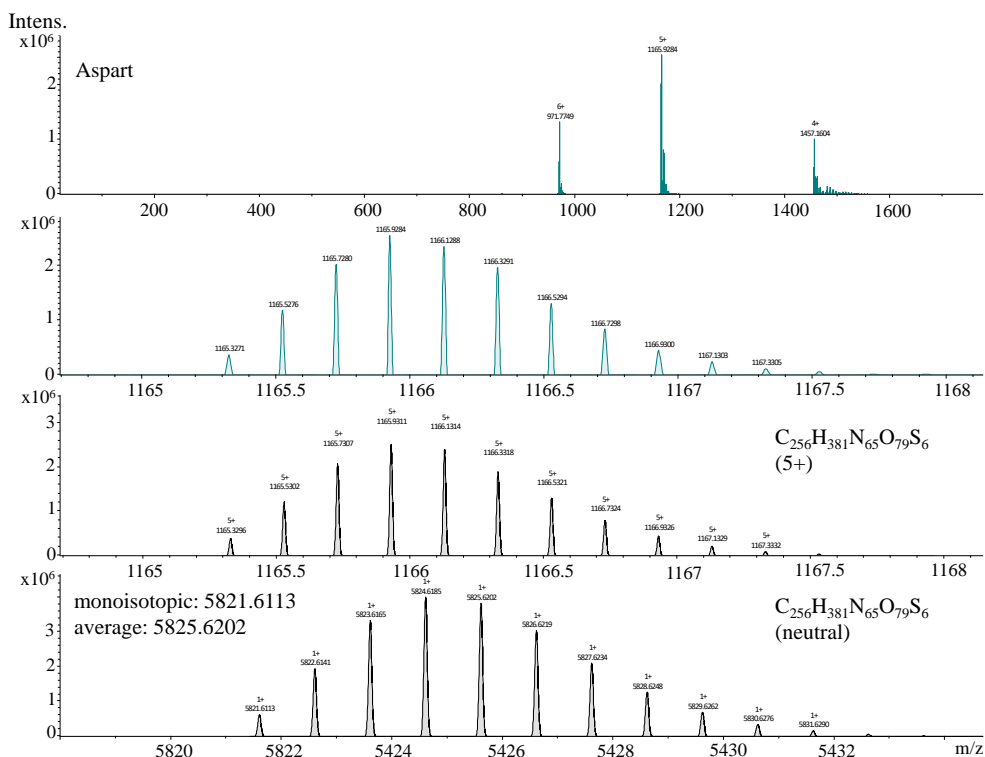


Figure 29. The isotopic mass envelope and the deconvolution of aspart insulin.

As insulins keep three S-S linkages on the peptide backbone, the aforementioned challenge holds true for them as well. Yet, intact top-down analysis of recombinant insulins using the CID technique can distinguish small mass or structural differences. It is possible since the varying amino acid residues are positioned outside the disulfide loop. The capability of MS/MS to differentiate

the analogues varying in the position of two amino acids exemplifies the applicability of this technique. Due to the presence of diagnostic fragments, the distinction between these insulins was possible without uncertainty [123, 124]. As insulin solutions were not exposed to reduction before the measurements, MS/MS analysis did not exhibit many product ion peak signals (Fig. 30).

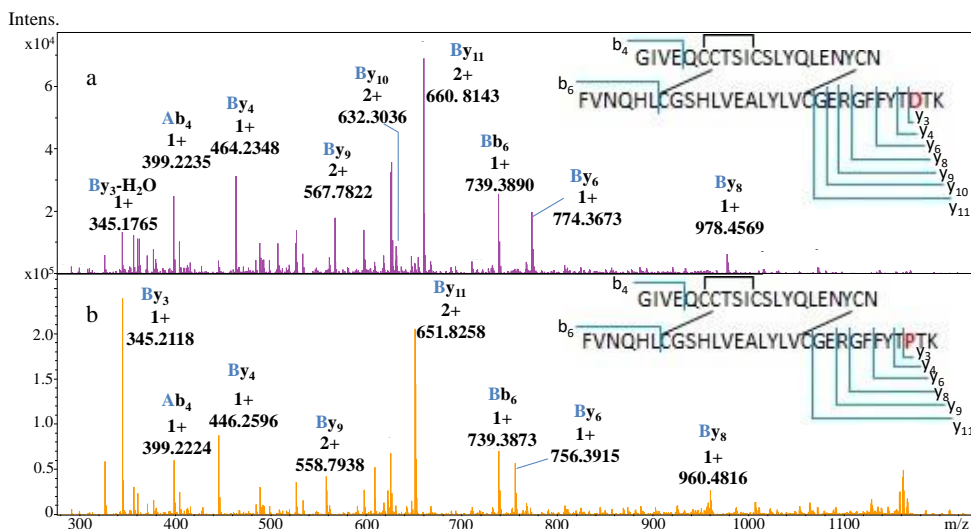
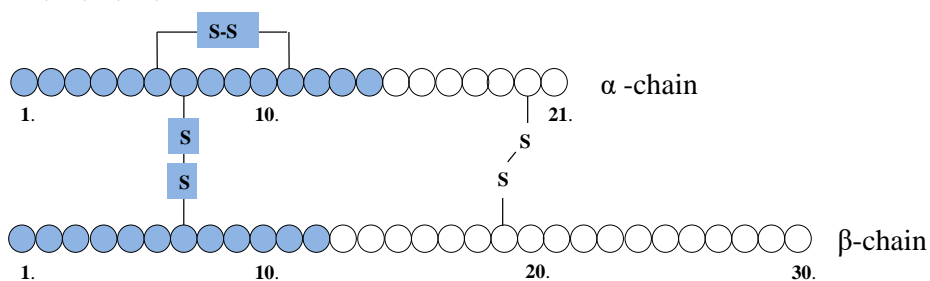


Figure 30. The spectra of (a) aspart and (b) human insulin from MS/MS analysis. The legends for the annotated peaks contain the chain (in blue) and the fragment type. Structure of the analogues are indicated, highlighting the difference in amino acid sequences in red as well as identified fragment types. Capillary voltage: 4.5 kV; end plate offset: 500 V; nebulization pressure: 0.3 bar (following 500 s no pressure application after sample introduction); dry gas temperature: 200 °C; dry gas flow rate: 4.0 L/min; mass scan range: 20-1800 m/z; spectra rate: 1 Hz; collision energy (CID): 45 eV.

Figure 30 displays our results from the limited fragmentation of recombinant insulins. For the intact TD analysis, aspart insulin is compared to human insulin, which presents a variation in a single amino acid at position  $\beta$ 28 (Pro is substituted with Asp). Due to this small alteration in the structure, a 17.9742 Da mass difference is obtained. As a result, the MS/MS spectra of the product

ions with the replaced amino acid residue revealed the existence of  $\beta$ 28-containing fragments. Figure 30 illustrates the spectra where a substantial amount of these ions and a large number of smaller fragments from outside of the disulfide loop are present. Usually, cleavages occurred at the amide bond, resulting in b- and y-type ions ("b" signifies ions from the N-termini, while "y" represents ions originating from the C-termini, and subscripts indicate the position of the amino acid where the cleavage took place) [125]. A closer look at the MS/MS spectra revealed the presence of larger peptides crossing the  $\alpha$ - $\beta$  chains (Fig. 31). The fragmentation pattern of these peptides was indicative of the b- or y-type ions [125], except the peptides bound by inter and/or intrachain S-S bonds. Table 7 displays the fragments obtained for aspart by MS/MS.

a,  $[\alpha_{(1-14)} \beta_{(1-12)}]b^{3+}$



b,  $[\alpha_{(15-21)} \beta_{(16-30)}]y^{3+}$

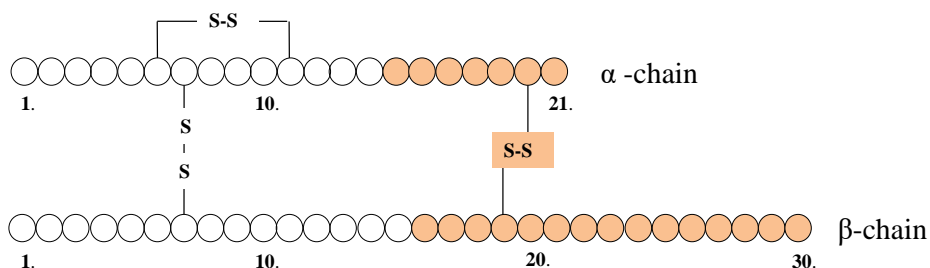


Figure 31. Fragmentation pattern of insulin yielding interchain ( $\alpha$ - $\beta$ ) fragments. (a) Blue color indicates the amino acids present in the identified b-type fragment ion (charge is retained on the N-terminus); (b) orange color highlights the amino acids present in a y-type fragment ion (charge is retained on the C-terminus).

Table 8. The list of peaks assigned on the MS/MS spectrum of insulin aspart

Experimental m/z	Theoretical m/z	Fragment type	Chain
345.1765	345.1769	$y_3 - H_2O$	$\beta$
363.1875	363.1874	$y_3$	$\beta$
399.2235	399.2238	$b_4$	$\alpha$
446.2245	446.2245	$y_4 - H_2O$	$\beta$
464.2348	464.2351	$y_4$	$\beta$
567.7822	567.7826	$y_9^{2+}$	$\beta$
632.3036	632.3039	$y_{10}^{2+}$	$\beta$
660.8143	660.8146	$y_{11}^{2+}$	$\beta$
739.3890	739.3886	$b_6$	$\beta$
774.3673	774.3668	$y_6$	$\beta$
851.0464	851.0471	$[\alpha_{(16-21)} \beta_{(16-30)}]y^{3+}$	$\alpha$ - $\beta$
893.7325	893.7333	$[\alpha_{(15-21)} \beta_{(16-30)}]y^{3+}$	$\alpha$ - $\beta$
934.9183	934.9183	$[\alpha_{(20-21)} \beta_{(17-30)}]y^{2+}$	$\alpha$ - $\beta$
944.4275	944.4306	$[\alpha_{(1-14)} \beta_{(1-12)}]b^{3+}$	$\alpha$ - $\beta$
954.0928	954.0940	$[\alpha_{(1-15)} \beta_{(1-11)}]b^{3+}$	$\alpha$ - $\beta$
978.4569	978.4567	$y_8$	$\beta$
1016.4501	1016.4506	$[\alpha_{(20-21)} \beta_{(16-30)}]y^{2+}$	$\alpha$ - $\beta$
1137.9930	1137.9934	$[\alpha_{(17-21)} \beta_{(17-30)}]y^{2+}$	$\alpha$ - $\beta$
1155.0043	1155.0037	$[\alpha_{(18-21)} \beta_{(16-30)}]y^{2+}$	$\alpha$ - $\beta$

The separation and detection capacity of the CZE-MS method optimised for seven insulin analyses was evaluated. Table 8 summarises the main analytical performance data. The linearity ranges of the calibration curves were determined using CZE-UV analyses on SMIL-coated capillaries. The linearity results obtained from these calibration diagram in the concentration

range between 1 mg/mL and 500 mg/mL were adequate, with a smallest  $R^2$  value of 0.9901 for detemir and a largest  $R^2$  value of 0.9997 for glargine.

The detection limit for CE-UV measurements varied from 0.3 to 1.2 mg/L, while for the base peak electropherograms (BPE) acquired from CZE-MS analyses, the LOD appeared to be in the 1.0 to 3.4 mg/L range, that is the detection sensitivity was similar for the two methods. The use of mass analyzers with greater sensitivity can certainly reduce the LOD values acquired from MS. Furthermore, in order to improve the LOD values and reduce the noise, MS/MS could also be beneficial. A slight sensitivity difference between UV and MS detections may be due to the broad charge envelope of the analytes, resulting in a reduced overall signal intensity for a certain charge state. The wide peak areas can be another factor contributing to the further reduction in sensitivity.

CE-MS is widely regarded as generating sensitivity levels that are at least one order of magnitude higher than that of CE-UV. This was confirmed to be valid for small molecules by Suneetha et al. [126], who compared the LC-UV and LC-MS analyses of teriflunomide, dimethyl fumarate, and fampridine from human plasma. However, there is a shortage of data comparing the sensitivity (LOD) performance of two detection techniques concerning the larger compounds (particularly, proteins). Table 9 illustrates the comparison of LOD data from previous studies (about 40 publications) acquired using CE-MS and CE-UV for proteins of varying sizes. It is evident from the searches that many publications include LOD values only for a single detection method (e.g., UV) in the validation even where both CE-UV and CE-MS were used for analysis. Due to variations in the analysis conditions (e.g., capillaries (coated or uncoated), application of on-line or off-line sample cleaning or stacking, the amount of injected analyte, performance and age of

the detector, etc.), it is challenging to compare the LOD values for CE-UV and CE-MS collected from various studies.

Based on our experience (Fig. 10, 11), it is evident that as the size of the protein increases, so does the strength of CE-UV over CE-MS in terms of detection sensitivity. As a small protein, insulin, with a mass spectra containing a fairly simple isotopic distribution and few charge states, yields comparable LOD values with UV and MS detection.

*Table 9. The comparison of LOD values obtained for insulin and other proteins by CE-UV and CE-MS. <sup>1</sup>Field amplified sample stacking or injection of large sample volume (50 mbar x 24 s) was applied.*

CE mode	LOD (mg/L)		Proteins measured	Ref.
	CE-UV	CE-MS		
<b>CZE-UV</b>	1	-	2 insulins	[Yeh2010]
<b>MEKC-MS</b>	-	10	6 insulins	[Ortner2009]
<b>MEKC-UV</b>	15	-	6 insulins	[Lamalle2015]
<b>CZE-UV</b>	3.6	-	2 insulins	[Pajaziti2020]
<b>CZE-MS</b>	-	0.06-0.81 <sup>1</sup>	Different proteins (MW > 33kDa)	[Taichrib2012]
<b>CZE-UV and CZE-MS</b>	1.4	-	Snake venom proteins (MW~7 kDa)	[Liu2021]
<b>CZE-MS</b>	-	50 100	Light chain (25 kDa) and heavy chain (50 kDa) of reduced mAb	[Hernandez2016]
<b>Current method</b>	0.3-1.2	1.0-3.4	7 insulins	

### 4.3 Applications

The applicability of CZE-MS for intact protein analysis has also been explored on various studies. In this chapter three quite different fields of the intact protein analysis are shown through the study of insulin deamidation, native protein analysis and the determination of mAb. These determinations were based on the results and expertise obtained by our work described in the previous chapters.

Deamidation of proteins is one of the most prominent non-enzymatic PTMs that results from the hydrolysis-mediated removal of amide groups from asparagine (Asn) and glutamine (Gln) residues, yielding free carboxylate groups. The deamidation was studied in case of human insulin. The presence of desamido isoforms in human insulin was predicted due to the availability of six of these residues (A5 (Gln), A15 (Gln), A18 (Asn), A21 (Asn), B3 (Asn), and B4 (Gln)) [127]. The deamidation of one amino acid residue increases the molecular mass of a protein by 0.984 Da, which may be identified by MS [128].

In our work the various deamidated forms were separated by CZE and identified by MS detections. Regarding the separation, the choice of BGEs was restricted given that they must be MS-compatible. Alkaline BGE ( $\text{NH}_4\text{Ac}$ , pH = 9) was selected for separations since, at this pH, free carboxyl groups generated as a result of deamidation impart negative charges to the protein and therefore become separated from the main human insulin peak. For CE-UV studies, 20% IPA was incorporated into the BGE to achieve high separation efficiency and resolution of isoforms. The deamidated forms could not be separated at pH values below 4.

The separation with CE-UV has been performed in BFS capillaries of 85 cm length, which yielded adequate resolution. Figure 32.a displays the

separation of human insulin and its six distinct isoforms, which formed 8 days after being exposed to conditions accelerating deamidation (pH=1).

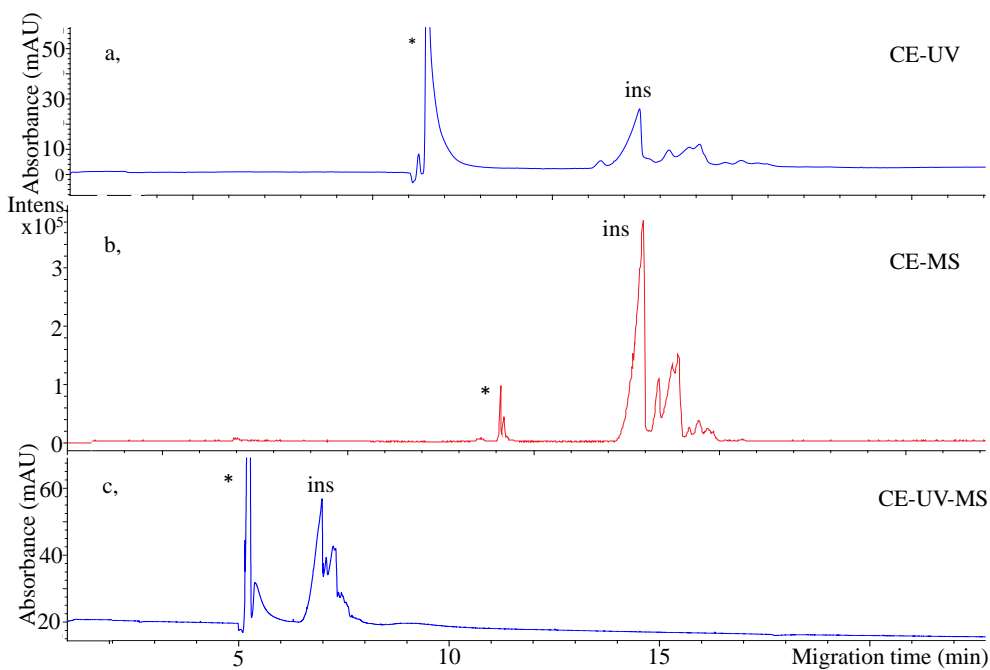
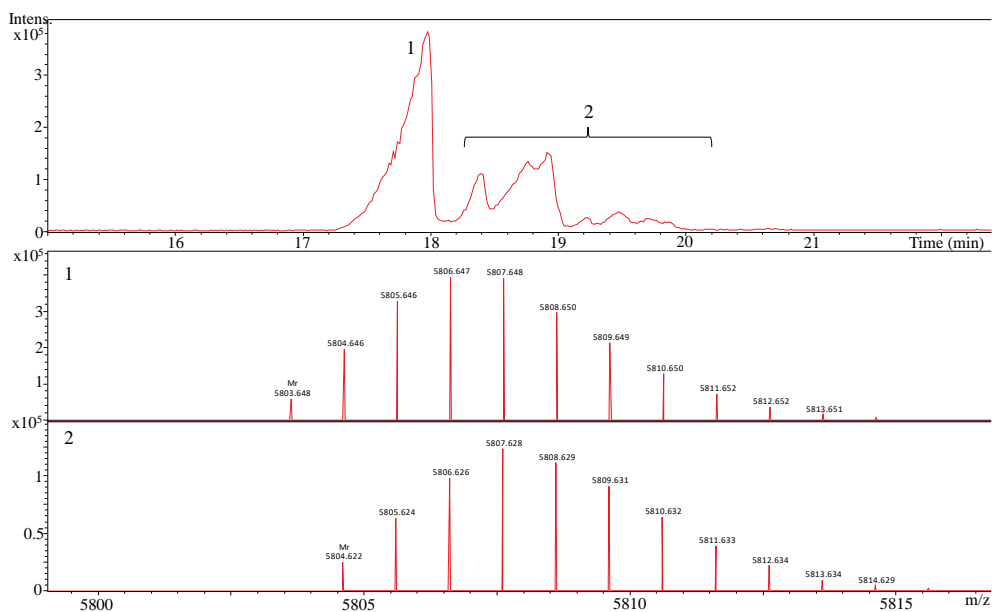


Figure 32. Analysis of human insulin and desamido-insulin isoforms with (a) CE-UV, (b) CE-MS and (c) CE-UV(-MS). (a) Sample: 3,43 mg/ml insulin stored in acidic condition (pH= 1) for 8 days at room temperature; capillary:  $L_{eff}$ : 77 cm; separation voltage: +25 kV; BGE: 50 mM  $NH_4Ac$  with 20% IPA (pH 9.0); conditioning: rinsing with 1 M NaOH (20 min), water (10 min) and BGE (20 min); (b) Capillary: 100 cm; BGE: 50 mM  $NH_4Ac$  (pH 9.0); nebulizer pressure: 0.4 bar; dry gas temperature: 220°C; dry gas flow rate: 8 L/min; capillary voltage: 4500 V; end plate offset: 500 V; spectra rate: 6 Hz; mass range: 800-2200 m/z; (c) capillary  $L_{eff}$ : 30 cm. The remaining parameters are same as (a); \*m-cresol.

Regarding the CZE-MS analysis, a 100 cm-long BFS capillary has been chosen in order to achieve a high separation efficiency and facilitate the proper coupling between CE and MS. The CZE-MS separation performance was comparable to that of CE-UV (Fig. 32.a,b). UV analysis can also be conducted during the CZE-MS analysis, but then much shorter effective separation length is possible to apply (Fig. 32.c), therefore the analytes could

be detected sooner than in the CZE-MS. Upon inspection of the spectra, it was evident that the acquired smaller peaks had a mass of only ~1 Da more than that of human insulin (Figure 33), indicating that they were monodesamido-insulin forms. (Our group was able to analyse 10 distinct desamido forms of human insulin, including 2-, 3- and 4-folds deamidated forms by extended incubation period [129].)



*Figure 33. Separation of human insulin from its desamido-insulin isoforms. Mass spectra of (1) human insulin and (2) desamido-insulin isoforms. The parameters are same as stated in Fig. 32.b.*

As previously discussed, in addition to intact analysis, TDMS can be also useful for the study of native proteins. Native MS yields a spectrum of folded proteins comprising non-covalent interactions and a complete higher-order structure. For native protein investigations these physiological conditions must be provided by BGE, the sample matrix and the sheath liquid, which must be free of acidic, basic or organic solvents. In our studies, 20 mM  $\text{NH}_4\text{Ac}$  (pH = 7.0) and 5 mM  $\text{NH}_4\text{Ac}$  (pH = 7.0) have been selected as the BGE

and the SL, respectively. Our target protein mixture contained lysozyme, myoglobin and HSA dissolved in 20 mM NH<sub>4</sub>Ac. The mixture was separated using a 65-cm-long LPA-coated capillary. Since no EOF is generated in this capillary owing to its neutral surface, current instabilities can be encountered [12]. To address this issue, high SL flow rates (0.7 μL/min) and an extra internal pressure (50 mbar) have been applied in the capillary during the electrophoretic run. With the aforementioned settings, it was possible to separate and detect lysozyme and myoglobin (Figure 34); however, the HSA peak did not appear in the electropherogram. Lysozyme (pI = 11.35) has a large net positive charge at neutral pH, while myoglobin (pI = 7.3) exhibits a slight positive net charge. However, HSA (pI = 4.7) kept a big negative net charge, which presumably did not migrate towards the cathode. On the other hand, it is questionable whether MS sensitivity would be sufficient to identify HSA peak, even if it was driven to reach MS (as in Fig. 11).

In Figure 34 the native mass spectra of lysozyme (Fig. 34.1) and myoglobin (Fig. 34.3) are compared with their denatured spectra (Fig. 34.2, 4). Notably, analytes generate fewer charge states in native CZE-MS than in denatured analysis. In the case of lysozyme, the maximum charge state in the native spectrum is  $[M+9H]^{9+}$ , whereas for denatured protein it is  $[M+11H]^{11+}$ . When it comes to myoglobin, in native settings the number of charged forms decrease considerably ( $[M+10H]^{10+}$  being the highest for native spectra while in denatured spectra more than 20 charge states are present). The difference between lysozyme and myoglobin denatured spectra may be explained by the distinct denaturation mechanisms of two proteins. Myoglobin, being a single-chain protein with no disulfide bridges, can easily loosen all of its non-covalent interactions and uncoil. Thus, it exposes more to the aqueous environment and produces more protonation sites. Nevertheless, acid denaturation is incapable

of disrupting four disulfide bridges of lysozyme, thereby lowering its exposed surface area and the likelihood of protonation.

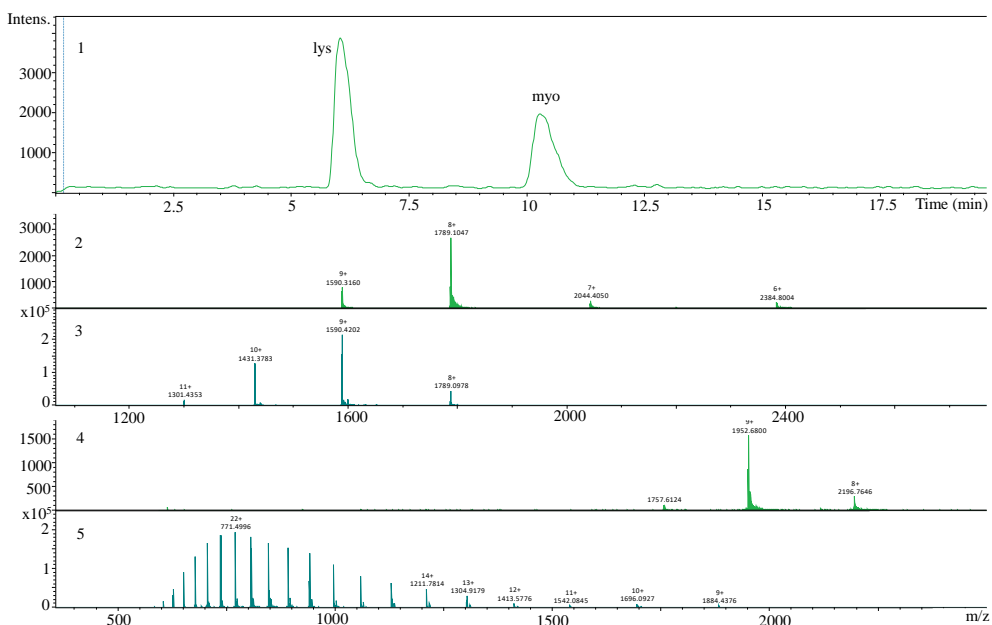


*Figure 34. Native CZE-MS analysis of (1) protein mixture and the spectra of (2) native lysozyme, (3) denatured lysozyme, (4) native myoglobin and (5) denatured myoglobin. Sample: 10 mg/mL lysozyme, myoglobin and HSA mixture; capillary: 65 cm LPA-coated capillary; separation voltage: +25 kV; injection: 50 mbar, 20 sec; BGE: 50 mM NH<sub>4</sub>Ac (pH 7.0); conditioning: BGE (5 min); nebulizer pressure: 0.5 bar (turned on 10 sec after sample injection); dry gas temperature: 220°C; dry gas flow rate: 8 L/min; capillary voltage: 4500 V; end plate offset: 500 V; spectra rate: 1 Hz; mass range: 600-4000 m/z; extra internal pressure: 50 mbar.*

The formation of higher number of charged forms in the denatured protein spectra could be expected to reduce the sensitivity; however, native protein spectra exhibits less intensive signal despite the less number of charge states. This could be presumably attributed to poorer ionization of the components in native settings. This phenomenon becomes even more pronounced in the case of bulkier components such as mAbs (Fig. 35).

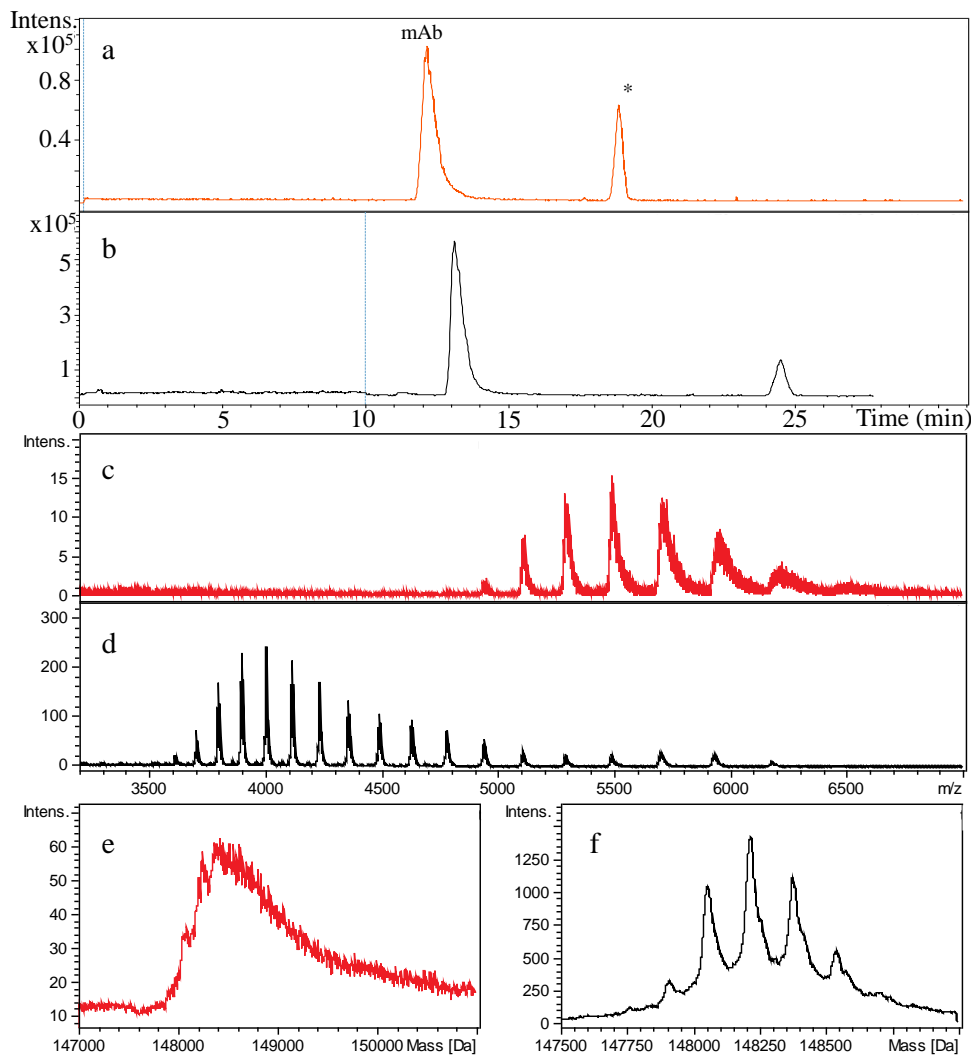
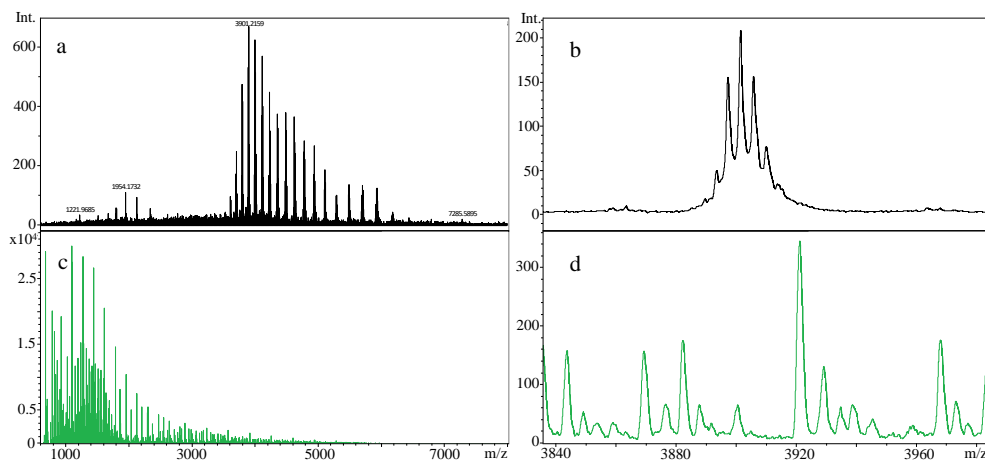


Figure 35. CZE-MS measurements of trastuzumab. (a) Native CZE-MS electropherogram, (c) mass spectra and (e) deconvoluted mass spectra of mAb obtained in native measurement conditions; (b) non-native CZE-MS electropherogram, (d) mass spectra and (f) deconvoluted mass spectra of mAb obtained in denatured conditions. Sample: 3 mg/mL trastuzumab; (a) capillary: 75 cm LPA-coated capillary; separation voltage: +30 kV; injection: 100 mbar, 5 sec; BGE and SL: 20 mM NH<sub>4</sub>Ac (pH 7.0); nebulizer pressure: 0.7 bar (turned on 10 sec after sample injection); conditioning: BGE (8 min); dry gas temperature: 220°C; dry gas flow rate: 5 L/min; capillary voltage: 4500 V; end plate offset: 500 V; spectra rate: 1 Hz; mass range: 600-8000 m/z; in-source CID: 120 eV; extra internal pressure: 50 mbar; (b) SL: 1 % acetic acid; nebulizer pressure was turned on 600 sec after injection; \*TWEEN (detergent); other parameters are same as (a).

Figure 35 demonstrates the comparison between native (native separation as well as detection) and non-native (native separation but denaturing MS detection) CZE-MS analysis of trastuzumab regarding the measured and deconvoluted mass spectra, and sensitivities of the two different techniques. Both analyses feature native CZE separation, proceeded with native (Fig. 35.a) and denaturing (Fig. 35.b) ESI-MS detection. The separation of mAb from its buffer detergent (TWEEN) was similar in both cases, with the only difference being a longer migration window owing to the extended (600 sec) off-nebulization time during non-native analysis. However, a clear difference in the compound and deconvoluted spectra is noticeable. In the native settings, mAb produces a lower number of charge states (Fig. 35.c) in a higher  $m/z$  range (5000–7000  $m/z$ ), while denaturing ESI-MS generates more charged forms in a lower  $m/z$  range (3500–5000  $m/z$ ) (Fig. 35.d). Moreover, native spectra appear to have wider peaks than that of denatured, which may be the contribution of a higher number of different adducts. The latter may also be the reason for suppressed sensitivity. Upon the magnification of the deconvoluted spectra (Fig. 35.e), non-native analysis is able to deliver more comprehensive information regarding the characterization of mAbs (Fig. 35.f), whereas it is very poor in the case of the deconvoluted native spectra (Fig. 35.e). The deconvoluted spectra of denatured mAb demonstrates several peaks with a mass difference of 162 Da, which is probably attributed to glycation (occurring in the N-termini or side chains of lysine due to the protein's exposure to reducing sugars). Glycation of mAbs is a non-enzymatic reaction that occurs both in vivo and during mAb production and storage [130]. Despite their presence in the MS spectra, glycated isoforms could not be separated from the main mAb form during CZE-MS analysis. Yet the separation of the mAb's main component from the detergent helped increase the detection sensitivity of trastuzumab. When compared to off-line MS analysis (Fig. 36.c, d) in

similar denaturing settings, it is evident that without separation, the suppression of the MS signal by TWEEN is rather high and therefore mAb is not detectable.



*Figure 36. The comparison of mAb MS signal (a, b) after CZE separation from TWEEN and (c, d) without CZE separation. a and c represent the mass spectra in wide m/z range, while b, d indicate the mass spectra for a narrow m/z range. (a, b) all the parameters are same as stated in Fig. 35.b; (c, d) sample: 10 mg/mL trastuzumab; BGE: 1% formic acid (pH = 2.75); all tuning parameters are same as stated in Fig 35.a.*

## 5. Summary

In the first part of my work, the performances of various capillaries (uncoated and coated) for intact protein analysis with CZE-UV have been examined and compared. For the comparisons, a protein mixture comprising myoglobin, human insulin, human serum albumin, human hemoglobin and lysozyme was employed. The operating parameters have been adjusted for each capillary in order to compare capillary performances fairly. In case of the BFS capillary, it has been demonstrated that the pH of the BGE and capillary conditioning have a significant influence on protein adsorption and consequently, the reproducibility and sensitivity of the method. Strongly acidic pH (pH = 1.8) and thorough capillary preconditioning enabled adequate repeatability and separation efficiency in BFS capillary. For migration time and area, precision data of less than 1 RSD% and 4 RSD% have been acquired. By comparing the results of UV and MS detection for the same protein mixture, it has been discussed why CZE-MS is unable to exceed the levels of sensitivity and separation efficiency as CZE-UV. The separation performances of static LPA-coated and semi-static PB-coated capillaries were compared to those of BFS capillary. Uncoated capillaries have been surprisingly shown to generate the highest number of theoretical plates (between 27 000/m and 322 000/m). However, in regard to resolution, PB and LPA-coated capillaries revealed the better resolution for the separation of proteoforms of hemoglobin (at a slightly higher pH that can be optimally applied in BFS capillary). According to the precision findings from 10 consecutive runs, uncoated and LPA-coated capillaries produced data that was equivalent, while PB-coated capillaries had slightly inferior reproducibility. We also briefly investigated the separation of globin chains and other unidentified haemoglobin proteoforms using PB-coated capillary.

Using all three previously examined capillaries as well as separation conditions, the analytical performance of CZE-MS methods for the analysis of complex cobra venom proteins has been assessed. As a consequence, it has been observed that BFS and LPA-coated capillaries enable the identification of a comparable number of venom proteins and peptides, whereas PB-coated capillary allowed the separation of even more components due to a wider detection window as a result of its superior resolving power. The ESI-MS was also revealed to have fairly good sensitivity for the smaller protein components ( $M < 25$  kDa); nevertheless, the MS detection was not sufficiently sensitive to identify numerous larger proteins (30 kDa – 100 kDa) included in venom. This findings was explained by a broad distribution of charged forms in large protein spectra and the presence of various adducts.

The proposed CZE-UV methods have been adjusted and applied to the separation of human insulin and its analogues as small proteins with similar (or the same) molecular mass and characteristics (pI, structures). Moreover, three-layer PB-DS-PB-coated SMIL capillary was employed instead of single-layer PB-coated capillary to alleviate the concerns about reproducibility and PB bleeding into ESI chamber. As a result, SMIL capillary yielded the highest number of theoretical plates, reproducibility and resolution of seven insulin analogues compared to LPA-coated and BFS capillaries. The precision data for migration times and peak areas in SMIL capillary varied from 0.08 to 0.5 RSD% and 5.8 to 8.8 RSD%, respectively. Insulins usually exhibited wide triangle-shaped peak morphologies producing large area values, which was also briefly discussed in this chapter. LOD values from CZE-UV observations varied from 0.3 to 1.2 mg/L, whereas the BPE of CZE-MS detection indicated considerably lower sensitivity (1.0 to 3.4 mg/L). This matter has been reviewed, and sensitivity variations have been evaluated against previous research findings.

CZE-MS analyses of insulin analogues have exhibited consistent outcomes with CZE-UV and allowed for component identification. In order to learn more about the structural variations, an MS/MS screening of human and aspart insulins—which differ only in one amino acid at position  $\beta$ 28 (Pro is replaced with Asp)—was conducted. The CID dissociation technique has been demonstrated to be sufficient for identifying these minor differences and the list of peptides attributed to aspart insulin has been presented.

The proposed CZE-MS methods were applied in several very diverse fields of the intact protein analysis. Human insulin is separated from its desamido-insulin isoforms, exhibiting the efficacy of CZE-MS to distinguish between components with mass differences of only 1 Da. A native CZE-MS analysis of lysozyme, myoglobin, and albumin has been performed where the detection of positively charged lysozyme and myoglobin has been achieved. Trastuzumab (mAb) has been analysed both with native and non-native (native separation combined with denaturing MS) CZE-MS to highlight the variations in detection sensitivity between these two methods.

CZE-MS was found beneficial for TDMS examinations of proteins, offering information ranging from deamidated forms to very large components like mAbs. Although MS detection sensitivity for larger species remains a challenge, it may be enhanced by the use of high-sensitivity mass analyzers or proper sample pretreatment/enrichment procedures. For the separation, coated capillaries may secure high resolving power and reproducibility; however, BFS capillaries can deliver a good separation efficiency for the simple protein mixtures while being the low-cost alternative.

Our comprehension of the topic also benefited from our participation in the CE-MS Initiative by the Consortium for Top-Down Proteomics

(<https://www.topdownproteomics.org/initiatives/ce-ms-initiative/>) on the analysis of proteins and protein complexes using CZE-MS.

## 6. References

1. B. Aslam, M. Basit, M.A. Nisar, M. Khurshid, M.H. Rasool, Proteomics: technologies and their applications, *J. Chromatogr. Sci.*, 55 (2016) 182–196.
2. M.R. Wilkins, J.-C. Sanchez, A.A. Gooley, R.D. Appel, I. Humphery-Smith, D.F. Hochstrasser, K.L. Williams, Progress with proteome projects: why all proteins expressed by a genome should be Identified and how to do it, *Biotech. Genet. Eng. Rev.*, 13 (1996) 19–50.
3. T.K. Toby, L. Fornelli, N.L. Kelleher, Progress in top-down proteomics and the analysis of proteoforms, *Ann. Rev. Anal. Chem.*, 9 (2016) 499–519.
4. A. Armirotti, G. Damonte, Achievements and perspectives of top-down proteomics, *Proteomics*, 10 (2010) 3566–3576.
5. J.A. Melby, D.S. Roberts, E.J. Larson, K.A. Brown, E.F. Bayne, S. Jin, Y. Ge, Novel strategies to address the challenges in top-down proteomics, *J. Am. Soc. Mass Spectrom.*, 32 (2021) 1278–1294.
6. N.L. Kelleher, H.Y. Lin, G.A. Valaskovic, D.J. Aaserud, E.K. Fridriksson, F.W. McLafferty, Top down versus bottom up protein characterization by tandem high-resolution mass spectrometry, *J. Am. Chem. Soc.*, 121 (1999) 806–812.
7. C. Nagy, M. Andrási, N. Hamidli, G. Gyémánt, A. Gáspár, Top-down proteomic analysis of monoclonal antibodies by capillary zone electrophoresis-mass spectrometry, *J. Chromatogr. Open.* 2 (2022) 100024.
8. A.D. Catherman, O.S. Skinner, N.L. Kelleher, Top down proteomics: facts and perspectives, *Biochem. Biophys. Res. Commun.*, 445 (2014) 683–693.
9. Stellan Hjertén, *Free Zone Electrophoresis*, Elsevier, 1967.
10. F.E.P. Mikkers, F.M. Everaerts, Th.P.E.M. Verheggen, High-performance zone electrophoresis, *J. Chromatogr. A.*, 169 (1979) 11–20.
11. J.W. Jorgenson, K.DeArman. Lukacs, Zone electrophoresis in open-tubular glass capillaries, *Anal. Chem.*, 53 (1981) 1298–1302.
12. Gerhardus de Jong, *Capillary electrophoresis - mass spectrometry (CE-MS)*, John Wiley & Sons, 2016.
13. S.P. Porras, M.-L. Riekkola, E. Kenndler, The principles of migration and dispersion in capillary zone electrophoresis in nonaqueous solvents, *Electrophoresis*, 24 (2003) 1485–1498.
14. H. Shintani, J. Polonski, *Handbook of capillary electrophoresis applications*, Blackie Academic and Professional, 1996.
15. J.R. Petersen, A.A. Mohammad, *Clinical and forensic applications of capillary electrophoresis*, Springer Science & Business Media, 2001.
16. S.F.Y. Li, Y.S. Wu, Capillary electrophoresis, *Electrophoresis*, (2000) 1176–1187.
17. R. Kuhn, S. Hoffstetter-Kuhn, *Capillary electrophoresis: principles and practice*, Springer Science & Business Media, 1993.
18. N.A. Lacher, K.E. Garrison, R.S. Martin, S.M. Lunte, Microchip capillary electrophoresis/ electrochemistry, *Electrophoresis*, 22 (2001) 2526–2536.
19. M. Ryvolová, M. Macka, M. Ryvolová, J. Preisler, M. Macka, Portable capillary-based (non-chip) capillary electrophoresis, *TrAC Trends Anal. Chem.*, 29 (2010) 339–353.

20. D. Barcelo, Downsizing the Methods, in: M. DeLaGuardia, S. Armata (Eds.), *Green Analytical Chemistry: Theory and Practice*, Elsevier, 2011.
21. J.L. Felhofer, L. Blanes, C.D. Garcia, Recent developments in instrumentation for capillary electrophoresis and microchip-capillary electrophoresis, *Electrophoresis*, 31 (2010) 2469–2486.
22. T. Wehr, Capillary Zone Electrophoresis, in: *Encyclopedia of physical science and technology*, 2003, 355–368.
23. S. Štěpánová, V. Kašička, Recent applications of capillary electromigration methods to separation and analysis of proteins, *Anal. Chim. Acta.*, 933 (2016) 23–42.
24. W.-L. Tseng, M.-M. Hsieh, S.-J. Wang, H.-T. Chang, Effect of ionic strength, pH and polymer concentration on the separation of DNA fragments in the presence of electroosmotic flow, *J. Chromatogr. A.*, 894 (2000) 219–230.
25. N. Volpi, *Capillary electrophoresis of carbohydrates*, Springer Science & Business Media, 2010.
26. R. Řemínek, F. Foret, Capillary electrophoretic methods for quality control analyses of pharmaceuticals: A review, *Electrophoresis*, 42 (2020) 19–37.
27. Y. He, N.A. Lacher, W. Hou, Q. Wang, C. Isele, J. Starkey, M. Ruesch, Analysis of identity, charge variants, and disulfide isomers of monoclonal antibodies with capillary zone electrophoresis in an uncoated capillary column, *Anal. Chem.*, 82 (2010) 3222–30.
28. R. Gahoual, J. Giorgetti, A. Beck, E. Leize-Wagner, Y.-N. François, Biopharmaceutical applications of capillary electromigration methods, *Capill. Electromigr. Sep. Methods.*, (2018) 453–480.
29. C.R. Jolliff, C.R. Blessum, Comparison of serum protein electrophoresis by agarose gel and capillary zone electrophoresis in a clinical setting, *Electrophoresis*, 18 (1997) 1781–1784.
30. C. Gay-Bellile, Automated multicapillary electrophoresis for analysis of human serum proteins, *Clin. Chem.*, 49 (2003) 1909–1915.
31. S.S. Zhao, D.D.Y. Chen, Applications of capillary electrophoresis in characterizing recombinant protein therapeutics, *Electrophoresis*, 35 (2013) 96–108.
32. F.-T.A. Chen, J.-H. Zang, Determination of milk proteins by capillary electrophoresis, *J. AOAC Int.*, 75 (1992) 905–909.
33. J. Sastre Toraño, R. Ramautar, G. de Jong, Advances in capillary electrophoresis for the life sciences, *J. Chromatogr. B.*, 1118-1119 (2019) 116–136.
34. C. Mathé, S. Devineau, J.-C. Aude, G. Lagniel, S. Chédin, V. Legros, M.-H. Mathon, J.-P. Renault, S. Pin, Y. Boulard, J. Labarre, Structural determinants for protein adsorption/non-adsorption to silica surface, *PLoS ONE*, 8 (2013) e81346.
35. K. Kubiak-Ossowska, M. Cwieka, A. Kaczynska, B. Jachimska, P.A. Mulheran, Lysozyme adsorption at a silica surface using simulation and experiment: effects of pH on protein layer structure, *Phys. Chem. Chem. Phys.*, 17 (2015) 24070–24077.
36. S. Olmo, *Capillary coatings in capillary electrophoresis (CE) analysis of biomolecules*, 2008.

37. C. Huhn, R. Ramautar, M. Wuhrer, G.W. Somsen, Relevance and use of capillary coatings in capillary electrophoresis–mass spectrometry, *Anal. Bioanal. Chem.*, 396 (2009) 297–314.
38. J.E. Melanson, N.E. Baryla, C.A. Lucy, Dynamic capillary coatings for electroosmotic flow control in capillary electrophoresis, *TrAC Trends Anal. Chem.*, 20 (2001) 365–374.
39. J. Horvath, V. Dolník, Polymer wall coatings for capillary electrophoresis, *Electrophoresis*, 22 (2001) 644–655.
40. L. Leclercq, M. Morvan, J. Koch, C. Neusüß, H. Cottet, Modulation of the electroosmotic mobility using polyelectrolyte multilayer coatings for protein analysis by capillary electrophoresis, *Anal. Chim. Acta.*, 1057 (2019) 152–161.
41. B. Domon, Mass spectrometry and protein analysis, *Science*, 312 (2006) 212–217.
42. J. Griffiths, A brief history of mass spectrometry, *Anal. Chem.*, 80 (2008) 5678–5683.
43. H. Awad, M.M. Khamis, A. El-Aneed, Mass spectrometry, review of the basics: ionization, *Appl. Spectrosc. Rev.*, 50 (2014) 158–175.
44. S. Medhe, Ionization techniques in mass spectrometry: a review, *Mass Spectrom. Purif. Tech.*, 04 (2018).
45. G.L. Glish, R.W. Vachet, The basics of mass spectrometry in the twenty-first century, *Nat. Rev. Drug Discov.*, 2 (2003) 140–150.
46. T.M. Annesley, Ion suppression in mass spectrometry, *Clin. Chem.*, 49 (2003)
47. R. Cramer, *Advances in MALDI and laser-induced soft ionization mass spectrometry*, Cham Springer International Publishing, 2016.
48. R. Aebersold, M. Mann, Mass spectrometry-based proteomics, *Nature*, 422 (2003) 198–207.
49. X. Han, A. Aslanian, J.R. Yates, Mass spectrometry for proteomics, *Curr. Opin. Chem. Biol.*, 12 (2008) 483–490.
50. A. Stolz, K. Jooß, O. Höcker, J. Römer, J. Schlecht, C. Neusüß, Recent advances in capillary electrophoresis-mass spectrometry: Instrumentation, methodology and applications, *Electrophoresis*, 40 (2018) 79–112.
51. F. Xian, C.L. Hendrickson, A.G. Marshall, High resolution mass spectrometry, *Anal. Chem.*, 84 (2012) 708–719.
52. R.A. Zubarev, A. Makarov, Orbitrap mass spectrometry, *Anal. Chem.*, 85 (2013) 5288–5296.
53. S. Medhe, Mass spectrometry: detectors review, *Chem. Biomol. Eng.*, 3 (2018) 51–58.
54. M. Biacchi, N. Said, A. Beck, E. Leize-Wagner, Y.-N. François, Top-down and middle-down approach by fraction collection enrichment using off-line capillary electrophoresis – mass spectrometry coupling: Application to monoclonal antibody F c/2 charge variants, *J. Chromatogr. A.*, 1498 (2017) 120–127.
55. J. Kruszewska, J. Sikorski, J. Samsonowicz-Górski, M. Matczuk, A CE-ICP-MS/MS method for the determination of superparamagnetic iron oxide nanoparticles under simulated physiological conditions, *Anal. and Bioanal. Chem.*, 412 (2020) 8145–8153.

56. W. Kolch, C. Neusüß, M. Pelzing, H. Mischak, Capillary electrophoresis-mass spectrometry as a powerful tool in clinical diagnosis and biomarker discovery, *Mass Spectrom. Rev.*, 24 (2005) 959–977.
57. H. Wu, K. Tang, Highly sensitive and robust capillary electrophoresis-electrospray ionization-mass spectrometry: interfaces, preconcentration techniques and applications, *Rev. Anal. Chem.*, 39 (2020) 45-55.
58. C.C. Liu, J. Zhang, N.J. Dovichi, A sheath-flow nanospray interface for capillary electrophoresis/mass spectrometry, *Rapid Commun. Mass Spectrom.*, 19 (2005) 187–192.
59. G. Bonvin, J. Schappler, S. Rudaz, Capillary electrophoresis–electrospray ionization-mass spectrometry interfaces: Fundamental concepts and technical developments, *J. Chromatogr. A.*, 1267 (2012) 17–31.
60. M. Moini, Simplifying CE–MS operation. 2. interfacing low-flow separation techniques to mass spectrometry using a porous tip, *Anal. Chem.*, 79 (2007) 4241–4246.
61. P. Pantůčková, P. Gebauer, P. Boček, L. Křivánková, Electrolyte systems for on-line CE-MS: Detection requirements and separation possibilities, *Electrophoresis*, 30 (2009) 203–214.
62. W. Zhang, T. Hankemeier, R. Ramautar, Next-generation capillary electrophoresis–mass spectrometry approaches in metabolomics, *Curr. Opin. Biotech.*, 43 (2017) 1–7.
63. E. Nevedomskaya, R. Ramautar, R. Derks, I. Westbroek, G. Zondag, I. van der Pluijm, A.M. Deelder, O.A. Mayboroda, CE-MS for metabolic profiling of volume-limited urine samples: application to accelerated aging TTD mice, *J. Proteome Res.*, 9 (2010) 4869–4874.
64. C.A. Nesbitt, H. Zhang, K.K.-C. . Yeung, Recent applications of capillary electrophoresis–mass spectrometry (CE–MS): CE performing functions beyond separation, *Anal. Chim. Acta.*, 627 (2008) 3–24.
65. A.M. Belov, R. Viner, M.R. Santos, D.M. Horn, M. Bern, B.L. Karger, A.R. Ivanov, Analysis of proteins, protein complexes and organellar proteomes using sheathless capillary zone electrophoresis - native mass spectrometry, *J. Am. Soc. Mass Spectrom.*, 28 (2017) 2614–2634.
66. G. van Schaick, R. Haselberg, G.W. Somsen, M. Wuhrer, E. Domínguez-Vega, Studying protein structure and function by native separation–mass spectrometry, *Nat. Rev. Chem.*, 6 (2022) 215–231.
67. D.P. Donnelly, C.M. Rawlins, C.J. DeHart, L. Fornelli, L.F. Schachner, Z. Lin, J.L. Lippens, K.C. Aluri, R. Sarin, B. Chen, C. Lantz, W. Jung, K.R. Johnson, A. Koller, J.J. Wolff, I.D.G. Campuzano, J.R. Auclair, A.R. Ivanov, J.P. Whitelegge, L. Paša-Tolić, Best practices and benchmarks for intact protein analysis for top-down mass spectrometry, *Nat. Methods*, 16 (2019) 587–594.
68. H. Wu, Studies on denaturation of proteins XIII. A theory of denaturation, *Chin. J. Physiol.*, 5 (1931) 6–26.
69. R. Haselberg, G.J. de Jong, G.W. Somsen, CE-MS for the analysis of intact proteins 2010-2012, *Electrophoresis*, 34 (2012) 99–112.
70. S. Vimer, G. Ben-Nissan, M. Sharon, Mass spectrometry analysis of intact proteins from crude samples, *Anal. Chem.*, 92 (2020) 12741–12749.

71. A.C. Leney, A.J.R. Heck, Native mass spectrometry: What is in the name?, *J Am. Soc. Mass Spectrom.*, 28 (2017) 5–13.
72. F.P. Gomes, J.R. Yates, Recent trends of capillary electrophoresis-mass spectrometry in proteomics research, *Mass Spectrom. Rev.* 38 (2019) 445–460.
73. K. Jooß, J.P. McGee, R.D. Melani, N.L. Kelleher, Standard procedures for native CZE-MS of proteins and protein complexes up to 800 kDa, *Electrophoresis*, 42 (2021) 1050–1059.
74. M. Rabe, D. Verdes, S. Seeger, Understanding protein adsorption phenomena at solid surfaces, *Adv. Colloid Interface Sci.*, 162 (2011) 87–106.
75. A. Staub, S. Comte, S. Rudaz, J.-L. Veuthey, J. Schappler, Use of organic solvent to prevent protein adsorption in CE-MS experiments, *Electrophoresis*, 31 (2010) 3326–3333.
76. M. Pioch, S.-C. Bunz, C. Neusüß, Capillary electrophoresis/mass spectrometry relevant to pharmaceutical and biotechnological applications, *Electrophoresis*, 33 (2012) 1517–1530.
77. J.A. Loo, H.R. Udseth, R.D. Smith, Peptide and protein analysis by electrospray ionization-mass spectrometry and capillary electrophoresis-mass spectrometry, *Anal. Biochem.*, 179 (1989) 404–412.
78. J. Shen, A. Buko, Rapid identification of proteins in polyethylene glycol-containing samples using capillary electrophoresis electrospray mass spectrometry, *Anal. Biochem.*, 311 (2002) 80–83.
79. H. Stutz, G. Bordin, A.R. Rodriguez, Capillary zone electrophoresis of metal-binding proteins in formic acid with UV- and mass spectrometric detection using cationic transient capillary isotachopheresis for preconcentration, *Electrophoresis*, 25 (2004) 1071–1089.
80. L.J. Deterding, J.M. Cutalo, M. Khaledi, K.B. Tomer, Separation and characterization of human high-density apolipoproteins using a nonaqueous modifier in capillary electrophoresis-mass spectrometry, *Electrophoresis*, 23 (2002) 2296.
81. C. Simó, M. Herrero, C. Neusüß, M. Pelzing, E. Kenndler, C. Barbas, E. Ibáñez, A. Cifuentes, Characterization of proteins from spirulina platensis microalga using capillary electrophoresis-ion trap-mass spectrometry and capillary electrophoresis-time of flight-mass spectrometry, *Electrophoresis*, 26 (2005) 2674–2683.
82. A. Staub, S. Rudaz, J.-L. Veuthey, J. Schappler, Multiple injection technique for the determination and quantitation of insulin formulations by capillary electrophoresis and time-of-flight mass spectrometry, *J. Chromatogr. A.*, 1217 (2010) 8041–8047.
83. R. Haselberg, G.J. de Jong, G.W. Somsen, Capillary electrophoresis–mass spectrometry for the analysis of intact proteins, *J. Chromatogr. A.*, 1159 (2007) 81–109.
84. R. Haselberg, G.J. de Jong, G.W. Somsen, Capillary electrophoresis-mass spectrometry for the analysis of intact proteins 2007-2010, *Electrophoresis*, 32 (2010) 66–82.

85. C. Neusüß, U. Demelbauer, M. Pelzing, Glycoform characterization of intact erythropoietin by capillary electrophoresis-electrospray-time of flight-mass spectrometry, *Electrophoresis*, 26 (2005) 1442–1450.
86. J.R. Catai, J.S. Torano, G.J. de Jong, G.W. Somsen, Capillary electrophoresis–mass spectrometry of proteins at medium pH using bilayer-coated capillaries, *Analyst*, 132 (2007) 75–81.
87. R. Haselberg, V. Brinks, A. Hawe, G.J. de Jong, G.W. Somsen, Capillary electrophoresis-mass spectrometry using noncovalently coated capillaries for the analysis of biopharmaceuticals, *Anal. Bioanal. Chem.*, 400 (2011) 295–303.
88. S. Ongay, C. Neusüß, Isoform differentiation of intact AGP from human serum by capillary electrophoresis–mass spectrometry, *Anal. Bioanal. Chem.*, 398 (2010) 845–855.
89. S. Ullsten, A. Zuberovic, M. Wetterhall, E. Hardenborg, K.E. Markides, J. Bergquist, A polyamine coating for enhanced capillary electrophoresis-electrospray ionization-mass spectrometry of proteins and peptides, *Electrophoresis*, 25 (2004) 2090–2099.
90. K. Jooß, J. Hühner, S. Kiessig, B. Moritz, C. Neusüß, Two-dimensional capillary zone electrophoresis–mass spectrometry for the characterization of intact monoclonal antibody charge variants, including deamidation products, *Anal. Bioanal. Chem.*, 409 (2017) 6057–6067.
91. M. Han, B.M. Rock, J.T. Pearson, D.A. Rock, Intact mass analysis of monoclonal antibodies by capillary electrophoresis—Mass spectrometry, *J. Chromatogr. B.*, 1011 (2016) 24–32.
92. S. Garza, S. Chang, M. Moini, Simplifying capillary electrophoresis–mass spectrometry operation: Eliminating capillary derivatization by using self-coating background electrolytes, *J. Chromatogr. A.*, 1159 (2007) 14–21.
93. S. Hjertén, High-performance electrophoresis, *J. Chromatogr. A.*, 347 (1985) 191–198.
94. J. Bodnar, L. Hajba, A. Guttman, A fully automated linear polyacrylamide coating and regeneration method for capillary electrophoresis of proteins, *Electrophoresis*, 37 (2016) 3154–3159.
95. H.H. Yeh, H.L. Wu, C.Y. Lu, S.H. Chen, Simultaneous determination of regular insulin and insulin aspart by capillary zone electrophoresis and application in drug formulations, *J. Pharm. Biomed. Anal.*, 53 (2010) 145–150.
96. C. Lamalle, A.C. Servais, R.P. Radermecker, J. Crommen, M. Fillet, Simultaneous determination of insulin and its analogues in pharmaceutical formulations by micellar electrokinetic chromatography, *J. Pharm. Biomed. Anal.*, 111 (2015) 344–350.
97. B. Pajaziti, R. Petkovska, M. Andradi, D. Nebija, Application of the capillary zone electrophoresis (CZE) and capillary gel electrophoresis (CGE) for the separation of human insulin, insulin lispro and their degradation products, *Pharmazie*, 75 (2020) 167–171.
98. M. Haunschmidt, K. Ortner, K. Hainz, E. Bradt, L. Sternbauer, W. Buchberger, C.W. Klampfl, Investigations on the migration behavior of insulin and related synthetic analogues in CZE, MEKC and MEEKC employing different surfactants, *Electrophoresis*, 31 (2010).

99. A. Kristl, A. Podgornik, M. Pompe, Simultaneous separation of insulin and six therapeutic analogues on a mixed mode column: HPLC-UV method development and application, *J. Chromatogr. B.*, 1171 (2021) 122557.
100. A. Thomas, W. Schänzer, M. Thevis, Determination of human insulin and its analogues in human blood using liquid chromatography coupled to ion mobility mass spectrometry (LC-IM-MS), *Drug Test. Anal.*, 6 (2014) 1125–1132.
101. J. Zielińska, J. Stadnik, A. Bierczyńska-Krzysik, D. Stadnik, Identification of N-terminally truncated derivatives of insulin analogs formed in pharmaceutical formulations, *Pharm. Res.*, 35 (2018).
102. A. Thomas, M. Thevis, Analysis of insulin and insulin analogs from dried blood spots by means of liquid chromatography–high resolution mass spectrometry, *Drug Test. Anal.*, 10 (2018) 1761–1768.
103. E. Balaguer, C. Neusüß, Intact glycoform characterization of erythropoietin- $\alpha$  and erythropoietin- $\beta$  by CZE-ESI-TOF-MS, *Chromatogr.*, 64 (2006) 351–357.
104. R. Haselberg, G.J. de Jong, G.W. Somsen, Capillary electrophoresis–mass spectrometry of intact basic proteins using Polybrene–dextran sulfate–Polybrene-coated capillaries: System optimization and performance, *Anal. Chim. Acta.*, 678 (2010) 128–134.
105. R. Haselberg, G.J. de Jong, G.W. Somsen, Capillary electrophoresis of intact basic proteins using noncovalently triple-layer coated capillaries, *J. Sep. Sci.*, 32 (2009) 2408–2415.
106. C. Vanhee, S. Janvier, G. Moens, E. Deconinck, P. Courselle, A simple dilute and shoot methodology for the identification and quantification of illegal insulin, *J. Pharm. Anal.*, 6 (2016) 326–334.
107. D. C. Kay, *An Introduction to Tissue-Biomaterial Interactions*, John Wiley & Sons, (2002) 1–50.
108. Á. Kecskeméti, C. Nagy, P. Biró, Z. Szabó, I. Pócsi, T. Bartók, A. Gáspár, Analysis of fumonisin mycotoxins with capillary electrophoresis – mass spectrometry, *Food Addit. Contam.: Part A.*, 37 (2020) 1553–1563.
109. A. Aich, M. Freundlich, P.G. Vekilov, The free heme concentration in healthy human erythrocytes, *Blood Cells Mol. Dis.*, 55 (2015) 402–409.
110. R.L. Edwards, A.J. Creese, M. Baumert, P. Griffiths, J. Bunch, H.J. Cooper, Hemoglobin variant analysis via direct surface sampling of dried blood spots coupled with high-resolution mass spectrometry, *Anal. Chem.*, 83 (2011) 2265–2270.
111. L. Leclercq, C. Renard, M. Martin, H. Cottet, Quantification of adsorption and optimization of separation of proteins in capillary electrophoresis, *Anal. Chem.*, 92 (2020) 10743–10750.
112. A.L. Gassner, S. Rudaz, J. Schappler, Static coatings for the analysis of intact monoclonal antibody drugs by capillary zone electrophoresis, *Electrophoresis*, 34 (2013) 2718–2724.
113. L. Goodwin, J.R. Startin, B.J. Keely, D.M. Goodall, Analysis of glyphosate and glufosinate by capillary electrophoresis–mass spectrometry utilising a sheathless microelectrospray interface, *J. Chromatogr. A.*, 1004 (2003) 107–119.
114. L. Hajba, A. Guttman, Recent advances in column coatings for capillary electrophoresis of proteins, *TrAC Trends Anal. Chem.*, 90 (2017) 38–44.

115. H. Katayama, Y. Ishihama, N. Asakawa, Stable capillary coating with successive multiple ionic polymer layers, *Anal. Chem.*, 70 (1998) 2254–2260.
116. A.T. Tu, Overview of snake venom chemistry, *Adv. Exp. Med. Biol.*, 391 (1996) 37–62.
117. K. Ortner, W. Buchberger, M. Himmelsbach, Capillary electrokinetic chromatography of insulin and related synthetic analogues, *J. Chromatogr. A.*, 1216 (2009) 2953–2957.
118. X. Yan, L. Sun, G. Zhu, O.F. Cox, N.J. Dovichi, Over 4100 protein identifications from a *Xenopus laevis* fertilized egg digest using reversed-phase chromatographic prefractionation followed by capillary zone electrophoresis-electrospray ionization-tandem mass spectrometry analysis, *Proteomics*, 16 (2016) 2945–2952.
119. O.O. Dada, Y. Zhao, N. Jaya, O. Salas-Solano, High-resolution capillary zone electrophoresis with mass spectrometry Peptide Mapping of Therapeutic proteins: improved separation with mixed aqueous–aprotic dipolar Solvents (N,N-dimethylacetamide and N,N-dimethylformamide) as the background electrolyte, *Anal. Chem.*, 89 (2017) 11227–11235.
120. S. Hjertén, S. Mohabbati, D. Westerlund, Influence of ignored and well-known zone distortions on the separation performance of proteins in capillary free zone electrophoresis with special reference to analysis in polyacrylamide-coated fused silica capillaries in various buffers, *J. Chromatogr. A.*, 1053 (2004) 181–199.
121. R. Haselberg, F.M. Flesch, A. Boerke, G.W. Somsen, Thickness and morphology of polyelectrolyte coatings on silica surfaces before and after protein exposure studied by atomic force microscopy, *Anal. Chim. Acta.*, 779 (2013) 90–95.
122. R.A. Zubarev, N.A. Kruger, E.K. Fridriksson, M.A. Lewis, D.M. Horn, B.K. Carpenter, F.W. McLafferty, Electron capture dissociation of gaseous multiply-charged proteins is favored at disulfide bonds and other sites of high hydrogen atom affinity, *J. Am. Chem. Soc.*, 121 (1999) 2857–2862.
123. M. Bhattacharyya, K. Gupta, K.H. Gowd, P. Balaram, Rapid mass spectrometric determination of disulfide connectivity in peptides and proteins, *Mol. BioSyst.*, 9 (2013) 1340.
124. J.M. Wells, J.L. Stephenson, S.A. McLuckey, Charge dependence of protonated insulin decompositions, *Int. J. Mass Spectrom.*, 203 (2000) A1–A9.
125. R.S. Johnson, S.A. Martin, Klaus. Biemann, J.T. Stults, J. Throck. Watson, Novel fragmentation process of peptides by collision-induced decomposition in a tandem mass spectrometer: differentiation of leucine and isoleucine, *Anal. Chem.*, 59 (1987) 2621–2625.
126. A. Suneetha, R.K. Raja, Comparison of LC-UV and LC-MS methods for simultaneous determination of teriflunomide, dimethyl fumarate and fampridine in human plasma: application to rat pharmacokinetic study, *Biomed. Chromatogr.*, 30 (2016) 1371–1377.
127. G. Mandrup, Rugged method for the determination of deamidation products in insulin solutions by free zone capillary electrophoresis using an untreated fused-silica capillary, *J. Chromatogr. A.*, 604 (1992) 267–281.
128. Y. Ying, H. Li, Recent progress in the analysis of protein deamidation using mass spectrometry, *Methods*, 200 (2020).

129. M. Andrasi, B. Pajaziti, B. Sipos, C. Nagy, N. Hamidli, A. Gaspar, Determination of deamidated isoforms of human insulin using capillary electrophoresis, *J. Chromatogr. A*, 1626 (2020) 461344.
130. J. Mo, R. Jin, Q. Yan, I. Sokolowska, M.J. Lewis, P. Hu, Quantitative analysis of glycation and its impact on antigen binding, *MAbs*, 10 (2018) 406–415.

## 7. Publications and conferences

### *Publications related to the dissertation:*

1. **Narmin Hamidli**, Blerta Pajaziti, Melinda Andrási, Cynthia Nagy, Attila Gáspár: Determination of human insulin and its six therapeutic analogues by capillary electrophoresis – mass spectrometry. *Journal of Chromatography A* (2022). IF: 4.601 Q1.
2. **Narmin Hamidli**, Melinda Andrási, Cynthia Nagy, Attila Gáspár: Analysis of intact proteins with capillary zone electrophoresis coupled to mass spectrometry using uncoated and coated capillaries. *Journal of Chromatography A* (2021). IF: 4.601 Q1.

### *Other publications:*

3. Cynthia Nagy, Melinda Andrási, **Narmin Hamidli**, Gyöngyi Gyémánt, Attila Gáspár: Top-down proteomic analysis of monoclonal antibodies by capillary zone electrophoresis-mass spectrometry. *Journal of Chromatography Open* (2022).
4. Melinda Andrási, Blerta Pajaziti, Bettina Sipos, Cynthia Nagy, **Narmin Hamidli**, A. Gáspár: Determination of deamidated isoforms of human insulin using capillary electrophoresis. *Journal of Chromatography A* (2020). IF: 4.759 Q1.

### *Conference lecture presentations related to the dissertation:*

1. Narmin Hamidli, Melinda Andrasi, Cynthia Nagy, Attila Gaspar: A comparison of bare silica and coated capillaries for CZE-MS analysis of native proteins. V4 Symposium “Flow Analysis & Capillary Electrophoresis” (FA&CE), 28 June-1 July, 2021, Krakow, Poland.
2. Narmin Hamidli, Melinda Andrasi, Cynthia Nagy, Attila Gaspar: Analysis of intact proteins with capillary zone electrophoresis coupled to mass spectrometry using uncoated and coated capillaries. XXV Spring Wind Conference, 6-8 May, 2022, Pecs, Hungary.
3. Narmin Hamidli, Melinda Andrasi, Cynthia Nagy, Attila Gaspar: Analysis of intact proteins with capillary zone electrophoresis coupled to mass spectrometry using uncoated and coated capillaries. 20th International Symposium and Summer School on Bioanalysis, 24-30 June, 2022, Pecs, Hungary.
4. Narmin Hamidli, Melinda Andrasi, Cynthia Nagy, Attila Gaspar: Analysis of intact proteins with capillary zone electrophoresis coupled to mass spectrometry using uncoated and coated capillaries. 26th International Symposium on Separation Sciences 28 June-1 July, 2022, Ljubljana, Slovenia.

*Conference poster presentations related to the dissertation*

Narmin Hamidli, Melinda Andrasi, Cynthia Nagy, Attila Gaspar: Analysis of intact proteins with capillary zone electrophoresis coupled to mass spectrometry using uncoated and coated capillaries. 33rd International Symposium on Chromatography, 18-22 September, 2022, Budapest, Hungary.